

MOLECULAR DISSECTION OF THE ALLOSTERIC
REGULATION OF YEAST PYRUVATE KINASE
BY FRUCTOSE-1,6-BISPHOSPHATE

By

ARON W. FENTON

Bachelor of Science

Oklahoma State University

Stillwater, Oklahoma

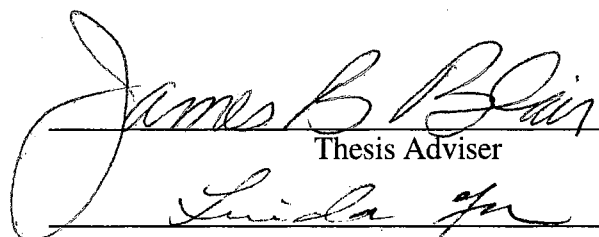
1993

Submitted to the Faculty of the
Graduate College of the
Oklahoma State University
In partial fulfillment of
the requirements for
the Degree of
DOCTOR OF PHILOSOPHY
December, 1999

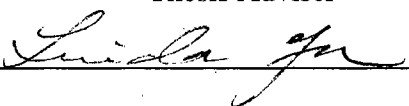
Thesis
1999D
F342m

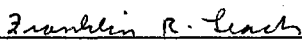
MOLECULAR DISSECTION OF THE ALLOSTERIC
REGULATION OF YEAST PYRUVATE KINASE
BY FRUCTOSE-1,6-BISPHOSPHATE

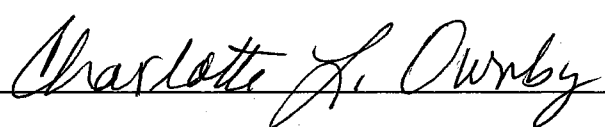
Thesis Approved:

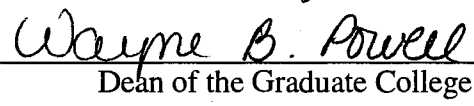


Thesis Adviser









Dean of the Graduate College

ACKNOWLEDGMENTS

I would like to thank my major advisor, Dr. James Blair, who has been both a wonderful supervisor and a dear friend. In addition, my committee members, Dr. Franklin Leach, Dr. Linda Yu, Dr. Charlotte Ownby, and Dr. Steven White have provided valuable guidance, encouragement, and assistance. Dr. George Odell has been a wonderful friend and motivator in my research. Dr. Olin Spivey, Dr. Ulrich Melcher, Dr. Steven Hartson, Eric Leoux, Ed Davis and Brad Scroggins have been wonderful colleagues offering encouragement and advice throughout my training. Janet Rogers and SueAnn Hudiburg have been very helpful in providing DNA services during my research. I have enjoyed working with a number of undergraduate and graduate students in the laboratory, all of who have contributed to my own training. Mr. Brian Stephens was a motivator of my scientific interest through his excellent classroom teaching in my high school career. I would like to express my appreciation to each of these individuals.

I would like to praise my wife, Shellee, and my three children, Anndrea, Crandel, and Christopher, who have been my encouragement, strength, and motivation in this work. They have lovingly and willingly made great sacrifices for my education. I would like to thank my parents for their support and encouragement.

I would like to express my gratitude to the Department of Biochemistry and Molecular Biology for the opportunity and financial support for this work.

TABLE OF CONTENTS

		PAGE
I.	INTRODUCTION	1
	Glycolysis in Metabolism.....	1
	Pyruvate Kinase in Regulation of Glycolysis and Gluconeogenesis.....	2
	Medical Importance of Pyruvate Kinase	3
	Pyruvate Kinase Structure.....	4
	Kinetic Properties of Pyruvate Kinase	4
	Pyruvate Kinase of <i>Saccharomyces cerevisiae</i>	8
	Fitting Pyruvate Kinase to Allosteric Models.....	9
	Changes in the Active Site Due to Allosteric Transition	11
	Allosteric Site(s)	11
	Allosteric Message Across C-C Subunit Interfaces	13
	Allosteric Message Across A-A Subunit Interfaces	14
	Allosteric Message within Subunits	14
	Red Blood Cell Pyruvate Kinase and Hemolytic Anemia.....	15
	Hypothesis.....	23
II.	MATERIALS AND METHODS.....	26
	Computer Modeling of Fructose-1,6-Bisphosphate.....	26
	Computer Modeling of Yeast Pyruvate Kinase	26
	Bacterial Growth and Transformation.....	27
	Mutagenesis.....	28
	Subcloning into an Expression Vector.....	35
	Screening for Proper Expression Construct.....	39
	Yeast Transformation.....	41
	Resin Preparation for Protein Purification	42
	Protein Purification.....	43
	Protein Gels.....	45
	Kinetic Assays.....	45
	Fluorescence Quench Titrations.....	47
	FBP Contamination in F1P and F6P	47
	Curve Fitting.....	48
III.	RESULTS	49
	Expression.....	49
	Wild Type Pyruvate Kinase.....	50
	Two Positive Charged Domain Interactions.....	64
	A-C Domain Contacts.....	66
	The Tyr 436 Pocket: A-C Domain Contacts	66
	The Arg 42 Pocket: A-C Domain Contacts	75
	C-C Interface Interactions	75
	A-A Interface Interactions	89

	Fructose-1,6-Bisphosphate Binding Site Mutants.....	100
	Fructose-1,6-Bisphosphate Analogs	102
IV.	DISCUSSION	115
	Sites of Pyruvate Kinase in Allosteric Regulation.....	115
	Non-expressing Yeast Pyruvate Kinase Mutations	116
	Yeast Pyruvate Kinase Mutations with Small Kinetic Effects.....	119
	A-C Domain Contacts in Allosteric Regulation.....	120
	R369A: A C-C Subunit Interface Mutation.....	123
	E392A: A C-C Subunit Interface Mutation	126
	Q299N: An A-A Subunit Interface Mutation	127
	T311M: An A-A Subunit Interface Mutation	131
	The Fructose-1,6-Bisphosphate Binding Site.....	132
	Pyruvate Kinase Regulation Speculation.....	137
	Future Studies.....	145
	Summary	148
V.	BIBLIOGRAPHY	152
VI.	APPENDIX	158
	Alignment of Pyruvate Kinase Sequences.....	159
	Point Mutations of Pyruvate Kinase Isozymes	174

LIST OF TABLES

	PAGE
Table 1. A Current List of Sequenced Human Red Blood Cell PK Single Amino Acid Replacement Mutations Associated with Hemolytic Anemia.....	17
Table 2. A Current List of Sequenced Human Red Blood Cell PK Mutations that Delete or Insert Three Amino Acids or Less.....	24
Table 3. A Current List of Sequenced, Naturally Occurring Single Amino Acid Replacement PK Mutations.....	25
Table 4. Purification of Wild Type Yeast PK.....	51
Table 5. Summary of the Kinetic Parameters of Wild Type Yeast PK and comparison with other Literature Reports.....	61
Table 6. Kinetic Parameters for Wild Type and K413E.....	74
Table 7. Kinetic Parameters for Wild Type and Mutations of Positive Residues of the Tyr 436 Pocket.....	81
Table 8. Kinetic Parameters for Wild Type and Mutations of Non-Positive Residues of the Tyr 436 Pocket.....	82
Table 9. Kinetic Parameters for Wild Type and R77Q.....	84
Table 10. Kinetic Parameters for Wild Type and R369A.....	88
Table 11. ADP Kinetic Parameters for Wild Type and Crude Extracts of Q299N.....	95
Table 12. Kinetic Parameters for Wild Type, T403K, T406R, and A458K.....	106
Table A1. A Current List of Site Directed Mutations in PK Isozymes.....	174

LIST OF FIGURES

	PAGE
Figure 1. Backbone Trace of a Rabbit Muscle PK Monomer.....	5
Figure 2. Two View of the Tetramer of Pyruvate Kinase.	6
Figure 3. Yeast PK with the Positions of Group I Red Blood Cell Mutations Highlighted.	21
Figure 4. Yeast PK with the Positions of Group II Red Blood Cell Mutations Highlighted.	21
Figure 5. Vector Circle Maps of pPYK101.....	29
Figure 6. Vector Circle Maps of pAlter (Promega) with PK Insert.....	30
Figure 7. Agarose Gel Electrophoresis of DNA from Restriction Digests of pAlter-PK Insert Constructs.....	33
Figure 8. Vector Circle Maps of pYES2 (Invetrogen) with PK Insert.....	37
Figure 9. Agarose Gel Electrophoresis of DNA from a Quick Screen.....	40
Figure 10. SDS PAGE Gel Electrophoresis of Yeast PK at Various Purification Steps.	54
Figure 11. SDS PAGE Gel Electrophoresis of Purified Wild Type PK.....	55
Figure 12. Kinetic Properties of Wild Type PK Under Two Different Salt Conditions.	56
Figure 13. Effects of $(\text{NH}_4)_2\text{SO}_4$ on PK Activities.	58
Figure 14. Effects of KCl Concentration on Activity (v) of Desalted Wild Type PK in the Presence (■) and Absence (○) of FBP.	59
Figure 15. Fluorescence Quench Titration Curves for Wild Type PK.....	63
Figure 16. A Hydrophobic/Hydrophilic Grid Map of the Energetically Minimized β -furanose FBP Model.....	65
Figure 17. Surface Charge Map of the Arg 42 Pocket.....	67
Figure 18. Surface Charge Map of the Tyr 436 Pocket.....	68
Figure 19. Alignment of Amino Acid Sequence of Pyruvate Kinase Sequences from Various Species In and Near the Tyr 436 and Arg 42 Pockets.....	69

Figure 20. A Proposed FBP Docking in the Tyr 436 Pocket.....	71
Figure 21. SDS PAGE Gel Electrophoresis Pattern of K413E.....	73
Figure 22. SDS PAGE Gel Electrophoresis Pattern of K236Q, K292Q, T406R, R409Q, K413Q, Y436F, and Y436S.	76
Figure 23. Kinetic Properties of Wild Type and K413Q.....	80
Figure 24. SDS PAGE Gel Electrophoresis of R77Q.	83
Figure 25. SDS PAGE Gel Electrophoresis of R369A and E392A.....	86
Figure 26. Kinetic Properties of Wild Type and E392A.....	90
Figure 27. Fluorescence Quench Titration Curves for Wild Type and E392A.....	91
Figure 28. Kinetic Properties of Wild Type and Crude Extracts of Q299N.	93
Figure 29. SDS PAGE Gel Electrophoresis Pattern of T311M.....	96
Figure 30. Kinetic Properties of Wild Type and Purified T311M.	97
Figure 31. Fluorescence Quench Titration Curves for Wild Type and T311M.....	99
Figure 32. The FBP Binding Site as Resolved by Co-Crystallization to Yeast PK.	101
Figure 33. SDS PAGE Gel Electrophoresis of T403E, T403K, T406R, A458K, and R459Q.	103
Figure 34. Kinetic Properties of Wild Type, T403E, and R459Q.	107
Figure 35. Fluorescence Quench Titration Curves for Wild Type, T403E, and A459Q.	109
Figure 36. FBP, F1P, and F6P Dependent Activations of Wild Type PK.....	112
Figure 37. FBP, F1P, and F6P Dependent Fluorescence Quench Titration Curves for Wild Type PK.	113
Figure 38. Location of Mutated residues of the Tyr 436 Pocket.....	117
Figure 39. Location of Non-expressing Mutations with Respect to the β -barrel.....	118
Figure 40. Location of the FBP Binding Site on the Surface Charge Map of the Yeast PK Model Developed in this Study.....	121
Figure 41. Location of Mutations with Little or No Effects on Monitored Kinetic Properties.....	122
Figure 42. Location of C-C Subunit Interface Mutations.....	125
Figure 43. Location of Amino Acids of a Possible Relay Involved in Allosteric Regulation.	128

Figure 44. Hand Alignment of Amino Acids of Crystallized PK Isozymes in the Arginine 459 Helix.....	135
Figure 45. Possible Communication Pathways Linking the PEP Binding Site With the C-C Subunit Interface.....	140
Figure 46. Possible Communication Pathways Across the C-C Subunit Interface.....	142
Figure 47. Possible Communication Pathways Linking the FBP Binding Site With the C-C Subunit Interface.....	144
Figure 48. Proposed Communication Pathways.....	146
Figure 49. Locations of Expressed Mutations.....	150
Figure A1. Sequence Alignment for Many PK Isozymes.....	159

LIST OF ABBREVIATIONS

All mutations are written as A###B, where A is the single letter amino acid code of the original amino acid, numbers represent the yeast PK residue position, and B is the single letter amino acid code of the replacement amino acid

Structural elements are labeled according to Larsen *et al.* (17) as shown in Figure A1.

A-A subunit contacts	One of two types of PK subunit contacts. Involves A, C, and N-terminus domains
ADP	Adenosine diphosphate
ATP	Adenosine triphosphate
Arg 42 pocket	A pocket between A and C domains of PK
C-C subunit contacts	One of two types of PK subunit contacts. Involves C domains
cdc19	A heat sensitive yeast strain
EDTA	Ethylenediamine-tetraacetic acid
FBP	Fructose-1,6-bisphosphate
F1P	Fructose-1-phosphate
F6P	Fructose-6-phosphate
$\square F_{\max}$	Maximum fluorescence quench
K_D	Binding constant
L	PK isozyme
LiAc	Lithium acetate
MES	2-[N-Morpholino]ethanesulfonic acid
M1	Mammalian muscle PK isozyme
M2	Mammalian fetal PK isozyme
NADH	β -nicotinamide adenine di-nucleotide
n_H	Hill coefficient
PEP	Phosphoenolpyruvate
PK	Pyruvate kinase
PKD screen	Use of pyruvate kinase deficiency as a screen to identify important amino acids
pyk1	Yeast gene that codes for pyruvate kinase
pyk2	Yeast gene that codes for a possible second pyruvate kinase
pPYK101	Yep24 based plasmid with a yeast pyruvate kinase gene inserted
R	Mammalian red blood cell PK isozyme
R-state	A high activity tetrameric state in thermodynamic models of cooperativity and allostery
r-	A high activity subunit state in thermodynamic models of cooperativity and allostery
$S_{1/2}$	Substrate concentration that gives a response equal to 1/2 the maximum response
T-state	A low activity tetrameric state in thermodynamic models of cooperativity and allostery
t-	A low activity subunit state in thermodynamic models of cooperativity and allostery

Tyr 436 pocket
 V_{\max}
YEPD media
YEPAG
1-5 pyk
121

A pocket between A and C domains of PK
Maximum activity
Dextrose based yeast growth media
Ethanol/Glycerol based yeast growth media
A yeast strain which lacks PK activity
A yeast strain with the pyk1 and pyk2 genes knocked out

INTRODUCTION

Glycolysis in Metabolism

All living organisms need to acquire and utilize free energy. These processes are collectively called metabolism. A chain of enzyme-catalyzed reactions that produce a specific product is a metabolic pathway. Metabolic pathways must be sensitive and responsive to substrate availability and needs of the total organism to avoid energy waste. This sensitivity and responsiveness is accomplished through regulation of key enzymatic reactions within the pathway.

Regulation of enzymes occurs at several levels. The quantity of enzyme present is dependent on the balance between the rate of biosynthesis and the rate of degradation. Biosynthesis requires transcription and translation of the gene coding for the regulator enzyme. A change in the rate of biosynthesis requires an altered rate of transcription and/or translation. Changes in enzyme quantity are generally considered to be a relatively slow and long-term form of metabolic regulation. Regulation of the catalytic activity of an enzyme can occur on a much shorter time scale. Feed-forward activation, feed-back inhibition, protein modification, allosteric regulation, and substrate channeling are all types of regulation that regulate catalysis at the enzyme level.

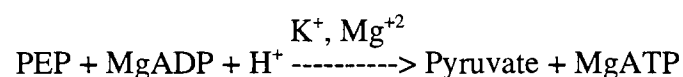
Glycolysis is one of the best characterized metabolic pathways. Glycolysis is metabolism of glucose to pyruvate with the production of two moles of ATP per mole of glucose. Nearly all living cells have the glycolytic pathway and many cell types are dependent on glycolysis as their primary source of energy. In addition glycolysis is responsible for producing metabolites that are substrates for a variety of other metabolic

pathways. Therefore understanding glycolysis is necessary to understanding metabolism as a whole.

Pyruvate Kinase in Regulation of Glycolysis and Gluconeogenesis

In opposition to glycolysis, gluconeogenesis is a major liver function that produces glucose. If regulation of glycolysis and gluconeogenesis in the liver is not coordinated, then production of glucose and utilization of glucose occur at the same time. This process called futile cycling, wastes energy. Regulation of glycolysis is accomplished by regulation of enzymes that catalyze crucial reactions in the glycolytic pathway. Due to the large free energies of the reactions catalyzed by hexokinase, phosphofructokinase, and pyruvate kinase, these three enzymes are the major sites of regulation in glycolysis. Control of pyruvate kinase activity is vital in preventing futile cycling in the liver.

Pyruvate kinase (PK) catalysis the last reaction in glycolysis and is one of two glycolytic reactions that produces ATP. The forward reaction catalyzed by PK has a negative free energy of -6.5 kcal/mole and is therefore essentially irreversible. The reaction transfers a phosphoryl group from phosphoenolpyruvate (PEP) to ADP to yield pyruvate and ATP. For most isozymes of PK two divalent cations and one monovalent cation are required for activity.



PK is regulated by a number of mechanisms. PEP and cations cooperatively regulate PK. This phenomenon is the ability of initial bound ligand to increase PK's affinity for late bound ligand and results in a sigmoidal shaped activity curve as the ligand concentration is varied. In some isozymes of PK, activity is regulated by phosphorylation/dephosphorylation. The effect of this covalent modification is to inhibit PK's activity.

Allosteric refers to "other site". Allosteric regulation therefore defines that an allosteric regulator binds at a site distant from the active site. However, binding of allosteric effectors to distant site(s) causes modification at the enzymes catalytic site. Fructose-1,6-bisphosphate (FBP) is an allosteric activator of many PK isozymes. ATP is an allosteric inhibitor of several PK isozymes.

Due to the importance of cooperative and allosteric regulation to PK's function as a regulation site in glycolysis, understanding how these regulation mechanisms function is important. The purpose of this study was to add to the understanding of allosteric regulation of PK by FBP.

Medical Importance of Pyruvate Kinase

Due to the importance of pyruvate kinase in metabolism, clinical importance of this enzyme is not surprising. Glycolysis, using glucose as a major nutrient, is the major energy-producing pathway of erythrocytes. Therefore, defective glycolytic enzymes have a drastic effect on the energy production and health of erythrocytes. Pyruvate kinase deficiency in human erythrocytes was first identified by Valentine *et al.* in 1961 (1). It is now recognized as the most common cause of hereditary nonspherocytic hemolytic anemia. Several reviews have been published on historical, clinical, and metabolic aspects of this deficiency (2-5). Hemolytic anemia has also been described in animals (6-10).

Protozoan such as *Trypanosoma brucei* lack a TCA cycle and are completely dependent of glycolysis for energy when in mammalian blood. Since phosphofructokinase is unregulated in these organisms, energy flux is controlled by PK (11-14). Unlike mammalian PK, PK of *T. brucei* is activated by fructose-2,6-bisphosphate (15). Therefore PK is a site that has been considered for drug design. Information that adds to the general knowledge of PK structure/function will be beneficial to understanding pyruvate kinase deficiency and to designing drugs that target PK of *T. brucei*.

Pyruvate Kinase Structure

In order to consider allosteric regulation of PK, one must first understand what is currently known about PK structure. A backbone trace of cat muscle PK was solved at 2.6 Å resolution in 1979 by X-ray crystallography (16). More recently, structures have been solved for rabbit M1, yeast, *Escherichia coli* type I, and *Leishmania mexicana* (17-22). The overall conformation of each of these PK's is similar. Crystallized PK enzymes are in tetrameric states consisting of four identical subunits. Each subunit consists of four domains: A, B, C, and N-terminus (Figure 1). There are two different subunit contacts resulting in a quaternary structure of a dimer of dimers (Figure 2). The N-terminus, A, and C domains are involved in one of the subunit contacts (referred to in this paper as the A-A subunit contacts) and only the C domains are involved in the second (referred to in this paper as the C-C subunit contacts). The A domain, located between the B and C domains, has a β -barrel structure (23). The active site lies between the A and B domains in each of PK's four subunits. One end of this β -barrel makes up part of the active site, while the highly dynamic B domain constitutes the remaining portion of the active site.

Several crystal structures have been published which contain various substrate analogs and cations bound in the active site (17-20). In addition, a large number of physical, chemical and kinetic experiments have been used to characterize the active site of the PK enzyme from several sources (see (24) for extensive review). Consequently interactions of PK with substrates and cations in the active site are reasonably well understood.

Kinetic Properties of Pyruvate Kinase

In mammals there are four isozymes (M1, M2, L, and R) which derive from two genes. M1 and M2 are both coded by the M-gene through alternative RNA splicing (25). The M1 isozyme is primarily found in muscle tissue. It demonstrates Michaelis-Menten hyperbolic kinetics with respect to PEP in the absence of allosteric effectors. M1 shows activation by FBP only if it has first been inhibited by the allosteric inhibitor, phenylalanine

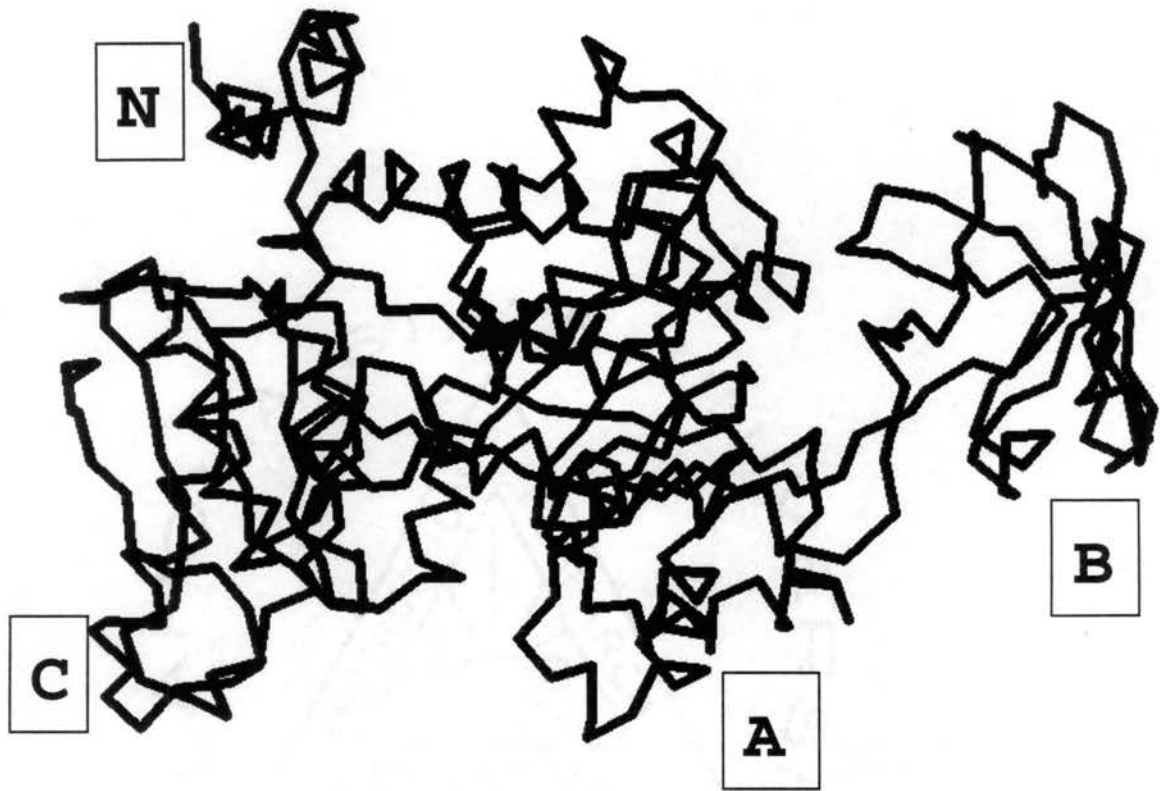
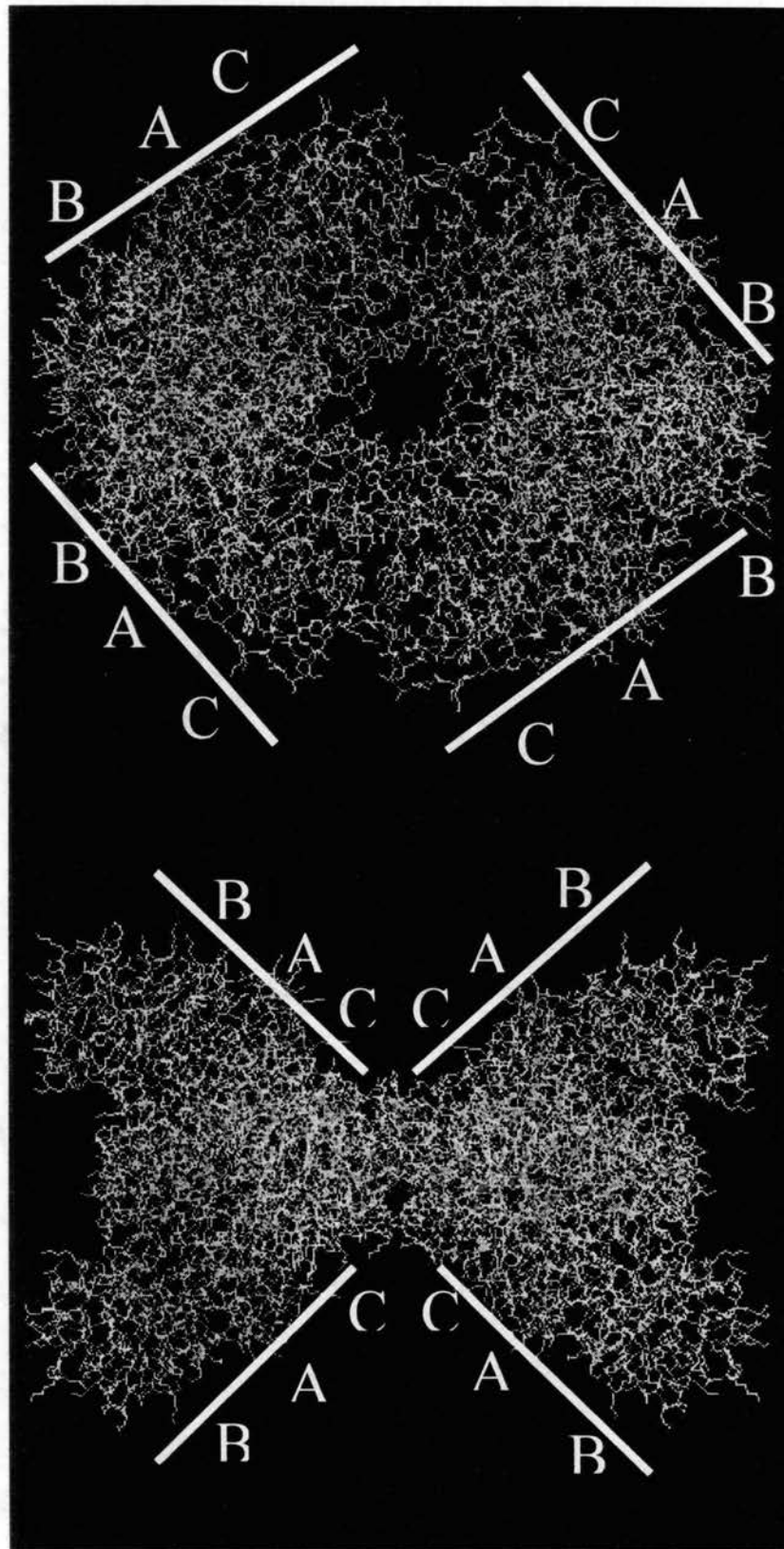


Figure 1. Backbone Trace of a Rabbit Muscle PK Monomer. Each of 4 subunits in a tetramer has 4 domains: A, B, C, and N-Terminus. The Active site lies between the B and A domains. Two types of subunit contacts are involved in making a tetramer. One type of contact involves only the C domains of two subunits while the other contact type involves A, C, and N-terminus domains of two subunits (17).

Figure 2. Two View of the Tetramer of Pyruvate Kinase. The A, B, and C domains of each subunit are labeled.



(26). The M2 isozyme is the fetal form of PK. It is also expressed in adult adipose tissue and lung (27,28). This isozyme has sigmoidal kinetics with respect to PEP in the absence of FBP. Upon activation by FBP the kinetic response shifts to a Michaelis-Menten hyperbolic response (28,29).

Liver (L) and red blood cell (R) PK's are both coded by a second mammalian gene (L-gene) as a result of different promoter sites (30). L and R isozymes are highly regulated isozymes that show sigmoidal kinetics with respect to PEP in the absence of FBP, but shift to hyperbolic kinetics in the presence of the activator. Both the L and R isozymes have phosphorylation sites near the N-terminus, which are regulated by the cAMP-dependent protein kinase (31,32).

Even though most non-mammalian enzymes currently studied show M1-like or L-like characteristics, not all PK's share activation by fructose-1,6-bisphosphate. The enzyme from *Bacillus stearothermophilus* is activated by ribose-5-phosphate (33,34). One of *E. coli*'s two isozymes is activated by AMP (35). PK from *T. brucei* is activated by fructose-2,6-bisphosphate in addition to fructose-1,6-bisphosphate (15). Pyruvate kinases from castor seeds and *Zymomonas mobilis* have not been demonstrated to have an allosteric activator (36-38). Even though PK isozymes with different regulation have been identified, most are activated by phosphorylated cyclic-sugar compounds. Therefore, structural changes induced by activators might be expected to be similar.

Pyruvate Kinase of *Saccharomyces cerevisiae*

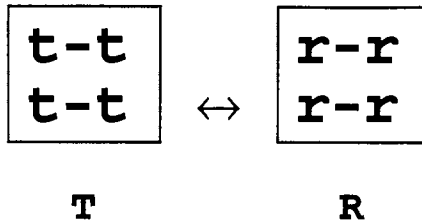
Saccharomyces cerevisiae (yeast) PK kinetics are similar to those reported for mammalian L-isozymes. Yeast PK shows hyperbolic curves when ADP is varied in the presence of saturating amounts of PEP both with and without FBP (39). PEP curves are sigmoidal in the absence of FBP (40). In the presence of FBP the apparent affinity for PEP is increased and the shape of the response curve becomes hyperbolic (40). Kinetic responses to varying concentrations of monovalent and divalent cations are sigmoidal and respond to FBP activation (41).

Unlike mammalian PK, allosteric regulation of PEP affinity of the yeast enzyme by alanine and phenylalanine has not been reported. Even though ATP inhibits yeast PK, the allosteric nature of this inhibition is uncertain (41). The yeast PK has a potential site for phosphorylation by cyclic-AMP dependent protein kinase, however, there is little evidence that the yeast isozyme is regulated by phosphorylation by this enzyme (42). Mck1, a member of the glycogen synthase kinase 3 family of protein kinases, has been found to suppress PK activity in yeast cells (43).

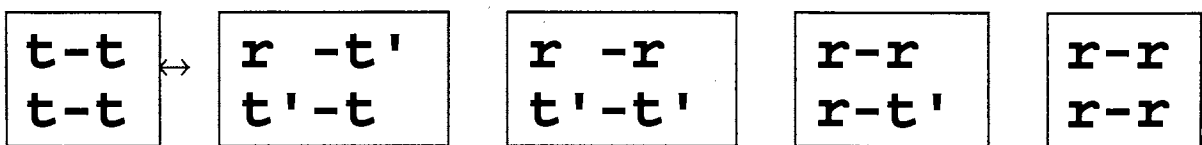
Yeast PK has been purified using many approaches and is well kinetically characterized with respect to substrates, ions, pH, and allosteric effectors (39-41,44-51). No crystallography data for yeast PK was available at the onset of this study in 1994. However a model for this enzyme, built from the rabbit M1 coordinates (17), was developed at the beginning of this study (see results). A yeast PK model based on the cat M1 coordinates has also been constructed (52). In 1998 the structure of yeast PK was solved (20). Since yeast shares allosteric activation by FBP with several other PK isozymes, yeast PK makes a useful PK model that can provide insight into allosteric regulation by FBP.

Fitting Pyruvate Kinase to Allosteric Models

There have been a variety of models developed to explain cooperative regulation. Of these, the concerted model of Monod *et al.* and the sequential model of Koshland *et al.* are most popular (53,54). The low affinity tense (T) state and the high affinity relaxed (R) state are assumed in both models. In both models, capital letters (R and T) are used to describe the conformation of the whole multimer. Lower case letters (r and t) are used to describe the conformation of a single subunit. The concerted model assumes that upon binding of a substrate the equilibrium between the all-T state multimer and the all-R states multimer is altered:



The sequential model states that the binding of substrate to one site induces a tertiary change and that each subunit affects the state of the neighboring subunit:



A more complicated model has been developed to describe cooperativity in hemoglobin (55). The advantage of the latter model is that the tetramer functions as a dimer of dimers. The dimer of dimers nature of PK has been noted based on structural data (56). The Ackers model may be valuable in understanding PK regulation once additional information is available.

It is conceptually easy to use the concerted and sequential models, originally developed to describe cooperativity, to describe allosteric regulation. Both models assume equilibrium between activity states and substrates shift this equilibrium. Allosteric regulators may shift the equilibrium independent of the substrates' effects. Because of the possible ties between cooperative and allosteric regulation, the term homotropic cooperativity has been used to imply the influence of a ligand on its own subsequent binding. Heterotropic cooperativity is used to imply the influence of a ligand on the affinity for different ligands.

Unlike cooperative regulation, explanation of allosteric regulation does not require multiple activity sites. However, since allosteric regulation of PK by FBP involves conversion of sigmoidal kinetic curves to hyperbolic, altered communications between

subunits is implied. Therefore, allosteric regulation of PK involves communication between multiple subunits.

Several studies have tried to fit data from PK to models. Kinetic data from mammalian isozymes has been found to fit a two-state model (26,57). Kinetic and fluorescent analysis of yeast and *B. stearothermophilus* PK's support an extended concerted model including a third, R_2T_2 , state (24,52,58,59).

Changes in the Active Site Due to Allosteric Transition

The purpose of this study was to add to the understanding of allosteric regulation of PK by FBP. The active site, the FBP binding site, and subunit interface(s) are all known to be important to allosteric regulation. Changes caused by FBP binding at the FBP binding site must be responsible for triggering all subsequent allosteric changes. Changes in the active site, resulting in the altered apparent affinities for PEP associated with allosteric regulation of many PK's, must be caused by FBP binding.

Changes in the active site of PK due to binding allosteric effectors have been followed in a number of studies. Recent work by Mesecar *et. al.* has demonstrated that FBP and PEP are coupled to the divalent ion but are not directly coupled to each other (60,61). Distances between the divalent and monovalent cations in the active site change in response to the presence of FBP (62-64). It is important to note that the kinetic response of PK to PEP is dependent on the type of cation present (65,75).

Allosteric Site(s)

At the onset of this study very little was known about the binding site(s) of allosteric effectors or their mechanism(s) of regulating the activity of the protein. However, several studies had investigated the nature of the allosteric activator, fructose-1,6-bisphosphate. Wurster *et al.* used structurally locked sugar-phosphate analogues to determine yeast PK's tautomeric and anomeric specificity for FBP (67). The β -furanose form of FBP was found as the activator. In a similar study Fishbein *et al.* suggested that yeast PK is nonspecific with respect to anomeric configuration of the activator, but that a C-2 hydroxyl is necessary

for activation (68). Speranza *et al.* used FBP analogs to study PK from *E.coli* (69). They concluded that both phosphates were important for binding, but the presence of a cyclic structure was not necessary. Haeckel *et al.* has shown that yeast PK is activated by glucose 1-phosphate, however, no activation was observed by the monophosphate fructose analogs (41).

At pH 6, crystals of cat M1-PK have been generated that contained ADP in a pocket (referred to in the literature as the arginine 42 pocket or the putative ATP binding site) in the region between the A and C domains (70). This might be a site for ATP regulation, but it was ADP, not ATP, that was bound in this pocket. This putative ATP site has often been generalized in the literature to be the allosteric binding site, suggesting that other allosteric effectors bind at this location (34,71,72).

Pyridoxal 5'-phosphate labeling and protection experiments have identified a lysine (equivalent to yeast 406) thought to be important to FBP binding (72,73). A lysine (equivalent to yeast 413) was also identified that was thought to be important to ADP binding at a site distant from the active site (72,73). However, the lysine residues identified are not located in the Arg 42 pocket. An ATP analog has been found to react with a lysine (equivalent to yeast 292) in the region between the A and C domains (74). Again this latter site differs from that labeled as the putative ATP binding site. Results of FBP binding studies using rat liver PK show that ATP has little effect on the binding of FBP, and therefore do not support a common binding site (75). The summary of the literature available at the beginning of this study suggested that the FBP binding site was distinct from the ATP binding site and that both sites were located between the A and C domains.

After the initiation of this study the crystal structure of yeast PK with FBP bound was reported (20). The FBP binding site is completely contained within the C domain. The 6'-phosphate of FBP binds to serine 402, serine 404, and threonine 407 through hydrogen bonds. The 1'-phosphate group of FBP is bound to arginine 459 through a strong

electrostatic interaction. The sugar ring provides additional interactions with tryptophan 452 and backbone atoms of 483 and 491.

Allosteric Message Across C-C Subunit Interfaces

Loss of cooperativity in apparent PEP binding is associated with allosteric regulation of PK by FBP. Since a single PEP binding site is contained in a single subunit of the PK tetramer, cooperativity in apparent PEP binding is dependent on changes at subunit interface(s). Therefore FBP must cause changes in the subunit interface(s) which give rise to the loss in cooperativity in apparent PEP binding.

Allosteric regulation may involve one or both types of subunit contacts. Only 22 amino acids differ between the mammalian M1 and M2 isozymes which demonstrate quite different kinetic and allosteric properties (25). These 22 amino acid differences fall into the C to C subunit contacts (17,56). M1 shows a hyperbolic PEP-dependent kinetic response in the absence of allosteric effectors but can be shifted to a sigmoidal response in the presence of phenylalanine (26). This isozyme can be activated by FBP if it is first inhibited by phenylalanine (26). M1 shows no kinetic response to FBP in the absence of phenylalanine (26). M2 shows a sigmoidal PEP-dependent kinetic response in the absence of effectors but can be shifted to a hyperbolic response in the presence of fructose-1,6-bisphosphate (26). These observations suggest that the two mammalian isozymes can have the same general properties but the equilibrium between the two states is altered due to their 22 amino acid differences. Fluorescence life-times of tryptophan residues in the PK isozymes provide evidence that in the absence of effectors the M1 enzyme exists almost exclusively in the R-state, while the M2 enzyme favors the T-state (26).

Residues that are non-conserved between mammalian M1 and M2 PK isozymes have been probed by mutagenesis. Replacing a cysteine with a leucine (at a position equivalent to yeast 394) causes the sigmoidal shape of M2's PEP dependent kinetic curve, in the absence of activator, to become hyperbolic (76). In the M1 isozyme, replacing an alanine with an arginine (at a position equivalent to yeast 369) shifted the kinetic response to

resemble that of the M2 isozyme (77). Mutations at the C-C interface of yeast and *B. stearothermophilus* isozymes also support the importance of the C-C subunit contact in allosteric regulation (59,78).

Pyruvate kinase from *Zymomonas mobilis* has been cloned and sequenced (36). This isozyme is active as a dimeric enzyme (37). It lacks both homotropic and heterotropic cooperativity (37). Comparing the amino acid sequence of *Z. mobilis* PK with the sequence and structure of yeast PK shows that conserved residues are on the interior of individual subunits as well as at the A-A interface. This suggests that the loss of regulation may be the consequences of changes in the C-C subunit interface contacts (20).

Allosteric Message Across A-A Subunit Interfaces

The differences in kinetic properties of M1 and M2 isozymes and the relatively small sequence differences between them emphasizes the role of the C-C subunit contacts in allosteric regulation. However, it is important to realize that both M1 and M2 isozymes maintain the ability to be regulated by allostery. Only the T to R equilibrium is shifted due to sequence differences (26). Therefore both isozymes have the ability to communicate changes at the C-C subunit interface to the active site. This communication must utilize residues distant from the C-C subunit interface.

There have been only a few studies that have investigated A-A subunit contacts, however the results of these studies indicate that residues at the A-A interface may play important roles in regulation. Lovell *et al.* found that mutating glutamine to asparagine, at a position equivalent to yeast 299, in the A-A interface altered allosteric regulation by ribose-5-phosphate (59). Duplicating an A-A interface mutation found in hemolytic anemia in both M1 and M2 isozymes also caused altered allosteric regulation (79,80).

Allosteric Message within Subunits

The goal of this study was to add to the understanding of allosteric regulation of PK by FBP. The active site, the FBP binding site, and the two types of subunit contacts are all of interest when considering allosteric regulation of PK. In addition, insight concerning

components within a subunit may be gained by comparing different PK structures. The crystal structure of *E. coli* type I PK has been compared with the crystal structures of cat and rabbit M1 PK's (21,81). This comparison must be interpreted with caution since the crystal structures are from enzymes of different species. The *E. coli* structure is considered to represent the low affinity T-state while the mammalian structures represent the high affinity R-state (21,81). The comparison suggests that two types of motions may occur during the T to R transition. The first motion is rotation of both the B and C domains with respect to the A domain within each subunit. This observation agrees well with closure of the B-domain discussed earlier with regard to the active site. The second motion is rotation of each subunit within the tetramer. Using comparison of PK structures, little motion within individual domains is predicted in the T to R transition.

Studies that support motion of the B-domain have already been described with respect to the active site (18,19,66). Salt bridges between the A and C domains and A and B domains have been predicted to be important to regulation of rabbit M1 PK (79) and of *B. stearothersophilus* PK (34), respectively. Mutations in the A-C domain contacts of *T. bruci* also support the role of this region in allosteric regulation (71).

Red Blood Cell Pyruvate Kinase and Hemolytic Anemia

To further identify residues important for PK structure and function, natural mutations of PK reported in the literature were examined. Pyruvate kinase deficiency, first identified by Valentine *et al.*, is now recognized as the most common cause of hereditary nonspherocytic hemolytic anemia (1). Mutations characterized to date represent single amino acid substitutions, splice site mutations, frame shift mutations, and termination mutations (82-86). A great deal could be learned if each of the single amino acid replacement mutations found associated with pyruvate kinase deficiency could be correlated with the activity and allosteric properties of the gene product. In 1979, the International Committee for Standardization in Haematology published standard methods for the analysis of PK protein variants. However, the characterizations that were recommended, and have

since been extensively used, have many shortcomings with respect to identifying properties of individual mutated proteins. The major shortcomings include: no attempt is made to separate PK activity into that contributed by the mutated R-PK and that contributed by M2-PK, which has been shown to express in PK deficient erythrocytes (5); in heterozygous mutations the two individual PK variants have not been separated; also, high reticulocyte counts may alter the activity values (87). With these shortcomings, most information on PK activity from pyruvate kinase deficiency patients is not useful for biochemical description of molecular effects of the individual amino acid substitutions.

However, if a patient exhibits pyruvate kinase deficiency, one can assume a functional mutation has occurred. Therefore, pyruvate kinase deficiency acts as a screen (PKD-screen) to identify residues important to the structure/function of PK. A similar approach has been used to identify important residues for site directed mutagenesis in rabbit muscle (80). Table 1 gives a current list of single amino acid replacements that cause hemolytic anemia.

The PKD-screen does not identify the function of mutated residues. An alignment of PK sequences was compiled and is shown in the Appendix (Figure A1). Amino acid sequences of PK's with many different types of regulation are represented, including some PK's with no known cooperative or allosteric regulation. If a residue is highly conserved it is likely to have common function in all PK's, i.e. active site or structure. Less conserved residues are more likely to be involved in roles that are not common to all isozymes, such as regulation. In an effort to identify amino acid residues important to regulation, hemolytic anemia mutations were separated into two groups (Figures 3 and 4). Group 1 contains residue positions that were highly conserved for function.

The positions of amino acids in the two groups are highlighted in the yeast PK structure in Figures 3 and 4 (20). Residues in the FBP binding site are identified in group II. Active site residues are identified in group I. Since residues in the FBP binding site and residues in the active site are identified in the predicted groups, the logic behind this screen

Table 1. A Current List of Sequenced Human Red Blood Cell PK Single Amino Acid Replacement Mutations Associated with Hemolytic Anemia. This list is restricted to mutations causing single amino acid substitutions. Mutations listed are from Baronciani *et al.*, Kanno *et al.*, Demina *et al.*, Cohen-Solal *et al.* and references therein (82-85). Structural assignments are based on the rabbit muscle PK structure (17).

<u>Mutation</u>	<u>Yeast#</u>	<u>2nd Structure</u>	<u>Super 2nd Structure</u>	<u>Domain</u>	<u>Specific Site Domain/tetramer</u>	<u>Amino Acid Conservation</u>
S80P	13	-		N	A-A SUB CONT	Group I
M107T	40	H3	β-BARREL	A		Group I
A115P	48	S2	β-BARREL	A		Group I
S120F	53	-		A	ACTIVE SITE	Group I
S130W	63	H4	β-BARREL	A		Group II
V134D	67	H4	β-BARREL	A		Group I
L155P	83	S3	β-BARREL	A		Group I
G159V	87	-		A		Group I
R163C	91	S4		B	ACTIVE SITE	Group I
E172Q	98	-		B		Group II
G263R	190	-		A		Group II
G263W	190	-		A		Group II
G275R	202	H5	β-BARREL	A		Group I
D281N	208	-		A		Group I
F287V	214	-		A	ACTIVE SITE	Group I
A295V	222	H6	β-BARREL	A		Group II
I310N	237	S14	β-BARREL	A		Group I
I314T	241	S14	β-BARREL	A	ACTIVE SITE	Group I
E315K	242	-		A	ACTIVE SITE	Group I
D331N	258	-		A	A-C DOM CONT	Group I
D331E	258	-		A	A-C DOM CONT	Group I
G332S	259	S15	β-BARREL	A		Group I
A336S	263	S15	β-BARREL	A		Group I
R337P	264	H9	β-BARREL	A	ACTIVE SITE A-ACONT	Group I
R337Q	264	H9	β-BARREL	A	ACTIVE SITE A-ACONT	Group I
D339Q	266	H9	β-BARREL	A	ACTIVE SITE	Group I
G341A	268	H9	β-BARREL	A	ACTIVE SITE A-ACONT	Group I
G341D	268	H9	β-BARREL	A	ACTIVE SITE A-ACONT	Group I
I342F	269	H9	β-BARREL	A	ACTIVE SITE A-ACONT	Group I
K348N	275	H10	β-BARREL	A	A-A SUB CONT	Group II
A352D	279	H10	β-BARREL	A	A-A SUB CONT	Group II
I357T	284	H10	β-BARREL	A	A-A SUB CONT	Group I
R359C	286	H10	β-BARREL	A	A-A SUB CONT	Group I
R359H	286	H10	β-BARREL	A	A-A SUB CONT	Group I
N361D	288	H10	β-BARREL	A	A-A SUB CONT	Group I
G364D	291	-		A	A-C DOM CONT	Group I
V368F	295	S16	β-BARREL	A		Group I
S376I	303	-		A	A-A SUB CONT	Group I
T384M	311	-		A	A-A SUB CONT	Group I
D390N	317	H11	β-BARREL	A	A-A SUB CONT	Group I
A392T	319	H11	β-BARREL	A	A-A SUB CONT	Group I
N393S	320	H11	β-BARREL	A	A-A SUB CONT	Group I
N393K	320	H11	β-BARREL	A	A-A SUB CONT	Group I
T408I	335	-		A		Group I
Q421K	348	H12	β-BARREL	A		Group II
R426W	353	H12	β-BARREL	A		Group II
R426Q	353	H12	β-BARREL	A		Group II

<u>Mutation</u>	<u>Yeast#</u>	<u>2nd</u> <u>Structure</u>	<u>Super 2nd</u> <u>Structure</u>	<u>Domain</u>	<u>Specific Site</u> <u>Domain/tetramer</u>	<u>Amino Acid</u> <u>Conservation</u>
E427D	354	H12	β -BARREL	A	A-A SUB CONT	Group II
A431T	358	H12	β -BARREL	A	A-A SUB CONT	Group II
G458D	385	H14		C	C-C SUB CONT	Group II
A459V	386	H14		C	C-C SUB CONT	Group II
V460M	387	H14		C	C-C SUB CONT	Group II
A468V	395	-		C	C-C SUB CONT	Group II
R479H	406	H15		C	FBPSITE A-C CONT	Group II
S485F	412	H15		C	A-C DOM CONT	Group II
R486W	413	H15		C	A-C DOM CONT	Group I
R490W	417	-		C		Group II
A495T	422	S19		C		Group II
A495V	422	S19		C		Group II
R498C	425	-		C	FBP SITE	Group II
R498H	425	-		C	FBP SITE	Group II
R504L	431	H16		C		Group II
R510Q	437	-		C		Group II
R518S	445	-		C		Group II
R532W	459	H17		C	FBP SITE	Group II
R532Q	459	H17		C	FBP SITE	Group II
V552M	479	S21		C	C-C SUB CONT	Group I
R559G	486	-		C	C-C SUB CONT	Group II
N566K	493	-		C	C-C SUB CONT	Group I

appears to be valid. Group II contains residues in the C domain, in the C-C subunit contacts, and in the A-A subunit contacts. Only 2 of 5 A-C domain contacts are identified in group II. These conclusions support the hypothesis that both the C-C and A-A domain contacts are important in regulation. However, involvement of A-C domain contacts in regulation is not supported.

Several other observations may prove to be valuable to the study of PK. Forty-six mutations were found in the A domain, 20 in the C domain, 2 in the B domain, and only 1 mutation in the N-terminus domain. The limited number of mutations found in the B domain suggest that this domain acts as a scaffold to hold active site residues in place and mutations in this scaffold do not greatly influence activity. Due to the large differences in the N-terminus between isozymes, this domain might have predicted to be involved in regulation.

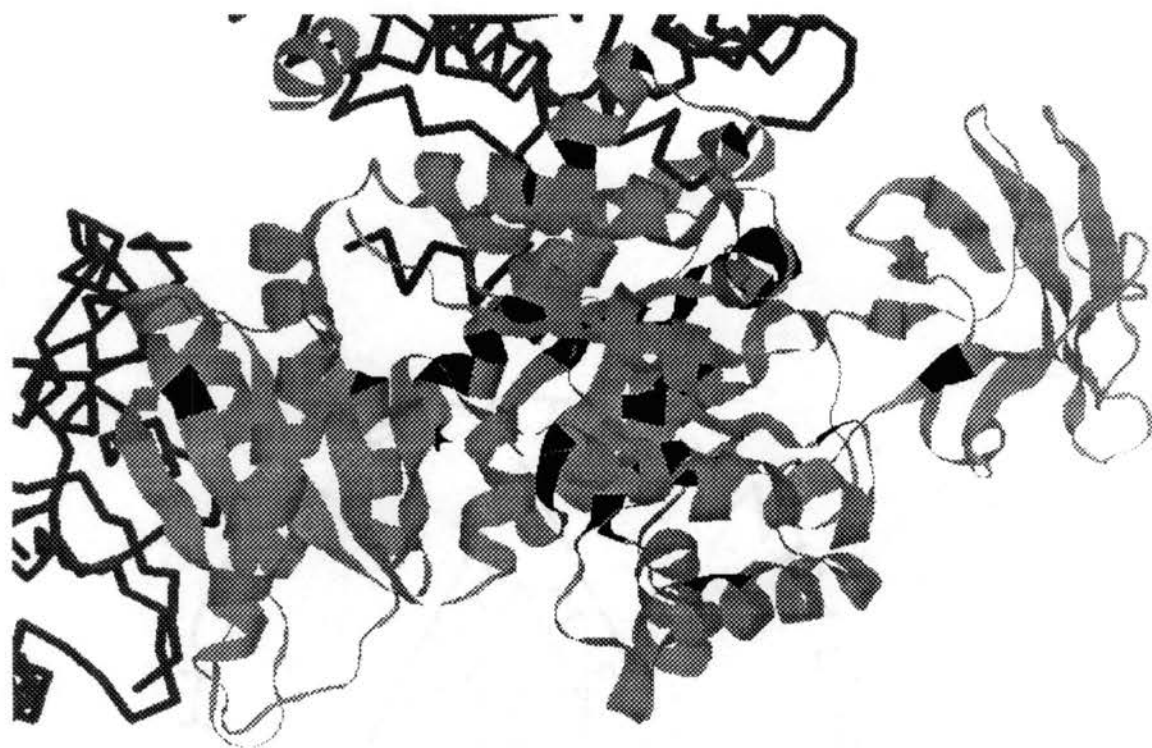
Helix regions contain the greatest number of mutations of any secondary structure. Together helix-9, helix-10, helix-11, and helix-12 hold the largest concentration of mutations. These secondary structures are both part of the β -barrel super secondary structure and are involved in A-A subunit contacts. Seven mutations are in the C-C subunit contacts.

Arginines are the most mutated residue in the screening (16 out of 59). This may show arginines importance in the structure/function or just that they are in positions that can not easily handle a different amino acid. If the positive charge of arginine is indeed the major factor for this observation then a similar observation should be made for lysine. On the contrary, lysine is not observed as a highly mutated residue.

Mutations that cause insertion or deletion of only a few amino acids may provide structural/functional information in addition to that provided by single amino acid replacement mutations. Table 2 lists mutations identified with pyruvate kinase deficiency that cause deletion or insertions of less than 3 amino acids.

Figure 3. Yeast PK with the Positions of Group 1 Red Blood Cell Mutations Highlighted. Group 1 contains residue positions that were highly conserved for function in the sequence alignment in Figure AI. The subunit of interest is shown in light gray with Group I red blood cell mutations shown in black. Neighboring subunits are shown in dark gray.

Figure 4. Yeast PK with the Positions of Group 2 Red Blood Cell Mutations Highlighted. Group 2 contains residue positions that were not as highly conserved for function as residue positions in Group 1 in the sequence alignment in Figure AI. The subunit of interest is shown in light gray with Group II red blood cell mutations shown in black. Neighboring subunits are shown in dark gray.



Along the same argument for the use of pyruvate kinase deficiency mutations as a screen for identification of structural/functional mutations, mutations that affect other PK isozymes may also provide structural/functional insights. Table 3 lists single amino acid mutations, other than those created by site directed mutageneses or those associated with pyruvate kinase deficiency in humans. Included in the list are two yeast mutants, G268D and S70F (88). G268D causes loss of PK activity in yeast strain *pyk 1-5* and S70F causes a temperature sensitive mutation in the yeast strain *cdc19* (88-92). Also included is the mutation responsible for pyruvate kinase deficiency in mice, G338D and a mutation causing increased ATP levels in human red blood cells, K37Q, (10,93). The two yeast mutations and the mouse mutation all occur in helix regions of the A domain's β -barrel. The human mutation is in the N-terminus domain.

Hypothesis

The purpose of this study was to add to the understanding of allosteric regulation of yeast PK by FBP. When this study was initiated, two positively charged pockets at the A-C domain interface were believed to be important in allosteric regulation. One of these two pockets was hypothesized to be the FBP binding site. Site directed mutagenesis of positive residues within the two pockets was used to test the two sites as possible FBP binding sites and their importance in allosteric regulation. After this study was initiated, the true FBP binding site was identified within the C domain (20). Specific residues within the FBP binding site were believed to be responsible for triggering an allosteric response. Site directed mutagenesis within the FBP binding site was used to test this hypothesis. Since the cooperative, sigmoidal response to PEP is lost during allosteric activation by FBP, subunit contacts were hypothesized to be important in allosteric regulation. Mutations within both the A-A and C-C subunit interfaces were created to test this possibility.

<u>Mutation</u>	<u>Yeast#</u>	<u>2nd Structure</u>	<u>Super 2nd Structure</u>	<u>Domain</u>	<u>Specific Site Domain/tetramer</u>
95/96 del G and P	28/29			A	-
131 del of I	64	H4	β -barrel	A	-
354 del of K	281	H10	β -barrel	A	A-A SUB CONT
221 D 222 ins	147			B	-
401 C 402 ins	328	S17	β -barrel	A	-
401 S 402 ins	328	S17	β -barrel	A	-

Table 2. A Current List of Sequenced Human Red Blood Cell PK Mutations that Delete or Insert Three Amino Acids or Less. Mutations are referenced from Baronciani *et al.*, Kanno *et al.*, Lenzner *et al.*, and references therein (84, 85, 147). Structural assignments are based on the rabbit muscle PK structure (17).

<u>Mutation</u>	<u>Yeast#</u>	<u>2nd Structure</u>	<u>Super 2nd Structure</u>	<u>Domain</u>	<u>Specific Site Domain/tetramer</u>	<u>Reference</u>
Human-R G37Q	None	-		N		(94)
Mouse-R G338D	265	H9	β -BARREL	A	ACTIVE SITE A-ACONT	(10)
Yeast ypk1-5 G268D	268	H9	β -BARREL	A	ACTIVE SITE A-ACONT	(89)
Yeast cdc19 S70F	70	H4	β -BARREL	A		This study

Table 3. A Current List of Sequenced, Naturally Occurring Single Amino Acid Replacement PK Mutations. This list includes mutations other than those identified with human pyruvate kinase deficiency. Structural assignments are based on the rabbit muscle PK structure (17).

MATERIALS AND METHODS

Computer Modeling of Fructose-1,6-Bisphosphate

In order to locate possible binding sites between FBP and yeast PK, types of bonds FBP is capable of forming was assessed. John Carment built a computer model of the β -furanose form of FBP. The Builder module in Insight II Version 2.3.0 (Biosym Technologies, 1993, 9685 Scranton Road, San Diego, CA 92121-2777) was used to construct the model. This model was minimized with Discover Version 2.9.5 (Biosym Technologies, 1994, 9685 Scranton Road, San Diego, CA 92121-4778). A hydrophilic/hydrophobic grid map was calculated by HINT! (Glen E. Kellogg and Donald J. Abraham, Dept. of Medicinal Chem., Virginia Commonwealth Univ., Richmond, VA 23298-0540) for the energetically minimized β -FBP furanose molecule. Due to general chemical knowledge of phosphated sugars, charge maps were not calculated for the minimized FBP structure.

Computer Modeling of Yeast Pyruvate Kinase

A yeast PK molecular structural model was needed to assist in possible FBP binding sites identification. Therefore, a yeast PK model was built using Insight II's Homology module Version 2.3.0 (Biosym Technologies, 1993, 9685 Scranton Road, San Diego, CA 92121-2777) by amino acid replacement into the coordinates of the rabbit muscle PK enzyme (17). After substitutions were made, amino acid side chains that conflicted in spatial orientation were rotated using the program's preset "highest occurrence" positions. The most accommodating orientation from these preset positions was used in the final yeast PK model. Differences in the length of amino acid sequence

between rabbit muscle PK and yeast PK cause either the lack of (Gaps) or addition of (Insertions) amino acids at given positions. These gaps and inserts can cause backbone rearrangement that must be accounted for in a model if the rearrangements could influence results of the study. Gaps and inserts were distant from the sites of interest in this study. Therefore no effort was made to correct gaps and inserts in the yeast PK model. As a control, all experiments using the yeast PK model were repeated using the rabbit muscle PK model (17). Similar results were found in both models. Since the hydrophilic/hydrophobic grid map of FBP indicated that most of FBP is hydrophilic, charge interactions would be expected to be most important in FBP binding to yeast PK, and a hydrophilic/hydrophobic grid map was not calculated for yeast PK.

Using the yeast PK model, a search was made for highly positive charged pockets that were solvent accessible. GRASP (Nicholls, A. 1993, GRASP: Graphical Representation and Analysis of Surface Properties, Columbia University, New York, NY) was used to generate a surface charge map of the yeast PK model as well as the rabbit M1 model.

Bacterial Growth and Transformation

Bacterial growth plates were made by combining 10 g bacto-peptone (Difco Laboratories, Detroit, MI), 5 g yeast extract (Difco Laboratories, Detroit, MI), 5 g NaCl, 15 g agar and 1 L H₂O. Ampicillin or tetracycline was added after the media was autoclaved to 100 mg/L or 10 mg/L respectively. Ten g of yeast extract, 20 g bacto-peptone, 20 g agar and 900 ml of H₂O were combined and autoclaved and then mixed with 50 ml of sterile 40% w/v dextrose to make YEPD plate media. To make YEPAG, 10 g of yeast extract, 20 g bacto peptone, 20 g agar, and 10 ml of glycerol and 900 ml of H₂O were mixed, autoclaved, and combined with 15 ml of ethanol. SOC media was made according to Sambrook *et al.* (94). All liquid medias were prepared identical to plate media, without the addition of agar.

All bacterial transformations in this study were completed in 1.5 ml microfuge tubes. Because these tubes have thicker walls than other tubes more commonly used in transformations, increased heatshock times were required to maintain transformation

efficiency. Mut S *E. coli* was heat shocked for 70 sec at 42°C. All other bacterial transformations were heat shocked for 90 sec at 42°C.

Mutagenesis

Site directed mutagenesis was used as probing technique to identify residues of importance for FBP binding and the allosteric regulation by FBP. Due to the low transformation efficiency of the pPYK101 (a yEP24 based shuttle vector; Figure 5) mutagenesis efforts within this plasmid were unsuccessful. After extensive efforts to circumvent these difficulties, this mutagenesis protocol was abandoned in favor of using a commercial mutagenesis kit.

Mutations were made using the Altered Sites II *in vitro* Mutagenesis System from Promega (Promega, Madison, WI). This kit utilizes pAlter as a plasmid and therefore the PK insert (containing the yeast PK promoter, gene, poly-A tail, and additional uncharacterized DNA) was subcloned into this plasmid (Figure 6). The plasmid, pAlter, was digested by combining 1 µl (1 µg/µl) pAlter with 0.4 µl React 3 10x buffer (Gibco BRL Life Technologies, Rockville, MD), 2.2 µl of H₂O, and 0.4 µl of *Bam*HI (Gibco BRL Life Technologies, Rockville, MD). After incubating the reaction for 2 hr at 37°C, 1 µl of 10x phosphatase buffer (Promega, Madison, WI), 3.5 µl of H₂O, and 1.5 µl alkaline phosphatase (Promega, Madison, WI) were added in order to phosphatase the cut vector. The reaction was incubated for 1.5 hr at 37°C. The reaction mix was mixed 1:1 with phenol/chloroform/isoamyl alcohol, vortexed briefly, and microfuged for 2 min. The top aqueous layer was removed and combined with an equal volume of 4 M ammonium acetate. The new volume was mixed with 2.5 times the new volume of ethanol, and placed at -80°C for 30 min. The sample was then microfuged, the supernatant removed, and the pellet dried. The pellet was resuspended in 10 µl of H₂O. Since a 50 µg/ml solution of double-stranded DNA gives an absorbance of 1 at 260 nm, absorbance at 260 nm was used to calculate DNA concentration (94).

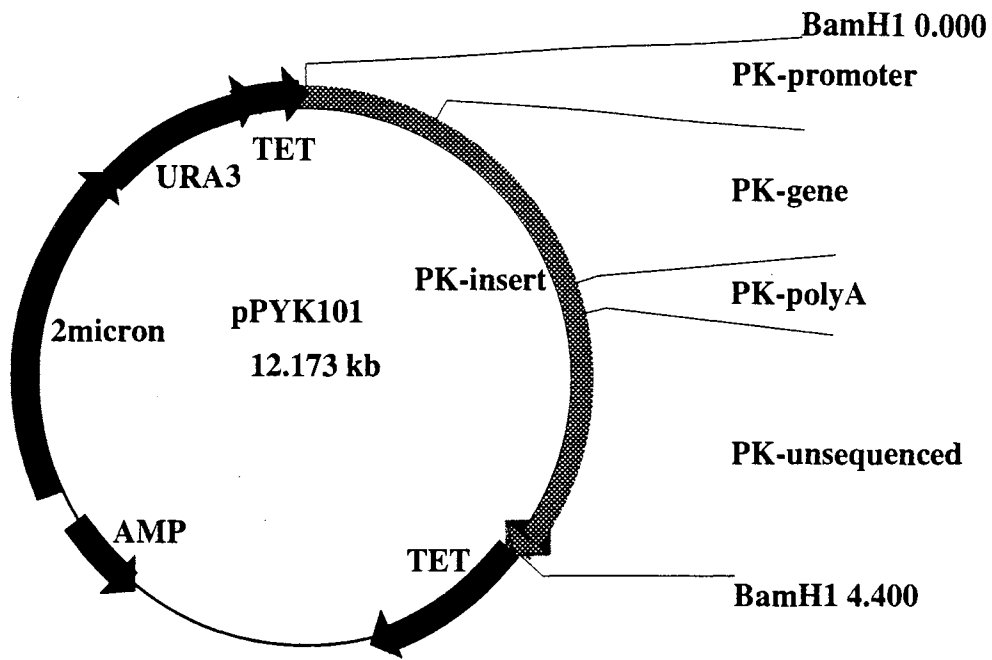


Figure 5. Vector Circle Maps of pPYK101. The PK insert contains the PK promoter, PK coding region, PK poly-A tail, and additional unsequenced DNA. pPYK101 was a gift from Dr. Patricia Tekamp-Olson (96).

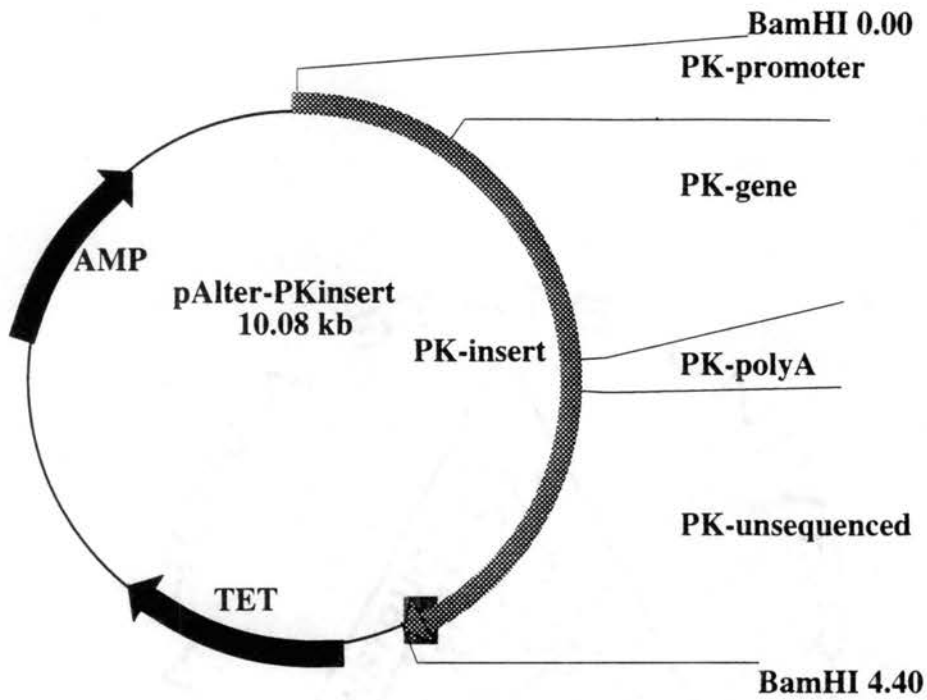


Figure 6. Vector Circle Maps of pAlter (Promega) with PK Insert. The PK insert, containing the PK promoter, PK coding region, PK poly-A tail, and additional unsequenced DNA, was subcloned from pPYK101. pPYK101 was a gift from Dr. Patricia Tekamp-Olson (96).

In order to isolate the PK insert, 25 μl of 1 $\mu\text{g}/\mu\text{l}$ pPYK101 (a kind gift from Tekamp-Olson; (95)) was combined with 3.5 μl of React 3 10x buffer (Gibco BRL Life Technologies, Rockville, MD) and 65 units of *Bam*HI (Gibco BRL Life Technologies, Rockville, MD). The reaction mix was incubated at 37°C for 2 hr. Four μl of DNA loading buffer (50% v/v glycerol, 0.1M EDTA, 0.2% bromophenol blue) was added to the mix and the sample was separated on a 0.9% agarose TAE gel according to Sambrook *et al.* (94). After the dye front reached the bottom on the gel, the gel was stained with ethidium bromide. The 4.4 kb band was cut out with a razor blade. Qiagen's gel extraction kit (Qiagen, Valencia, CA), used according to the manufacture's instructions, was used to isolate the DNA from the gel slice. Absorbance at 260 nm was used to calculate DNA concentration.

For ligation of the PK insert into pAlter, 0.32 μl of cut, phosphatased pAlter (0.62 $\mu\text{g}/\mu\text{l}$), 11.5 μl of cut, isolated PK insert (0.025 $\mu\text{g}/\mu\text{l}$), and 4 μl of H₂O were combined and incubated at 45°C for 5 min. Two μl of ligase buffer (Promega, Madison, WI) and 2 μl of ligase (Promega, Madison, WI) were then added to the ligation reaction. The reaction was incubated at 14°C overnight.

After the ligation reaction was completed, the entire reaction was combined with 100 μl of freshly prepared, competent JM109 cells (Promega, Madison, WI). The cells were prepared according to the protocol provided in the Altered Sites II kit manual. The cells were transformed according to the transformation protocol for JM109 cells provided in the Altered Sites II kit manual. However, only 200 μl of SOC media were added during the procedure, and all of the transformed cell mix was plated onto bacteria growth plate with tetracycline, 5-bromo-4-chloro-3-indolyl- β -D-galactoside, and isopropylthio- β -D-galactoside. Plates were incubated in the dark at 37°C overnight. White colonies were grown in 5 ml bacteria growth culture with tetracycline, at 37°C overnight. Plasmid from cultures were purified using Qiagen spin prep's (Qiagen, Valencia, CA) according to manufacture's instructions.

To determine proper size and orientation of insertions, purified plasmid was restricted in reactions containing 6 μ l DNA, 1 μ l restriction buffer, and 1 μ l of each restriction enzyme used. Reactions were incubated at the temperatures and times recommended by the manufacture for the individual enzyme. *Bam*HI, *Hind*III, and *Bst*XI used in size/orientation determination were obtained from Gibco (Gibco BRL Life Technologies, Rockville, MD). Reaction mixes were separated on a 0.9% agarose gel (Figure 7).

Mutagenesis in the pAlter clones was carried out according to the manufacturer's instructions, with the exception of Qiagen Spin prep DNA isolation (Qiagen, Valencia, CA). Denatured DNA template was combined with a kinased mutagenesis primer and repair and/or knockout primers provided with the kit. All of the designed mutations were obtained using the wild type gene as an initial template with the exception of T403E. Multiple tries to obtain the T403E mutation using the wild type gene template were unsuccessful. The mutation was obtained using the mutated T403K gene as a template. Mutagenesis primers were made by the Oklahoma State University Recombinant DNA/Protein Resource Facility. DNA sequence surrounding target codons caused unfavorable primer design in some mutagenesis primers. In these cases mutations in addition to the desired codon switch were created which improved primer design without changing amino acid sequence. The primers were annealed to the template, and then elongated and ligated.

The mutation reactions were transformed into ES1301 competent Mut S *E. coli* (Promega, Madison, WI) and inoculated onto bacteria growth media with the appropriate antibiotic to select for the newly created mutant strand of DNA. After the *E. coli* grew overnight, plasmid DNA was isolated using Qiagen Spin preps (Qiagen, Valencia, CA). The plasmid DNA was then transformed into JM109 cells and plated on bacteria growth plates with the appropriate antibiotic for overnight growth. Single colonies were selected and grown in 5 ml mini-cultures overnight. Plasmid DNA was isolated using Quiagen spin preps (Qiagen, Valencia, CA) according to the manufacture's instructions. The DNA was

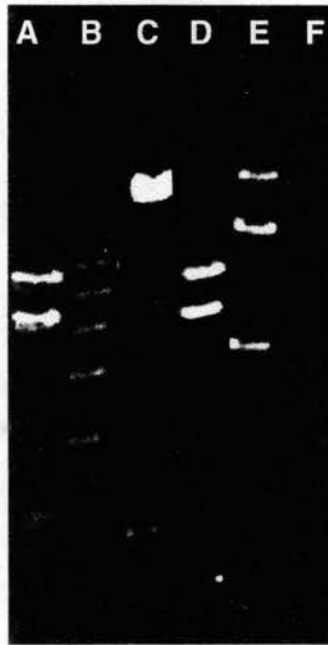


Figure 7. Agarose Gel Electrophoresis of DNA from Restriction Digests of pAlter-PK Insert Constructs. Lanes B and F are a one Kb ladder. Lane A is sample 1 restricted with BamHI. Lane C is sample 1 restricted with *HindIII* and *BstXI*. Lane D is sample 2 restricted with *BamHI*. Lane E is sample 2 restricted with *HindIII* and *BstXI*. *BamHI* restriction of both plasmids confirms proper sizes for insert and plasmid at 4.4 Kb and 5.68, respectively. *HindIII* cuts the vector and *BstXI* cuts the insert so that restriction patterns reveal how close the two restriction sites are. Lane C shows that sample 1 has the insert orientated in the forward direction. Lane E shows that sample 2 has the insert orientated in the reverse direction. Sample 1 was used for future work with this plasmid.

sequenced across the site of the desired mutation. Colonies that contained the correct mutation were stored by combining 1:1 with 30% sterile glycerol and frozen at -80°C.

List of Mutagenesis Primers:

	5'	3'
K292Q	GCTGGTCAGCCAGTTATCTGTGC	
K413Q	GTTTCCCAGTACAGACC	
K236Q	CGTCCAGATCATTGTCAAGATTG	
Y436F	TGCTAGATTCTCTCACTTGTTTCAGAGGTGTCTTCC	
R77Q	ATTGTACCCAGGTCAACCATTG	
R19Q	GTTCTGACTTGCAGAGAACCTCCATCATTGGTAC	
R409Q	GTACCACCCCACAATTAGTTTCCAAGTACAGACC	
T406R	CGGTAGAACCCCAAGATTGGTTTCCAAGTACAGAC	
K236E	CGTCGAGATCATTGTCAAGATTGAAAACC	
K292E	GGTGAGCCAGTTATCTGTGCTACC	
R409E	GTACCACCCCAGAATTGGTTTCCAAGTACAG	
K413E	GGTTTCCGAGTACAGACCAAACGTCCAATC	
R415Q	GTACCAAACCAAACGTCCAATCATCTTG	
Y436S	TGCTAGATTCTCTCACTTGTCAGAGGTGTCTTCC	
Q299N	GCCTGTTATCTGTGCTACTAATATGTTGGAATC	
R459Q	GGACTGATGATGTAGAAGCCCAGATCAAC	
E392A	TCCGCTGTCGCTGCTGTATTCGCTCAAAG	
R369A	CAAAC TACGATGATATGGCAAACGTACTC	
T311M	CCCAAGACCAATGAGAGCAGAAGTTCCGATG	
T403E	AGGCTATCATTGTCTTGTCCAGAATCGGGCACCAC	
T403K	AGGCTATCATTGTCTTGTCCAGAATCGGGCACCAC	
A458R	GGACTGATGATGTAGAACGCCGTATCAAC	

List of Sequencing Primers designed with SoYeon Park:

PRIMER	5'	3'	POSITION #
(Tekamp-Olson sequence)			
+1	GGATCCTGCTTGTGATGTCTTCCAAGTG	587	
+2	AAGACACCAATCAA	877	
+3	CAAGAACATCACCA	1301	
+4	TCCCAGCCCCAGAAGTC		1723
+5	CGTGTCGCTGCTGTT	2064	
+6	TCAAGAACGGTGTCCAC		1519
+7	CTCTCACGGTTCTTACG		1067
+8	ACCAGATGCCCAAGAGC		2181
+9	CATGGTCCCCTTTCA	769	
+10	CCAAGGTCCAGAAATC		1165
-1	GGATCCGATTATCTTGCGATGGGAGG		2669
-2	ACGGTAGAGACTTGC	2394	
-3	CGAATGGGAAGACACCT		2220
-4	CGGTTTCAGCCATAGTG		1941
-5	GTGGACACCGTTCCTTGA		1519
-6	GGTGGGATTGGGTAGTC		1209
-7	GGCAAGTAAGCGATAGC		1983
-8	TGGGGCTGGGATTTCAA		1715
-9	ACGACAATTGGAGAC	2589	
-10	CTACCAGCGGAGATGAC		1317

Subcloning into an Expression Vector

In addition to difficulties in mutating the PK gene within the yEP24-based pPYK101, subcloning of mutated PK genes from pAlter into yEP24 was unsuccessful. The reasons for this difficulty are still unclear. However, low transformation efficiency of this plasmid, size of insert, and non-directional cloning may have contributed to this failure.

PCR was used to add a new restriction site to allow for directional cloning. Desired PK mutants in pAlter were used as templates in PCR reactions using Gibco's PCR Reagent System (Gibco BRL Life Technologies, Rockville, MD). The upstream primer included the *Bam*HI site that was used to ligate the PK insert into the pAlter vector. The down stream primer was at position 2853 of the Tekamp-Olson sequence, and included a *Hind*III restriction site. The down stream primer position was chosen to include the poly-A tail but not include the unsequenced portion of the Tekamp-Olson insert. The sequence of each primer and the position of its components are shown below. The PCR reaction mixes and conditions are also listed. Since the PCR products have unique *Bam*HI and *Hind*III sites,

the products could be directionally cloned into the pYES2 vector (Invitrogen, Carlsbad, CA) (Figure 8).

PCR Primer Sequences:

Upstream-

5'CTCGGGGATCCAAATGTAAATAACAATCAC3'
*Bam*HI

Downstream-

5'AATATAAGCTTCCACCAAACGAAGGCCAGAAGC3'
*Hind*III

Primer Mix:

3.6 µl of the upstream primer (1.04 µg/µl)
3.4 µl of the down stream primer (1.05 µg/µl)
dilute to a total volume of 40 µl with H₂O

PCR reaction mix:

10 µl 10x PCR buffer minus MgCl₂
3 µl 50 mM MgCl₂
2 µl 10 mM dNTP's
2 µl DNA template or 1 µl kit control template
5 µl primer mix from above or 5 µl kit control primer mix
dilute to a total volume of 100 µl with H₂O
add 0.5 µl Taq DNA polymerase

PCR reaction times:

Pre-incubate at 94°C for 3 minutes
PCR cycle for 35 cycles where a cycle is:
Denature step at 94°C for 45 seconds
Annealing step at 55°C for 30 seconds
Extension step at 72°C for 2 minutes and 30 seconds
post incubation at 72°C for 10 minutes

For ligation of the PCR product into pYES2, the PCR product was purified using Quiagen's PCR purification kit (Quiagen, Valencia, CA) according to the manufacturer's protocol. Purified PCR products were cleaved at the newly created *Bam*HI and *Hind*III sites. Fifty µl of purified PCR product was combined with 5 µl React 2 (Gibco BRL Life Technologies, Rockville, MD), 2.5 µl *Hind*III (Gibco BRL Life Technologies, Rockville, MD), and 2.5 µl *Bam*HI (Gibco BRL Life Technologies, Rockville, MD) and incubated at 37°C for 2 to 6 hours. In like manner 20 µl of pYES2 was combined with 2.5 µl of React

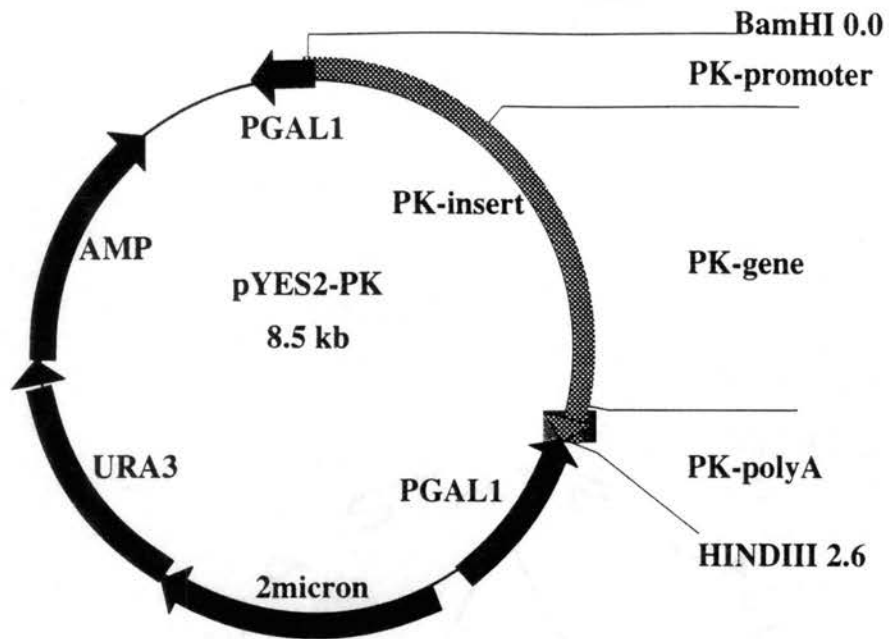


Figure 8. Vector Circle Maps of pYES2 (Invetrogen) with PK Insert. The PK insert contains the PK promoter, PK coding region, and PK poly-A tail.

2 (Gibco BRL Life Technologies, Rockville, MD), 1.25 μ l of *Hind*III (Gibco BRL Life Technologies, Rockville, MD), and 1.25 μ l of *Bam*HI (Gibco BRL Life Technologies, Rockville, MD) and incubated 6 hr to overnight at 37°C.

Restriction reactions were mixed 1:1 with phenol/chloroform/isoamyl alcohol (25/24/1). The samples were briefly vortexed and the microfuged for 2 min. The top, aqueous layer was removed and combined with an equal volume of 4 M ammonium acetate. Using the new total volume, 2.5 times the total volume of 95% ethanol was added to the sample. After 15 min at -80°C, the samples were microfuged for 10 min. The supernatant was removed and the microfuge tubes were inverted on a paper-towel and allowed to dry. The pellet was resuspended in 15 μ l of H₂O.

After digestion, the pYES2 was purified by the use of Qiagen's PCR purification kit (Qiagen, Valencia, CA), used according to the manufacturer's protocol. The vector was further purified using a phenol/chloroform/isoamyl alcohol extraction followed by ethanol precipitation, as described above for purification of the inserts. The dried pellet was resuspended in 25 μ l of H₂O.

A₂₆₀ of the DNA samples were used to calculate the DNA concentration. For ligation, approximately 100 ng of *Bam*HI/*Hind*III cut pYES2 and 100 ng of *Bam*HI/*Hind*III cut PCR product were combined in a total of 8 μ l. Two μ l were removed for visualization on an agarose gel. The remaining 6 μ l of ligation reaction was incubated at 45°C for 5 min and then cooled to 15°C. After cooling, 0.75 μ l of ligase buffer (Promega, Madison, WI) and 0.6 μ l of ligase were added to the reaction. The reaction was then incubated at 15°C overnight.

Two and one half μ l of the ligation reaction were used to transform 50 μ l of DH5 α library efficiency competent cells (Gibco BRL Life Technologies, Rockville, MD). Cells were thawed on ice. Immediately after thawing, cells were allocated 50 μ l /pre-chilled 1.5 ml microfuge tube. To one 50 μ l allocate of cells, 2.5 μ l of ligation reaction was added. A flicking motion was used to mix the samples, and then they were placed on ice for 30 min.

After the ice incubation, the samples were heat shocked at 42°C for 90 sec. The samples were immediately placed on ice for 2 min. Two hundred µl of SOC or bacteria growth media without antibiotics was added to each sample. Samples were incubated at 37°C for one hr. The samples were then transferred onto bacteria growth plates with ampicillin, and spread using a sterile glass rod. Plates were incubated at 37°C for 18 hr.

Screening for Expression Construct

Individual colonies were selected from 18 hr plates and used to inoculate 5 ml mini-cultures of bacteria growth media with ampicillin. Mini-cultures were grown over night at 37°C. Mini-cultures were screened using a modified phenol quick screen (96). In a 1.5 µl microfuge, 750 µl of culture was pelleted, and the supernatant removed. To the pellet, 8µl of DNA loading buffer (50% v/v glycerol, 0.1M EDTA, 0.2% bromophenol blue) was added while stirring the pellet with the pipette tip. The sample was briefly vortexed. Twenty-five µl of phenol/chloroform/isoamyl alcohol (25/24/1) was added and the sample was vortexed. The samples were microfuged for 5 min. Three layers were visible, an aqueous layer on top, a solid white intermediate layer, and a phenol layer on bottom. For each sample, 8 µl of the top aqueous layer was removed and loaded directly into a well of a 0.9% agarose gel. A one kb ladder and uncut, supercoiled vector were loaded as controls. The gel was stained with ethidium bromide after the dye front reached the bottom of the gel.

An example of a quick screen gel is shown in Figure 9. The largest band (above 12 kb) is genomic DNA, while the two low molecular weight (below 4.1 kb) bands are RNA bands. The intermediate bands are supercoiled plasmid DNA's. Comparisons of screened samples were compared with the uncut, supercoiled vector to see which samples contain plasmids larger than the vector alone. This screening method does not give detailed information about the insert.

Quiagen spin prep columns (Quiagen, Valencia, CA) were used to purify plasmid DNA from colonies with proper sized plasmid according to the quick screen. The purified plasmid was either stored at -20°C until sequenced or immediately sequenced. An

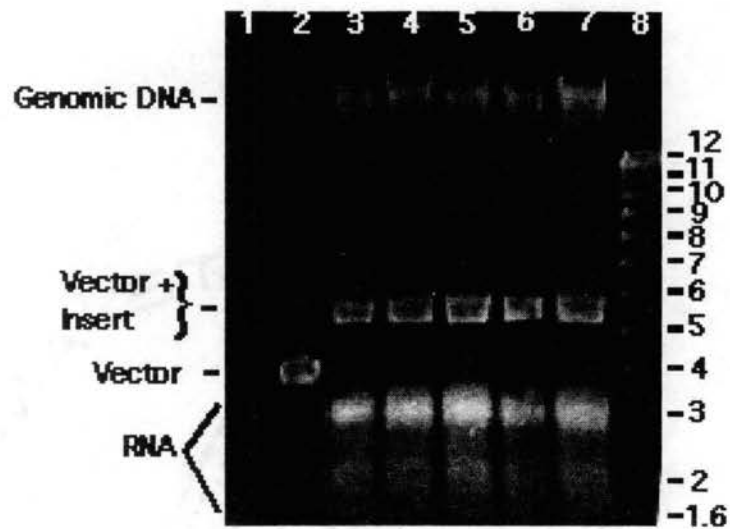


Figure 9. Agarose Gel Electrophoresis of DNA from a Quick Screen. Lanes 1 and 8 are 1kb ladder standards. Lane 2 is uncut pYES2 (Promega) without an insert. Lanes 3-7 are quick screen DNA preps from mini-cultures of single colonies transformed with pYES2/PK insert ligation reaction. DNA is supercoiled and therefore comparison with supercoiled vector alone was used to identify expression vectors with inserts. Two bands below the 4.1 kb standard are RNA and the band above the 12 kb standard is genomic DNA. Bands beneath the genomic DNA and above the RNA are supercoiled plasmid bands.

automated sequencing service offered by the Oklahoma State University Recombinant DNA/Protein Resource Facility was utilized in sequencing DNA of the mutants. A sequencing primer selected to sequence across the mutated site was used for the sequencing. A sample of the mini-cultures that contained correct mutations was mixed 1:1 with sterile 30% glycerol and stored at -80°C as a stock for future use.

Yeast Transformation

Quiagen column purified expression plasmids with the desired yeast PK inserts were transformed into yeast using the lithium acetate method (97). The 121 yeast strain (EBY121E-pyk1Δ::HIS3 pyk2Δ::URA3) was a generous gift of Dr. Eckhard Boles (98). The 1-5 ypk yeast strain (90) was obtained from the Yeast Genetic Stock Center (Department of Molecular and Cell Biology, 229 Stanley Hall #3206, University of California, Berkeley, CA 94720-3206). Fifty ml of 121 yeast were grown in YEPAG liquid media to an optical density (OD) at a 600 nm wavelength of between 1 and 2 (works best at OD of 2). The cells were pelleted by centrifugation at 3000xg for 5 min. The cells were resuspended in 25 ml H₂O, and then pelleted as before. The cell pellet was resuspended in 1 ml of filter sterilized 100 mM lithium acetate (LiAc), and transferred to a 1.5 ml microfuge tube. The cells were again pelleted by briefly spinning in a tabletop microfuge. The cell pellet was diluted up to a final volume of 500 μl in 100 mM LiAc. The cell pellet was vortexed to assure mixing, and then allocated 50 μl/1.5 ml microfuge tube. Aliquots were pelleted in a tabletop microfuge, and the supernatants were removed. Single stranded carrier DNA (Sigma D-7656, Salmon Testes DNA) was boiled for 5min, and then immediately placed in ice water until used. The following were added in order to each cell aliquot: 240μl sterilized 50% w/v polyethylene glycol (MW-4000); 36μl filter sterile 1.0 M LiAc; 25 μl ssDNA (10.6 mg/ml); 50 μl plasmid (10 to 100 μg). Each tube was vortexed until the cell pellet was resuspended. The samples were placed at 30°C for 30 min and then at 42°C for 22 min. Cells were briefly microfuged in a tabletop microfuge to pellet cells. The cell pellet was resuspended in 1 ml of H₂O by gently pipeting up and down as few as times as

possible. Two to 200 μ l of the transformed samples were spread/YEPD plate. Plates were allowed to sit at room temperature until all liquid was absorbed into the media, and then placed at 30°C until yeast growth appeared. Single colonies were selected from yeast transformation plates and used to inoculate 5 ml of liquid YEPD media. These mini-cultures were grown at 30°C until they became dense, and then mixed 1:1 with 30% glycerol for long term storage at -80°C.

Resin Preparation for Protein Purification

Coarse-mesh cellulose-P (catalog number C2508) and fast-flow;fibrous DEAE-cellulose (catalog number D6418) were obtained from Sigma Chemical Company (St. Louis, MO). Both resins were washed before use in protein purification. After cellulose-P powder was mixed with an excess of water, the slurry was allowed to sit until the resin settled. Excess water was decanted. This procedure was repeated until liquid above settled resin was clear. The pH of resuspended cellulose-P was adjusted to 7.0 and collected by water aspiration through a Buchner funnel. The pH of resuspended cellulose-P was adjusted to 6.0 and collected by water aspiration through a Buchner funnel. Cellulose-P was then resuspended in 10 mM K_2HPO_4 , 5 mM EDTA, 5 mM β -mercaptoethanol, pH 6.0, 600 mM KCl. The resin was collected by aspiration filtration. Cellulose-P was then resuspended in 10 mM K_2HPO_4 , 5 mM EDTA, 5 mM β -mercaptoethanol, pH 6.0 and collected by aspiration filtration with the use of a Buchner funnel.

DEAE-cellulose was mixed with an excess of water and the slurry was allowed to sit until resin settled. Excess water was decanted. This procedure was repeated until liquid above settled resin was clear. The pH of resuspended DEAE-cellulose was adjusted to 8.6 and collected by water aspiration through a Buchner funnel. The pH of resuspended DEAE-cellulose was adjusted to 7.0 and collected by water aspiration through a Buchner funnel. The resin was cycled between pH 8.6 and 7.0 two additional times. After the resin had been thoroughly rinsed with water, it was resuspended in 10 mM K_2HPO_4 , 5 mM EDTA, 5 mM

β -mercaptoethanol, pH 8.3 and collected by aspiration filtration with the use of a Buchner funnel.

Protein Purification

For purification of PK, YEPD plates were streaked from frozen stocks of yeast strain 121 containing the desired mutated PK gene/expression plasmid (98). Single colonies were used to inoculate 5 ml mini-cultures of liquid YEPD. After the mini-cultures grew to high density at 30°C, they were used to inoculate 2 L cultures of YEPD. Two L cultures were grown to an OD₆₀₀ between 10 and 20 before cells were pelleted in a GSA rotor at 5000 rpm for 10 min.

After the pellet was resuspended in 5 ml of 1.2 M sorbitol at pH 6.8 per gram of cells, 2 mg of Zymolase-20T (Seikagaku Kogyo Co., 2-1-5, Nihonbashi-honcho, Chuo-ku, Tokyo, 103 Japan) per gram of cells was added. The slurry was allowed to incubate for 1.25 hr while gently shaking. The suspended cells were pelleted by centrifugation as before and resuspended in 5 ml of lysing buffer (10 mM K₂HPO₄, 5 mM EDTA, 5 mM β -mercaptoethanol, pH 7.5) per gram of cells and vortexed vigorously. This solution was centrifuged to remove cell debris. It should be noted that PK activity is found in the sorbitol fraction if frozen yeast cells are used as a starting material. In this study fresh yeast cells were used as starting material and therefore PK activity was in the lysing buffer fraction.

Four grams of DEAE cellulose (Sigma Chemical Co., St. Louis, MO) per gram of cells was added to the lysing buffer fraction. Immediately after adding the DEAE cellulose, the pH was adjusted to 8.3 using a 3 M KOH solution and the slurry was allowed to stand for 5 minutes. The pH of 8.3 was used based on Murcott's proposal that yeast PK is a "slippery" protein and does not bind to a strong anion exchanger at pH 8.3 even though its pI is 6.6 (52). Using a Buchner funnel and Whatman 3MMChr filter paper, the filtrate was recovered by aspiration filtration. Flow through was collected and the pH was adjusted to 6.0 with a 1 M H₃PO₄ solution. Washed and dried fibrous cellulose phosphate (Sigma Chemical Co., St. Louis, MO) was added to the flow through fraction, while maintaining the

pH at 6.0, until 90% of the PK activity was removed from solution. The cellulose phosphate-PK complex was recovered by removing the liquid fraction with a Buchner funnel, Whatman 3MMChr filter paper, and aspiration filtration. Care was given not to allow the resin to be completely dried. PK was eluted from cellulose phosphate using 300 mM KCl in lysing buffer at pH 6.0. This elution was accomplished by resuspending the resin in KCl in a beaker and allowing the resuspension to sit for 5 to 10 min before filtering resin in a Buchner funnel. An additional KCl rinse was added to the Buchner funnel after the resin had been collected. The rinse was added to the primary effluent. The enzyme lysis, DEAE cellulose batch binding, and cellulose-phosphate batch binding steps, developed in this lab, have also been used by Mesecar and Nowak (24,60,61).

Solid ammonium sulfate was added to the KCl effluent to obtain 1.95 M ammonium sulfate (50% saturated ammonium sulfate at 4°C). Samples at 1.95 M ammonium sulfate were incubated a minimum of 4 hr at 4°C with stirring before precipitated proteins were pelleted in a SA600 rotor at 10,000 rpm for 30 min. Solid ammonium sulfate was added to the supernatant to a total 2.54 M (65% saturated ammonium sulfate at 4°C). The samples were held at 4°C for 4 to 10 hr with stirring before precipitated protein was pelleted as before. The 65% ammonium sulfate pellet was diluted to 50% saturated ammonium sulfate (4°C). Precipitated protein was pelleted, and ammonium sulfate was added to the supernatant to a total of 65% saturated ammonium sulfate (4°C). The pellet was stored at 4°C saturated ammonium sulfate.

Activity during purification was measured according to the method of Bucher and Pfeleiderer (99). Up to 10 µl of PK sample was added to 660 µl of assay reaction (121 mM MES pH6.2, 121 mM KCl, 30 mM MgCl₂, 10 units/ml L-lactic dehydrogenase (Sigma L-7525), 282 µM β-nicotinamide adenine di-nucleotide, reduced form (β-NADH), 3.2 mM ADP, 4.4 mM PEP, and 0.77 mM FBP). Changes in A₃₄₀ were measured with a Hewlett Packard 8452A diode array spectrophotometer. Protein measurements on samples from the steps of protein purification were made using the reagents and protocol of Bio-Rad Protein

Assay (Bio-Rad Laboratories, Richmond, CA) using bovine serum albumin as a standard. A_{595} readings for the protein measurements were taken with a Gilford 300N micro-sample spectrophotometer.

Protein Gels

Electrophoresis using a 9% resolving/4% stacking polyacrylamide gel was used to monitor protein purification and estimate protein purity. Gels were run with a constant step voltage of 25 V for 1.5 hr, 50V for 0.5 hr, 75 V for 0.5 hr and 100 V for 0.75 hr. Protein bands were transferred onto Immobilon-P PVDF type membrane (Millipore, Bedford, MA), and stained with G-250 Coomassie or Western blotted with goat anti-yeast PK antiserum. The goat anti-yeast PK antiserum used in this study was developed by Dr. James Blair.

Kinetic Assays

Kinetics of yeast PK was measured using a modified version of the coupled assay (99). Using a Hewlett Packard 8452A diode array spectrophotometer disappearance of NADH was monitored at A_{340} . All reactions were thermostated at 25°C. All kinetic reactions were started by the addition of enzyme. PEP and ADP dependent kinetic curves with and without FBP were obtained from the same reaction. The presence of $(\text{NH}_4)_2\text{SO}_4$ was required to stabilize the activities of some mutant PK's. However, $(\text{NH}_4)_2\text{SO}_4$ affected kinetic parameters. Therefore, two standard reaction mixes were used for obtaining PEP and FBP dependent kinetic curves. A standard assay mix for PEP dependent kinetics, in the absence of $(\text{NH}_4)_2\text{SO}_4$, included 110 mM MES pH 6.2, 335 mM KCl, 28 mM MgCl_2 , 10 units/ml L-lactic dehydrogenase (L-7525, Sigma, St. Louis, MO), 300 μM β -nicotinamide adenine di-nucleotide, reduced form (β -NADH), and 8.2 mM ADP in a total of 725 μl and with or without 10 μl of 174 mM FBP. A standard assay mix for PEP dependent kinetics in the presence of $(\text{NH}_4)_2\text{SO}_4$ included 110 mM MES pH 6.2, 113 mM KCl, 55 mM $(\text{NH}_4)_2\text{SO}_4$, 28 mM MgCl_2 , 10 units/ml L-lactic dehydrogenase, 300 μM β -nicotinamide adenine di-nucleotide, reduced form (β -NADH), and 5.9 mM ADP in a total of 710 μl and with or without 30 μl of 58.3 mM FBP. A standard assay mix for FBP dependent kinetic

activation in the absence of $(\text{NH}_4)_2\text{SO}_4$ includes 110 mM MES pH 6.2, 335 mM KCl, 28mM MgCl_2 , 10 units/ml L-lactic dehydrogenase, 300 μM β -nicotinamide adenine dinucleotide, reduced form (β -NADH), 8.2 mM ADP, and the appropriate 10% V_{max} PEP level in a total of 735 μl . A standard assay mix for FBP dependent kinetic activation in the presence of $(\text{NH}_4)_2\text{SO}_4$ includes 110 mM MES pH 6.2, 113 mM KCl, 55 mM $(\text{NH}_4)_2\text{SO}_4$, 28 mM MgCl_2 , 10 units/ml L-lactic dehydrogenase, 300 μM β -nicotinamide adenine dinucleotide, reduced form (β -NADH), 5.9 mM ADP, and the appropriate 10% V_{max} PEP level in a total of 735 μl . It is important to note that L-lactic dehydrogenase was desalted to remove $(\text{NH}_4)_2\text{SO}_4$. PK was diluted into dilution buffer (100 mM K_2HPO_4 , 200 mM KCl, 5 mM EDTA, 1 $\mu\text{l/ml}$ β -mercaptoethanol, 20% glycerol, pH 6.2) so that 10 μl of diluted protein added to the standard PEP assay mix gave a V_{max} of 1.0. A unit (U) of PK activity is defined as μmoles of product produced per minute. To determine the concentrations of fructose-1,6-bisphosphate, enzymatic assays described by Michal and Beutler were employed (100). PEP and ADP concentrations were determined using the kinetic reaction described here with the substrate of interest in limiting amounts following the procedure described by (101).

It is important to note that ADP is known to chelate Mg^{++} . In this study, MgSO_4 concentrations were saturating. The free Mg^{++} concentration should therefore be saturating at all ADP concentrations.

Purified PK's were stored suspended in saturated $(\text{NH}_4)_2\text{SO}_4$. Unless noted, proteins were desalted before use in either kinetic or fluorescence studies. To desalt, ammonium sulfate suspensions of PK were microfuged and the supernatant discarded. Pellets were resuspended to a total of 250 μl in dilution buffer (100 mM K_2HPO_4 , 200 mM KCl, 5 mM EDTA, 1 $\mu\text{l/ml}$ β -mercaptoethanol, 20% glycerol, pH 6.2). The total 250 μl was loaded onto a BioRad (Hercules, CA) Bio-Spin column packed with 1.1 ml G-50 Sephadex (G-50-150, Sigma, St. Louis, MO) pre-equilibrated with dilution buffer. The first 250 μl off the column were discarded. The next 475 μl off of the column were collected as

desalted protein. Protein concentrations were monitored by A_{280} using an extinction coefficient of $0.51 \text{ (mg/ml)}^{-1}$ in a 1 cm cuvette (50). $(\text{NH}_4)_2\text{SO}_4$ levels were monitored by the method of Lehoux *et al.* (102).

Fluorescence Quench Titrations

The direct binding method of Blair and Walker was not useful in obtaining binding data for FBP to wild type PK (75). In the absence of direct binding data, fluorescence quench caused by titration with FBP were used to monitor FBP binding. This method has been used extensively (44,59,60,103). A Perkin-Elmer 650-40 Fluorescence Spectrophotometer was used to monitor fluorescence. An excitation wavelength of 276 nm and an emission wavelength of 330 nm were used in combination with ratio mode and high pm gain options. Fifty μl of PK, 0.49 to .57 mg/ml, desalted in dilution buffer was added in 350 μl of filtered fluorescence buffer (134 mM MES pH 6.2, 405 mM KCl, 112 mM MgCl_2) with or without 25 μl of 236 mM PEP. It was necessary to let this reaction mix equilibrate 11 min. at 25°C before initiation of fluorescence readings. This reaction mix was titrated with FBP such that the total volume of FBP did not exceed 10% of the original reaction mix. Dilution corrections were performed before fluorescence data was fitted.

FBP Contamination in F1P and F6P

To determine the concentrations of fructose-1,6-bisphosphate contamination in F6P, the enzymatic assay described by Michal and Beutler was used (100). The enzymatic assay did not detect FBP contamination in the F6P used in this study. The Sigma Chemical Company (St. Louis, MO.) used an enzymatic assay to determine FBP contamination of F6P to be less than 0.001 mole%.

The enzymatic assay used to quantitate FBP in this study detects F1P. Therefore, contamination of F1P by FBP could not be measured. F1P used in this study was obtained from the Sigma Chemical Company (St. Louis, MO.). The company used thin layer chromatography to determine that F1P was 98.5% pure with no detectable amount of FBP.

Curve Fitting

Kinetic data was fit to the Hill equation (104) in the form:

$$V=(V_{\max} * [S]^n)/(S_{1/2}^n + [S]^n)$$

using Kalidagraph (Kalidagraph, Synergy Software, Reading, PA). V is velocity, V_{\max} is the maximum velocity, $S_{1/2}$ is the substrate concentration that gives a velocity equal to one half of the maximum velocity, $[S]$ is the substrate concentration, and n is the Hill coefficient. To fit FBP dependent activation curves, the velocity without FBP was subtracted from all velocity data before fitting.

Fluorescence quench titrations were fit to the Hill equation (104). Unlike activity measurements, fluorescence measurements in the absence of ligand are nonzero values. Therefore with the help of Dr. Olin Spivey, the Hill equation was rearranged to allow fitting to the initial fluorescence reading as well as other parameters. The following form of the Hill equation was used to fit fluorescence data:

$$F_{\text{corr}}=F_0 - \{(F_0 - F_{\text{inf}}) / [1 + (L_{1/2}/L)^n]\}$$

$$F_{\text{corr}}=(F_{\text{exp}} - F_{\text{BG}}) * V_{\text{tot}} / V_{\text{int}}$$

using a program written by Chandler *et al.* (105). F_{corr} is fluorescence corrected for background (FBG) and dilution. F_{exp} is the experimental fluorescence value. V_{tot} is the total volume at the experimental fluorescence point. V_{int} is the volume of the initial fluorescence reading. F_0 is the initial fluorescence reading with no ligand present, F_{inf} is fluorescence at infinite concentrations of ligand, $L_{1/2}$ is the concentration of ligand to obtain 1/2 of the difference between F_0 and F_{inf} , and L is the concentration of ligand at the F_{corr} reading. The Hill coefficient is represented by n . $-\Delta F_{\text{max}}$ (intensity) shown in the text and figures is F_{inf} minus F_0 .

RESULTS

Expression

The purpose of this study was to add to the understanding of allosteric regulation of PK by FBP using yeast PK as a model system. The active site, the FBP binding site, and the subunit interface(s) are all important in allosteric regulation. In order to probe sites of interest by site directed mutagenesis a system was needed that insured all PK protein was coded by the mutated gene. An expression system, which does not interfere with production of the desired mutated pyruvate kinase, needed to be identified. Three yeast expression systems were examined.

A yeast strain without endogenous PK activity, *pyk 1-5* (90), has previously been used in this laboratory to express wild type PK. Recently, the mutation of the PK gene in *pyk 1-5* was sequenced. Loss of PK activity appears to be due to a G268D point mutation near the active site (88). Even though the PK gene mutation in *pyk 1-5* causes a loss of PK activity, PK protein is still expressed in *pyk 1-5* (88). The use of *pyk 1-5* as an expression system might result in the production of mixed tetramers with the *pyk 1-5* PK protein contributing to PK phenotypes.

A heat sensitive PK yeast strain, *cdc 19*, was also available (92). With the assistance of Mr. Jeff Frazier, PK from *cdc 19* was sequenced in this study. A single amino acid substitution, S70F, causes the *cdc 19* phenotype. However, before exploration of *cdc 19* as a possible expression system was completed, a knockout yeast PK became available (98). The knockout yeast strain, 121, has the *pyk1* gene knocked out as well as a second possible PK gene, *pyk2* (98). Dr. Eckhard Boles generously shared this double knockout yeast strain and 121 was selected as the expression yeast strain for this study.

Transformation of yeast strain 121 with the wild type PK/pYES2 construct gives a high level of expression such that PK represents between 20 to 30 % of total soluble protein.

Yeast can not survive on glucose as a sole carbon source unless active pyruvate kinase is present. The knockout yeast used as an expression system in this study has the yeast genomic PK gene disrupted. Therefore growth of transformed knockout yeast on glucose acts as a screen for active PK proteins. All mutations studied in this investigation were designed to restore growth of yeast strain 121 on glucose. Therefore mutations which disrupt the enzyme activity were selected against in this study.

Wild Type Pyruvate Kinase

Kinetic activation as a function of FBP concentration is sensitive to changes in FBP binding affinity, as well as interruptions in communication between the FBP binding site and the active site. If FBP binding of mutant PK's is compared with the kinetic response to FBP, the effect of a mutation can be characterized as having effects on FBP binding and/or effects on communication between the activator binding site with the active site. Therefore, the design of this study was to use purified wild type and mutant PK's to obtain kinetic parameters. Mutations that showed altered FBP dependent kinetic activation were further examined for altered FBP binding. Since the direct FBP binding technique of Blair and Walker (75) was not useful for the investigation of yeast PK, FBP binding was indirectly evaluated using the fluorescence quench titration technique of Kuczynski and Suelter (44).

The current protein purification protocol is simple and quick. Up to three preparations have been completed in a single day. General information in the purification scheme is presented in Table 4. The measured protein concentration of fractions eluted from cellulose-phosphate was repeatedly lower than expected. As discussed later, KCl and ammonium sulfate used in specific purification steps markedly alters yeast PK activity. Therefore, the purification table (Table 4) is not a good indication of PK purity or yield. However, SDS-PAGE gel electrophoresis shows this simple, rapid purification scheme gives rise to homogenous wild type yeast PK protein (Figure 10).

Table 4. Purification of Wild Type Yeast PK. Pelleted yeast cells were lysed with Zymolase, and cell debris was removed by centrifugation. Supernatant was combined with DEAE-cellulose at pH 8.3, and filtered. Since yeast PK does not bind to DEAE-cellulose, the flow through was combined with cellulose-phosphate. PK bound to cellulose-phosphate was eluted with 300 mM KCl and further purified by two rounds of ammonium sulfate fractionation as described in the Materials and Methods. *The measured protein concentration of KCl elutions from cellulose-phosphate was consistently low.

Purification Step	Total Activity (U)	Total Protein (mg)	Specific Activity (U/mg)	Yield (%)	Fold Purification
Lysis	210,000	1,600	131	100	1
DEAE-cellulose	154,000	1,006	153	73	1.17
Cellulose-phosphate	70,500	(18)*	-	-	-
Ammonium sulfate fractionation	27,500	86	320	13	2.44

Electrophoresis gels at serial dilutions of purified wild type protein show that the protein is highly purified (Figure 11). Contaminating bands are only observed when the lanes are overloaded with PK protein. Analysis of Western blots show that some of the contaminating bands are recognized by goat anti-yeast PK antiserum, indicating a small amount of proteolysis during purification (Figure 11). If contaminating bands represent proteolysis of a subunit within a tetramer, further purification will be difficult.

To minimize problems due to instabilities in mutant proteins produced in this study, initial kinetic screens were with wild type (Figure 12) and various mutated PK's diluted in saturated $(\text{NH}_4)_2\text{SO}_4$. The specific activity of wild type PK assayed in the presence of $(\text{NH}_4)_2\text{SO}_4$ does not agree with specific activities previously reported in the literature. Ammonium ions are known to fulfill yeast PK's monovalent cation requirement (44,47,49,106). To determine the maximum concentration of $(\text{NH}_4)_2\text{SO}_4$ which does not affect PK activity, PK was desalted as described in Materials and Methods and assayed at varying concentrations of added $(\text{NH}_4)_2\text{SO}_4$ (Figure 13). $(\text{NH}_4)_2\text{SO}_4$ concentrations greater than 0.4 mM decrease V_{\max} activity and increase the activity at 4.31 mM PEP in the absence of FBP. Desalting L-lactic dehydrogenase and PK as described in Materials and Methods reduces the final assay concentration of $(\text{NH}_4)_2\text{SO}_4$ to less than 0.15 mM, as detected by the $(\text{NH}_4)_2\text{SO}_4$ assay of Lehoux *et al.*(102).

The V_{\max} of PEP dependent kinetic curves in the absence of FBP obtained with desalted PK is not equivalent to the same parameter when FBP is present. Since removal of monovalent cations (NH_4^+) causes this effect, the concentration of KCl was varied to determine if a sub-saturating concentration of monovalent cation is responsible for the V_{\max} difference. Increasing KCl in the kinetic assays with desalted PK's causes the two curves to obtain equivalent V_{\max} quantities (Figure 14). For further studies, kinetic assays using desalted PK had 335 mM KCl.

The kinetic parameters of desalted wild type PK in the presence of 335 mM KCl are shown in Figure 12. The major effect of high concentrations of $(\text{NH}_4)_2\text{SO}_4$ on wild type

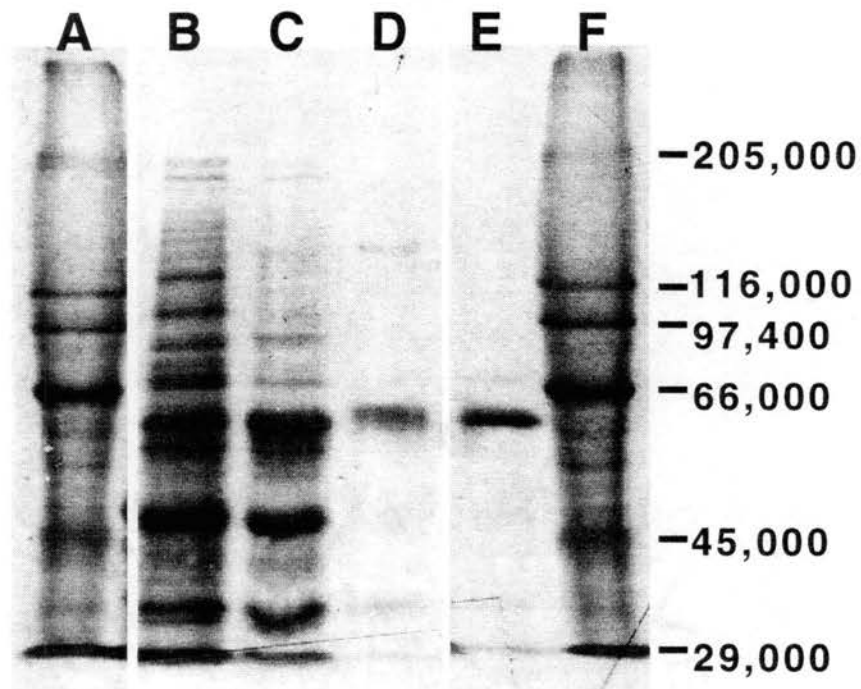


Figure 10. SDS PAGE Gel Electrophoresis of Yeast PK at Various Purification Steps. Lanes A and F are protein molecular weight standards: Carbonic Anhydrase MW=29,000; Egg Albumin MW=45,000; Bovine Albumin MW=66,000; Phosphorylase b MW=97,400; β -Galactosidase MW=116,000; Myosin MW=205,000. PK lanes were loaded with 1.2 units of activity per lane. Lane B=Cell lysate, Lane C=DEAE-cellulose wash through, Lane D= cellulose-phosphate effluent, Lane E= $(\text{NH}_4)_2\text{SO}_4$ fractionation.

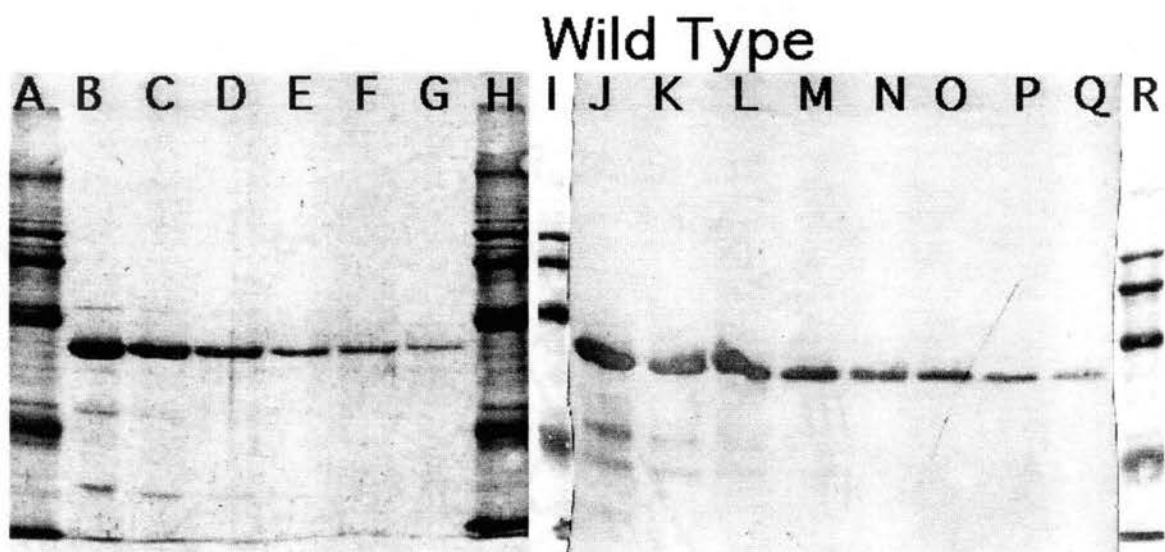
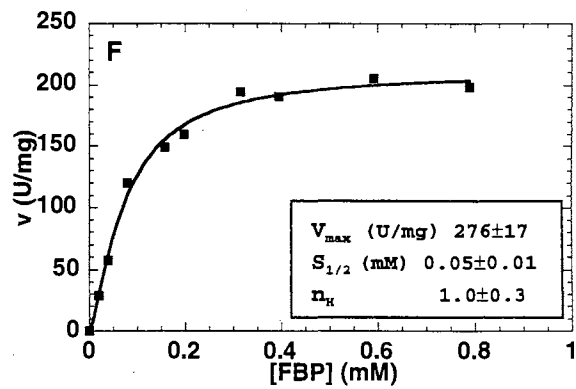
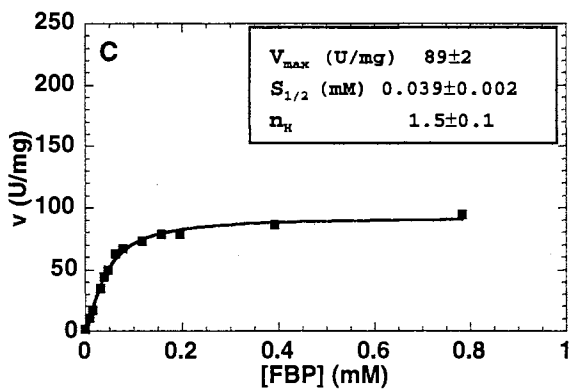
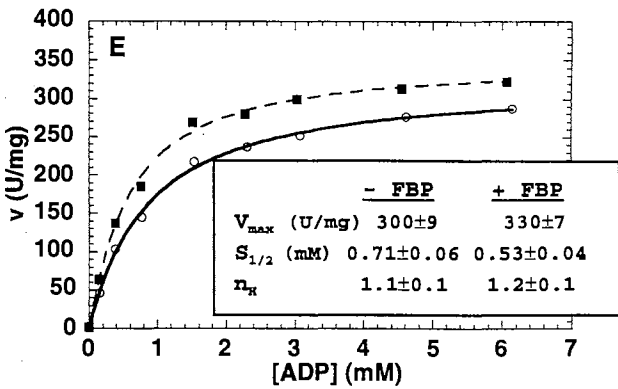
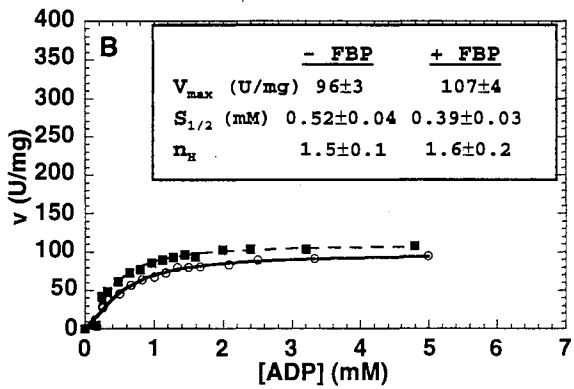
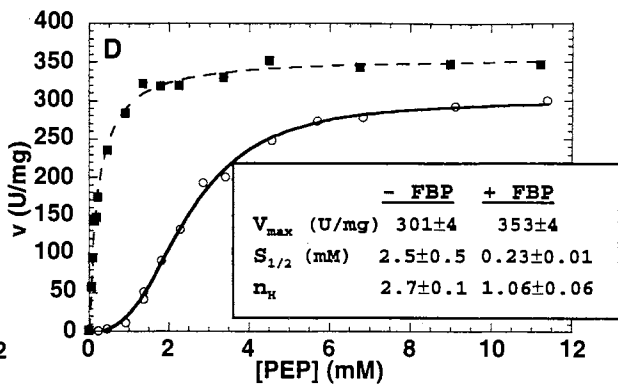
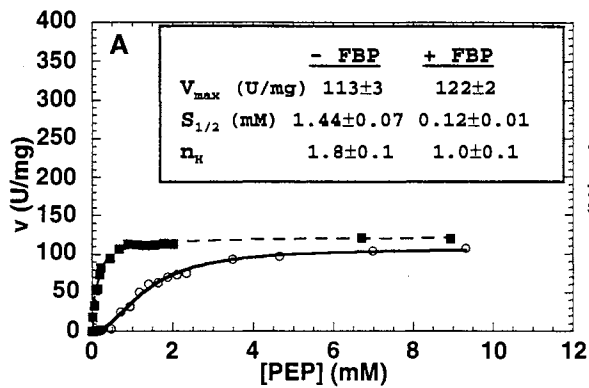


Figure 11. SDS PAGE Gel Electrophoresis of Purified Wild Type PK. Lanes B-G and J-Q represent serial 1:1 dilutions of purified protein. Protein concentrations in lanes B and J are 2.7 $\mu\text{g}/\text{lane}$. Lanes A-H, R, and I are stained with G-250 Coomassie blue. Lanes J-Q are Western blotted. Lanes A, H, R, and I are protein molecular weight standards: Carbonic Anhydrase MW=29,000; Egg Albumin MW=45,000; Bovine Albumin MW=66,000; Phosphorylase b MW=97,400; β -Galactosidase MW=116,000; Myosin MW=205,000.

Figure 12. Kinetic Properties of Wild Type PK Under Two Different Salt Conditions.

The catalytic activity (v) of purified wild type PK was measured at varying concentrations of substrate (PEP and ADP) and the allosteric activator (FBP). Panels A, B and C represent studies with PK stored in saturated ammonium sulfate and giving a final concentration of 55 mM ammonium sulfate in the assay solution. Panels D, E and F represent studies with desalted PK samples as described in Materials and Methods with final ammonium sulfate in the assay solution less than 0.15 mM. Activation by FBP was monitored at a PEP concentration that gives a 10% V_{\max} activity (in absence of FBP). The precise PEP concentration that gives 10% V_{\max} was dependent on the experimental conditions used. Kinetic parameters determined by fitting the results to the Hill equation are presented in the inserts.

Panel A. Varying concentrations of PEP without (○) or with 2.4 mM FBP (■). Panel B. Varying concentrations of ADP with 12 mM PEP and without (○) or with 2.4 mM FBP (■). Panel C. Varying concentrations of FBP with 0.67 mM PEP. Panel D. Varying concentrations of PEP without (○) or with 2.4 mM FBP (■). Panel E. Varying concentrations of ADP with 12 mM PEP and without (○) or with 2.4 mM FBP (■). Panel F. Varying concentrations of FBP with 1.9 mM PEP.



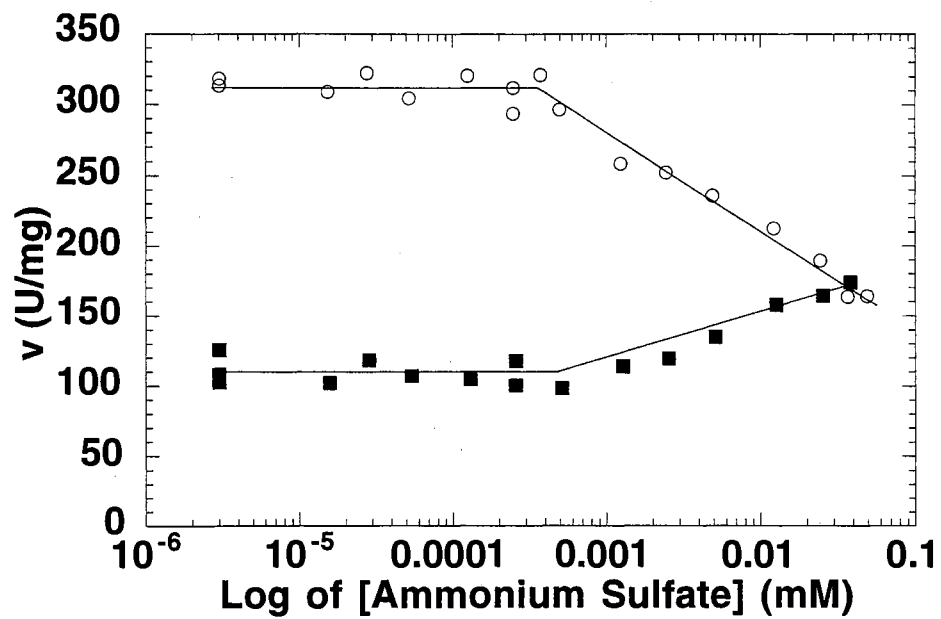


Figure 13. Effects of $(\text{NH}_4)_2\text{SO}_4$ on PK Activities. PK activity (v) was measured in the presence of 110 mM MES, 28 mM MgCl_2 , 113 mM KCl, 5.4 mM ADP, 4.31 mM PEP, and with (○) or without 2.3 mM FBP (■). Lines are drawn to show the general pattern of the data.

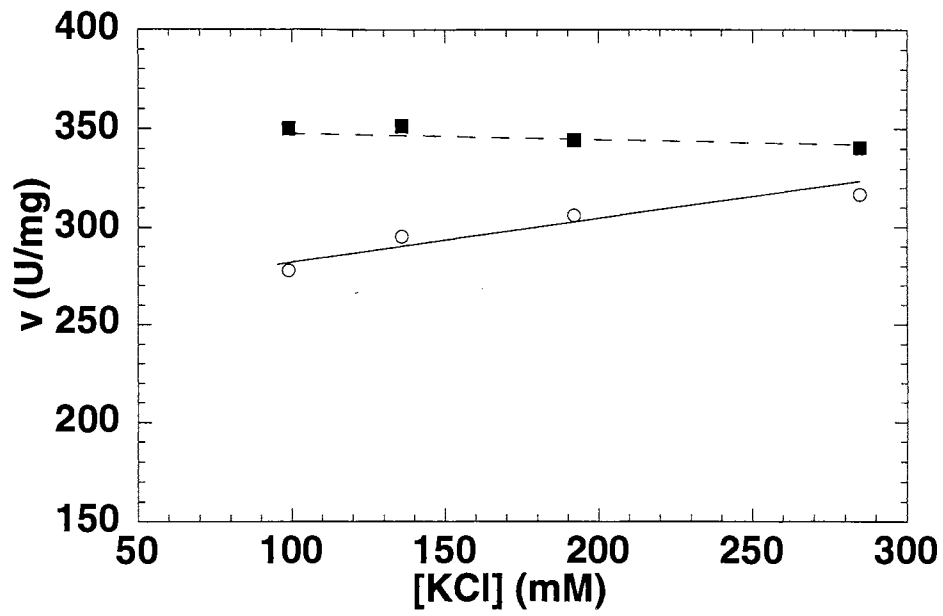


Figure 14. Effects of KCl Concentration on Activity (v) of Desalted Wild Type PK in the Presence (■) and Absence (○) of FBP.

activity is to decrease the V_{\max} . However, the $S_{1/2}$ and n_H for PEP dependent kinetics, both in the presence and absence of FBP, are also affected by the presence of $(\text{NH}_4)_2\text{SO}_4$.

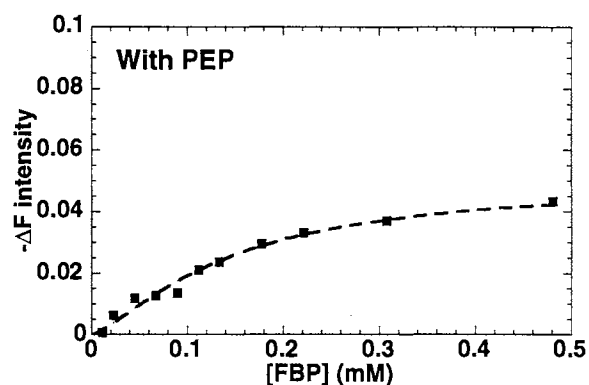
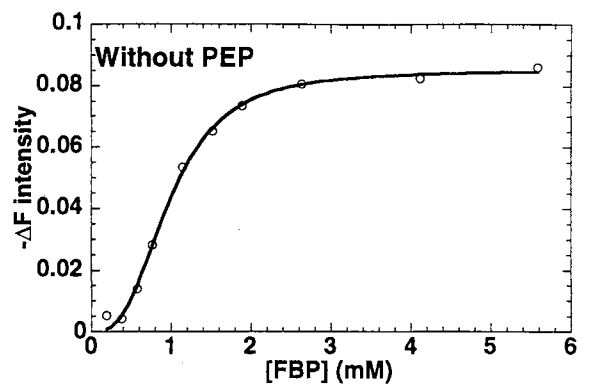
A comparison of kinetic parameters for wild type PK from this preparation and preparations reported in the literature is shown in Table 5. The kinetic parameters for purified wild type yeast PK assayed at low concentrations of $(\text{NH}_4)_2\text{SO}_4$ in this study are very similar to those previously reported.

Buffer conditions similar to those used in standard kinetic assays without $(\text{NH}_4)_2\text{SO}_4$ were used to study fluorescence quench titrations of desalted PK with FBP (Figure 15). It should be noted that both FBP and PEP independently cause a fluorescence quench of yeast PK (44). Therefore the monitored $-\Delta F_{\max}$ in response to FBP in the absence of PEP is not equivalent to that obtained in the presence of PEP. Estimates of FBP binding parameters of wild type PK obtained in this study are similar to results previously reported by others (44).

At the beginning of this investigation very little evidence was available to indicate that ADP interacts with allosteric regulation by FBP (41,44,49,51). Therefore, the activity responses of various mutant PK's to varying concentrations of ADP were not measured, unless noted. The kinetic parameters of wild type and mutant PK's for PEP in the presence and absence of 2.4 mM FBP, and the kinetic parameters of FBP activation of PK were used as an initial screen to define those mutations influencing FBP activation of the enzyme. Activation by FBP was monitored at a PEP concentration that gives a 10% V_{\max} activity (in absence of FBP). At this PEP concentration, the largest FBP activation is observed. The precise PEP concentration that gives 10% V_{\max} was dependent on the mutation used and experimental conditions used. With the exceptions Q299N, R396A, and K413E, PK enzymes used in kinetic and fluorescent studies were desalted as detailed in Materials and Methods. Only large changes in kinetic properties of mutant PK's were emphasized in this study.

Table 5. Summary of the Kinetic Parameters of Wild Type Yeast PK and comparison with other Literature Reports.

Reference:	This Study	(41)	(49)	(50)	(52)	(78)
<u>PEP (-FBP)</u>						
$S_{1/2}$ (mM)	2.5	4.5	1.8	1.8	3.7	2.8
n_H	2.7	2.8	2.9	2.3	2.9	2.9
<u>PEP (+FBP)</u>						
$S_{1/2}$ (mM)	0.23	0.46	0.13	0.10	0.16	0.22
n_H	1.06	1.0	0.94	fit to 1	fit to 1	1.72
<u>ADP (-FBP)</u>						
$S_{1/2}$ (mM)	0.71	-	0.40	0.34	-	0.25
n_H	1.1	-	1.2	fit to 1	-	1.5
<u>ADP (+FBP)</u>						
$S_{1/2}$ (mM)	0.53	-	0.20	0.16	-	0.15
n_H	1.2	-	1.1	fit to 1	-	1.0
<u>FBP activation</u>						
$S_{1/2}$ (mM)	0.05	-	0.028	0.014	-	-
n_H	1.0	-	2.3	1.3	-	-
<u>Specific Activity</u>						
(U/mg)	320	200	220	375	367	325



	<u>- PEP</u>	<u>+ PEP</u>
$-\Delta F_{\max}$	0.085	0.050
$\text{FBP}_{1/2}$ (mM)	0.98 ± 0.03	0.14 ± 0.01
n_H	2.9 ± 0.2	1.4 ± 0.1

Figure 15. Fluorescence Quench Titration Curves for Wild Type PK. Fluorescence of purified yeast PK was measured at an excitation wavelength of 276 nm and an emission wavelength of 330 nm at varying concentrations of FBP in the absence (○) and presence of 15 mM PEP (■). $-\Delta F$ values are per $\mu\text{g/ml}$ protein. The scale of FBP concentration is different on the two graphs. The responses of fluorescence (ΔF) were fit to the Hill equation for cooperative interactions and are presented in the insert.

Two Positive Charged Domain Interactions

At the onset of this study the location of PK's FBP binding site was unknown. One goal of this study was to identify the FBP binding site of yeast PK. In search of a possible binding site for FBP, it was first necessary to identify possible bond types available for FBP binding. Based on the results of Wurster *et al.*, an energetically minimized β -furanose FBP model was built with the assistance of Mr. John Carment (67). A hydrophilic/hydrophobic grid map was calculated for the model (Figure 16). This map shows two large hydrophilic regions. The first hydrophilic region includes areas around the 6'-phosphate group and the second hydrophilic region encompasses the 1'-phosphate group and the C2 and C3 OH groups. A small hydrophilic region from the OH group of C4, and a single hydrophobic region centered around C4, C5, and C6 of FBP are also predicted by this analysis. The phosphate groups of FBP are negatively charged at pH's greater than 2 (107). Therefore the phosphate groups are predicted to play major roles in binding through ionic bonds. FBP is also capable of hydrogen bonding from OH groups of the sugar ring. Hydrophobic interactions with the sugar ring backbone are possible. Hydrophilic/hydrophobic predictions are in agreement with analog studies that suggests FBP's two phosphate groups are important for binding to PK (69). Due to the negative charge of FBP's two phosphate groups, positive pockets on the surface of PK were considered as potential sites for FBP docking.

The major draw back to using yeast PK, initially, was the lack of structural data. Therefore, a yeast PK model was built by replacing the amino acid sequence of yeast PK into the structure of rabbit muscle PK (17). Using a surface charge map of the yeast PK model, two highly positively charged pockets which are solvent accessible were identified in the region between the A and C domains. One pocket (Figure 17) corresponds to the Arginine 42 (Arg 42) pocket previously characterized as an ADP binding site by X-ray analysis (70). Mutagenesis of residues in the Arg 42 pocket in PK of *T. bruci* also supports this site's importance in allosteric regulation by FBP (71).

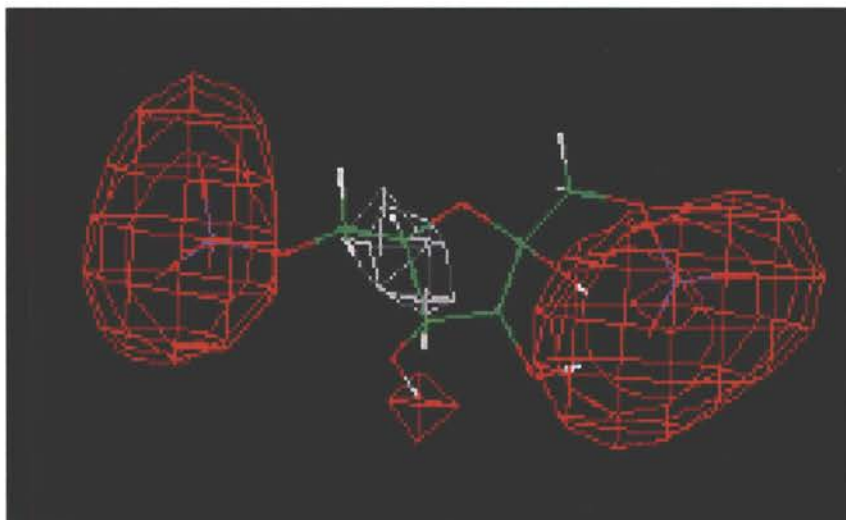


Figure 16. A Hydrophobic/Hydrophilic Grid Map of the Energetically Minimized β -furanose FBP Model. The energy-minimized β -furanose FBP was built using the Builder module in Insight II Version 2.3.0 (Biosym Technologies, 1993, 9685 Scranton Road, San Diego, CA 92121-2777) and minimized with Discover Version 2.9.5 (Biosym Technologies, 1994, 9685 Scranton Road, San Diego, CA 92121-4778). Hydrophobic regions are presented as white shells and hydrophilic regions are shown as red shells.

The second positively charged pocket identified by molecular modeling is close in space to the Arg 42 pocket, although on the opposite side of the monomer. Tyrosine 436 has a dominating presence in the second pocket and therefore this site will be referred to as the Tyr 436 pocket (Figure 18). The Tyr 436 pocket corresponds to a site identified as a possible FBP/ADP binding site by a chemical labeling/protection experiment with *E. coli* type I PK (72,73). This pocket has also been identified as a possible ATP binding site by labeling experiments with the *E. coli* type I isozyme (74). An alignment of the yeast PK sequence with a variety of other allosteric PK's shows that positive residues in the Tyr 436 and Arg 42 pockets are highly conserved across many species (Figure 19).

A-C Domain Contacts

It is interesting to note that both the Tyr 436 and Arg 42 pockets are contained in the A and C domain contacts. Mattevi *et al.* suggested that transition between T and R states involve little motion within domains, but rather involves motions between domain (21,81). Therefore, contacts between domains may be important in stabilizing activity states. Additional support for the involvement of A-C domain contacts in allosteric regulation is provided by mutagenesis of amino acids near the Tyr 436 pocket of *B. stearothermophilus* (34). The *B. stearothermophilus* study suggests a salt bridge between the A and C domains may be important in allosteric regulation (34). Therefore, probing the Arg 42 and Tyr 436 pockets in the current study was not only valuable for locating the FBP binding site but also for analyzing A-C domain contacts for roles in allosteric regulation.

The Tyr 436 Pocket: A-C Domain Contacts

The Tyr 436 and Arg 42 pockets identified in this study by surface charge mapping have both been previously proposed as binding sites for allosteric effectors (34,70-74). We considered the possibility that separate ATP and FBP binding sites may be located in areas between the A and C domains. FBP binding studies with liver PK suggests that ATP regulation of this isozyme is not through competition at the same site to which FBP binds (75).

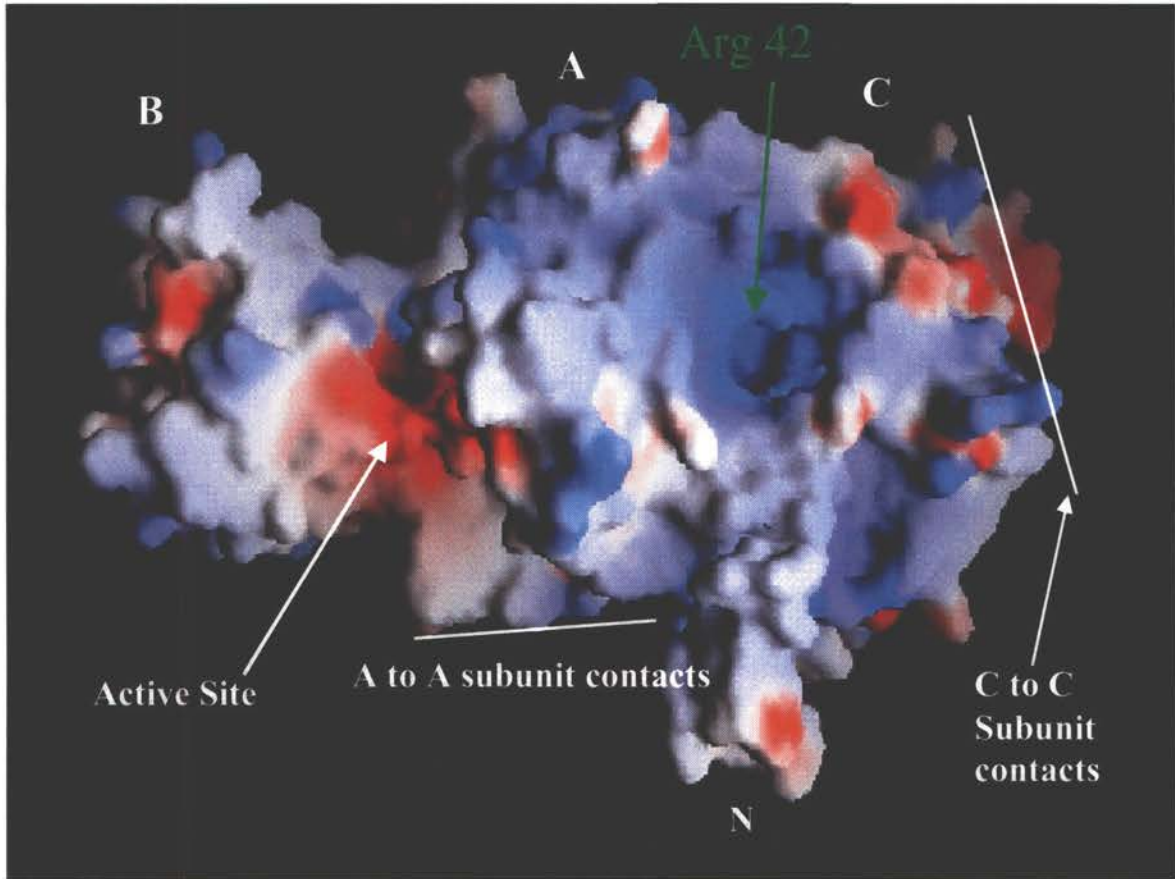


Figure 17. Surface Charge Map of the Arg 42 Pocket. A surface charge map, generated by molecular modeling as described in Materials and Methods, of a subunit of yeast PK and orientated to show the Arg 42 pocket. Red indicates negatively charged areas and blue represents positively charged areas. White represents neutral charged areas. The Arg 42 pocket is labeled based on ADP interactions with cat muscle PK's arginine 42 (equivalent to yeast arginine 19) (70).

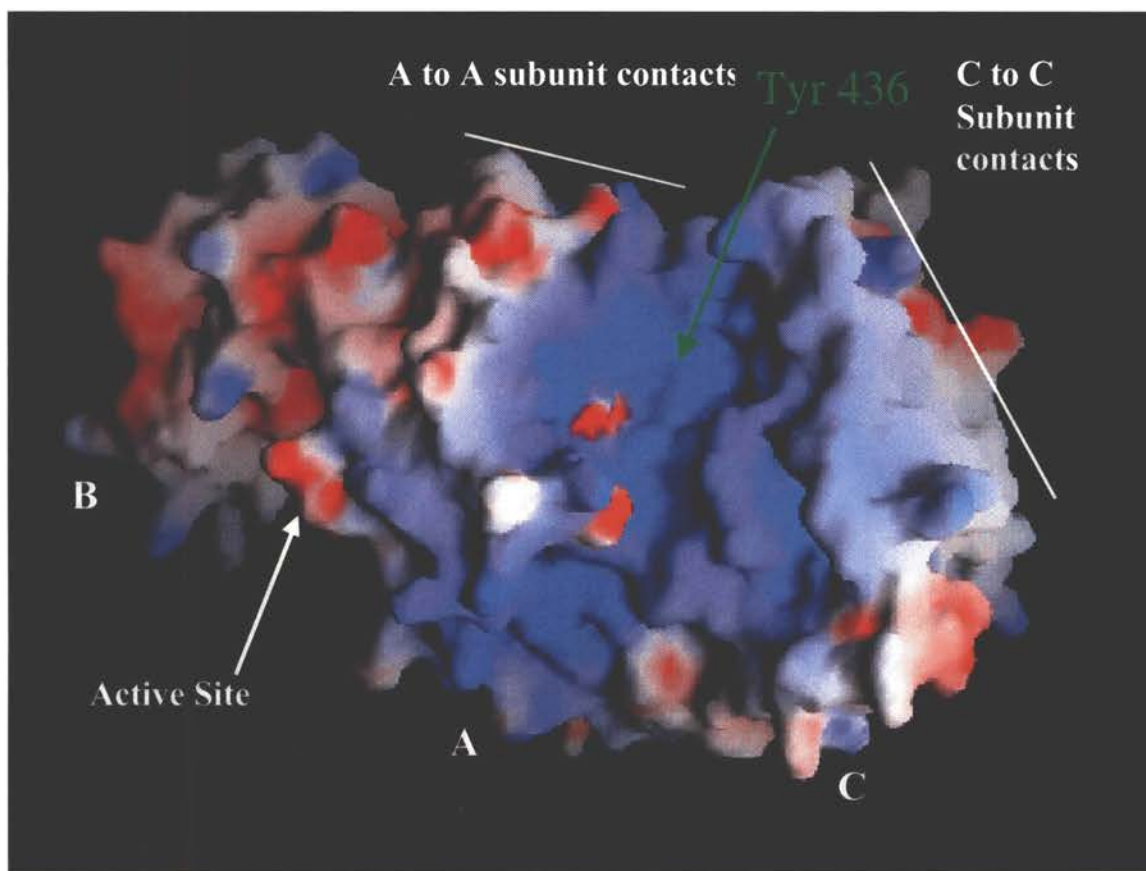


Figure 18. Surface Charge Map of the Tyr 436 Pocket. A surface charge map, generated by molecular modeling as described in Materials and Methods, of a subunit of yeast PK and orientated to show the Tyr 436 pocket. Red indicates negatively charged areas and blue represents positively charged areas. White represents neutral charged areas.

Tyr436 POCKET CONSENSUS SEQUENCE

Yeast numbering	Lys236	Lys292	Arg406/409	Arg415	Tyr436
				Lys413	
1)RatR	GQNIKIISKIE	CNLAGKPVVC	LTKTGRSAQLLSQYRPRAA	RQVHLSRGVF	
2)RatL	GQNIKIISKIE	CNLAGKPVVC	LTKTGRSAQLLSQYRPRAA	RQVHLSRGVF	
3)RatM2	GKNIKIISKIE	CNRAGKPVIC	LTKSGRSAHQVARYRPRAP	RQAHLYRGIF	
4)RatM1	GKNIKIISKIE	CNRAGKPVIC	LTESGRSAHQVARYRPRAP	RQAHLYRGIF	
5)RabbitM1	GKNIKIISKIE	CNRAGKPVIC	LTESGRSAHQVARYRPRAP	RQAHLYRGIF	
6)chickenM1	GKHIIISKIE	CNRAGKPIIC	MTESGRSAHLVSRYPNPAP	RQAHLYRGVF	
7)Aspergillus	GKEIQIIAKIE	CNIKGPVIC	LTTSKGKTARYLSKYRNPVCP	RYSHLYRGVW	
8)S.cerevisiae1	GKDVKIIIVKIE	SNLAGKPVIC	LSTSGTTPRLVSKYRPNCP	RFSHLYRGVF	
9)T.bruci	GKDILIIISKIE	CNVVGPVIC	LSNTGRSARLISKYRPNCP	RQLNVTRSVV	
10)EcoliTypeI	GENIHIISKIE	CIRARKVVIT	ATQGGKSARAVRKYFPDAT	HQLVLSKGVV	
11)EcoliTypeII	GCDAKIVAKVE	ARQLNRAVIT	MTESGRTALMTRSRISSGLP	NLTALYRGVT	
12)Bstearotherm	ALHIQIIAKIE	CNMLGKPVIT	PTVSGKTPQMVAKYRPAK	RRALALVWGVV	

ARG42 POCKET CONSENSUS SEQUENCE

Yeast numbering	Arg19	Lys42	Asn46	Arg77	His349	Arg353	His434	Arg470
1)RatR	PVAA.RSTSI	EMIKAGMNIARL	PLSYRPVAI	VMMQHAIAREAEA	ARQVHLSRG	SGKLRGFLR		
2)RatL	PVAA.RSTSI	EMIKAGMNIARL	PLSYRPVAI	VMMQHAIAREAEA	ARQVHLSRG	SGKLRGFLR		
3)RatM2	PITA.RNTGI	EMIKSGMNVARL	PILYRPVAV	VRMQHLIAREAEA	ARQAHLYRG	VGKARGFFK		
4)RatM1	PITA.RNTGI	EMIKSGMNVARL	PILYRPVAV	VRMQHLIAREAEA	ARQAHLYRG	VGKARGFFK		
5)RabbitM1	PITA.RNTGI	EMIKSGMNVARM	PILYRPVAV	VRMQHLIAREAEA	ARQAHLYRG	VGKARGFFK		
6)chickenM1	PTIA.RNTGI	EMIKSGMNVARL	PITYRPVAI	VRMQHAIAREAEA	ARQAHLYRG	VGKARGFFK		
7)Aspergillus	PSKNFRRTSI	SLRTAGLNVVRM	...RPLAI	VKMMSETCLLAEV	SRYSHLYRG	HALKLGIIIN		
8)S.cerevisiae1	AGSDLRRTSI	ALRKAGLNIVRM	...RPLAI	VTTMAETAVIAEQ	ARFSHLYRG	KAKEFGILK		
9)T.bruci	PVAKHRANRI	NLMKSGMSVARM	...LHIGI	VQYMARICVEAQS	CRQLNVTRS	FAKKEYAS		
10)EcoliTypeI	MKKTKI	MLADAGMNVML	...KTAAI	VSIMATICERTDR	AHQLVLSKG	LALQSGLAH		
11)EcoliTypeII	SRRLRRTKI	KVIAAGANVVRM	...RHVAI	VAAMARVCLGAEK	LNLALYRG	LLRDKGYLM		
12)Bstearotherm	MKRKTKI	VQLEAGMNVARL	...RTVAI	VKTMHQIALRTEQ	SRRLALVWG	AAVRSGLVK		

Figure 19. Alignment of Amino Acid Sequence of Pyruvate Kinase Sequences from Various Species In and Near the Tyr 436 and Arg 42 Pockets. Positive Charged residues are show in bold. Sequence codes and references are provided in the Appendix (Figure A1).

When the Tyr 436 pocket of the yeast model was considered in detail and compared with other PK sequences, five highly conserved positive charges were identified as possible interactants with the phosphate groups of FBP. Yeast residues at the conserved position are lysine #236, lysine #292, arginine #409, lysine #413, arginine #415. A sixth residue (tyrosine #436) may interact with FBP's C4 OH via hydrogen bonding (Figure 20).

Comparison of conserved residues identifies six highly conserved positive residues in the Tyr 436 pocket. In addition to the five positive residues of the yeast PK's Tyr 436 pocket, several PK isozymes have a conserved positive charge at a position equivalent to yeast PK's threonine 406. When comparing sequence with location on the 3-D structure of rabbit muscle (17) at least four of six conserved positively charged residues are present in any one FBP regulated PK isozyme. The orientation of these conserved residues suggested that FBP might bind within the Tyr 436 pocket similar to that shown in the binding model presented in Figure 20. We considered that the number and positions of positively charged residues in the Tyr 436 pocket might cause different PK isozymes to have different affinities for FBP.

To probe the Tyr 436 pocket as a possible FBP binding site, several mutations were designed in this site: K236Q, K236E, K292Q, K292E, T406R, R409Q, R409E, K413Q, K413E, R415Q, Y436F, and Y436S. If FBP binds in the Tyr 436 pocket in a similar fashion to the depiction in Figure 20, then mutations changing positive side chains to neutral should decrease FBP binding. Replacement of positive charges with negative charges should repulse FBP, and therefore eliminate or greatly diminish FBP binding. Creating an additional positive residue at position 406 might be expected to increase PK's affinity for FBP.

Removing the hydrogen bonding capacity of the 436 residue by creating Y436F may decrease FBP affinity. Due to the prediction that FBP binds to PK mainly through ionic interactions, the effects of the Y436F mutation was expected to be less than effects caused by altering charged residues. Substituting a serine into the 436 position, Y436S,

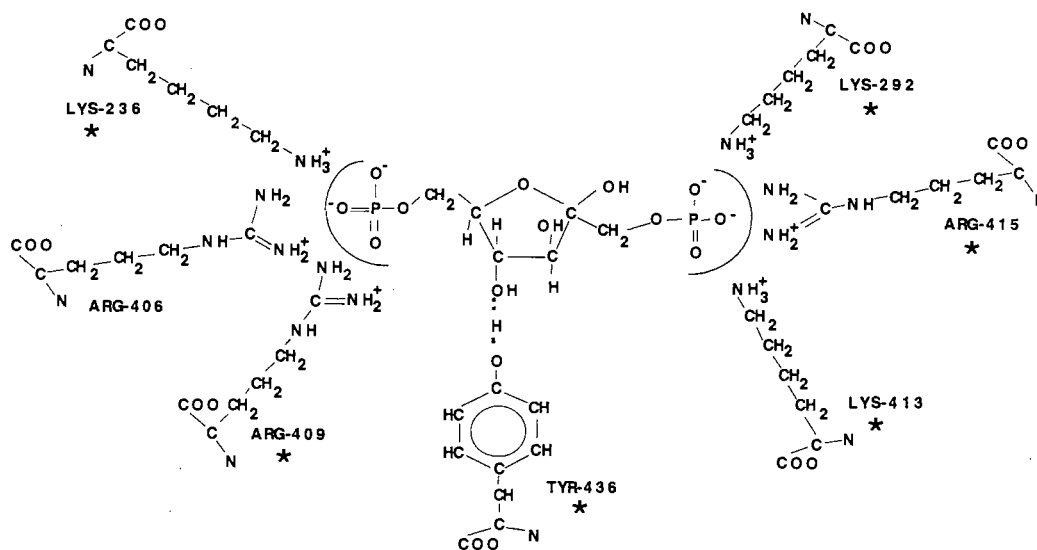


Figure 20. A Proposed FBP Docking in the Tyr 436 Pocket. At least four positive residues, two each on opposite sides of the Tyr 436 pocket, are present in any one FBP regulated isozyme of PK. Residues marked with an asterisk are present in yeast PK. Numbering and residue type are for yeast residues. FBP is orientated to allow H-bonding between tyrosine 436 and the C4 OH group of FBP.

conserves hydrogen-bonding capabilities. Y436F and Y436S could provide insight into the possible hydrogen-bonding role of the 436 position if the Tyr 436 pocket were the true FBP binding site.

K236E, K292E, R409E and R415Q were not expressed in the yeast system. As previously discussed, growth of transformed knockout yeast on glucose selects for plasmids that carry gene coding for active PK. Therefore, these amino acid replacements probably cause total loss of enzyme activity.

K413E was a functional enzyme that rescued deficient yeast growth. However, only very low levels of enzyme activity were obtained, and the standard purification scheme was not fully successful (Figure 21). For that reason, kinetic parameters of K413E were determined using protein diluted in saturated $(\text{NH}_4)_2\text{SO}_4$ (Table 6). The V_{max} of K413E is greatly reduced compared to that of wild type PK. Since the V_{max} is equivalent to maximum activity per total mg of protein, contaminating proteins can contribute to lowering this value. The reduced V_{max} of the K413E mutation may be due to contaminating proteins which can be seen using SDS-PAGE in Figure 21. K413E has no major change in response to varying FBP concentrations. Therefore no further analysis of this mutation was performed.

The mutant PK proteins K236Q, K292Q, T406R, R409Q, K413Q, Y436F, and Y436S were all successfully purified to near homogeneity by the protocol described in Materials and Methods (Figure 22). Kinetic parameters for these proteins were determined using desalted proteins (Tables 7 and 8 and Figure 23). K413Q reduces the V_{max} to less than three hundredths that of wild type PK (Figure 23). The level of contaminating proteins in purified K413Q as revealed by SDS-PAGE (Figure 22) does not support that the lowered V_{max} is due to contaminating proteins. In the absence of FBP, the V_{max} for PEP was not obtained, and therefore fitting of this curve was not possible (Figure 23). Even though K413Q's apparent affinity for PEP is greatly diminished in the absence of FBP, the apparent affinity for PEP in the presence of FBP is not different from wild type.

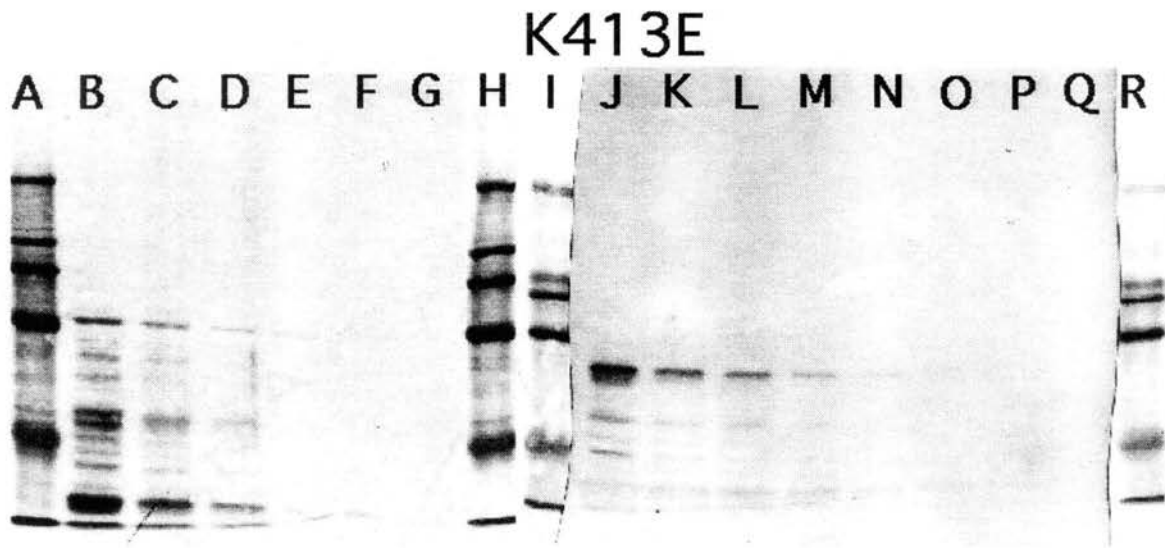


Figure 21. SDS PAGE Gel Electrophoresis Pattern of K413E. The K413E mutant protein was only partially purified by the protein purification procedure detailed in Materials and Methods. Lanes B-G and J-Q represent serial 1:1 dilutions of the partially purified protein. Protein concentrations in lanes B and J are 9.5 $\mu\text{g}/\text{lane}$. Lanes A-H, R, and I are stained with G-250 Coomassie blue. Lanes J-Q are Western blotted using Ab against yeast PK. Lanes A, H, R, and I are protein standards: Carbonic Anhydrase MW=29,000; Egg Albumin MW=45,000; Bovine Albumin MW=66,000; Phosphorylase b MW=97,400; β -Galactosidase MW=116,000; Myosin MW=205,000.

Table 6. Kinetic Parameters for Wild Type and K413E.

<u>Kinetic Property</u>	<u>Enzyme Source</u>	
	<u>Wild Type</u>	<u>K413E</u>
<u>PEP(-FBP)</u>		
V_{max} (U/mg)	113±3	1.78±0.02
$PEP_{1/2}$ (mM)	1.4±0.1	1.04±0.02
n_H	1.8±0.1	2.1±0.1
<u>PEP(+FBP)</u>		
V_{max} (U/mg)	122±2	1.90±0.02
$PEP_{1/2}$ (mM)	0.12±0.01	0.102±0.005
n_H	1.0±0.1	1.1±0.1
<u>FBP</u>		
V_{max} (U/mg)	89±2	1.46±0.01
$FBP_{1/2}$ (mM)	0.039±0.002	0.046±0.001
n_H	1.5±0.1	1.3±0.1

The kinetic properties of wild type and K413E yeast PK were determined as described in Figure 11 and in the Materials and Methods using enzyme preparations stored in saturated ammonium sulfate. FBP activation of wild type and K413E PK's were determined in the presence of 0.67 mM and 0.46 mM PEP, respectively.

K292Q, R409Q, Y436F, and Y436S also have effects on the V_{\max} (Tables 7 and 8). Of these mutants, Y436F has the largest effect with a V_{\max} one third that of the wild type. Concentrations of contaminating proteins in these mutant PK's as revealed by SDS-PAGE do not support that the low V_{\max} values are due to contaminating proteins (Figure 22). R409Q and K236Q both have $S_{1/2}$ of FBP activation that are three fold higher than that of wild type PK (Table 7).

However, the lack of predicted large effects of mutations on apparent affinity for FBP do not support the Tyr 436 pocket as the FBP binding site. R409Q and K236Q may have some importance in the allosteric regulation by FBP, however the effects of these mutations are relatively small. Therefore further studies with these mutations were not pursued in this investigation.

The Arg 42 Pocket: A-C Domain Contacts

The Arg 42 pocket was also probed by mutagenesis as a possible FBP binding site. Within the Arg 42 pocket two positive groups were identified for mutagenesis. Creating R77Q and R19Q mutated these two positive residues. Both arginine 77 and arginine 19 were mutated to glutamine to neutralize the positive charge while maintaining the hydrophilic nature of the side chain. If FBP binds in the Arg 42 pocket by interactions with arginine 77 or arginine 19, then mutations changing positive to neutral amino acids should decrease FBP binding.

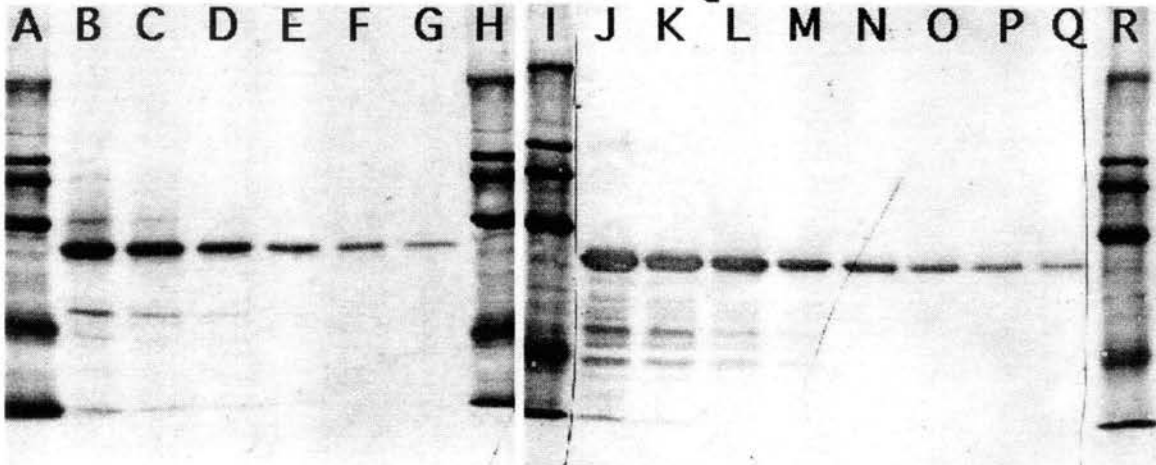
Expression of the R19Q mutation was not obtained, suggesting the protein is inactive. The R77Q mutation was obtained and purified (Figure 24). The kinetic parameters for R77Q are very similar to those for the wild type enzyme (Table 9). No further analysis of this mutation was performed.

C-C Interface Interactions

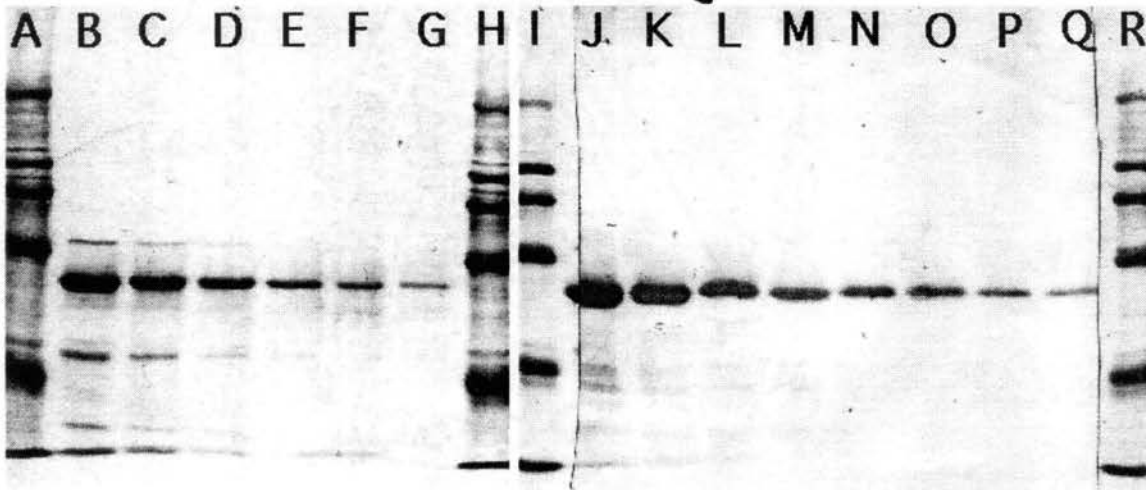
Yeast PK's activity response to PEP is sigmoidal. The sigmoidal shaped response curve indicates communication between PEP binding sites (53,54). In the presence of FBP the response to increasing PEP concentrations becomes hyperbolic indicating that

Figure 22. SDS PAGE Gel Electrophoresis Pattern of K236Q, K292Q, T406R, R409Q, K413Q, Y436F, and Y436S. Lanes B-G and J-Q represent serial 1:1 dilutions of purified proteins. Protein concentrations in lanes B and J for K236Q, K292Q, T406R, R409Q, K413Q, Y436F, and Y436S are 3.4, 3.2, 3.0, 11, 13, 3.8, and 2.1 $\mu\text{g}/\text{lane}$, respectively. Lanes A-H, R, and I are stained with G-250 Coomassie blue. Lanes J-Q are Western blotted. Lanes A, H, R, and I are protein molecular weight standards: Carbonic Anhydrase MW=29,000; Egg Albumin MW=45,000; Bovine Albumin MW=66,000; Phosphorylase b MW=97,400; β -Galactosidase MW=116,000; Myosin MW=205,000.

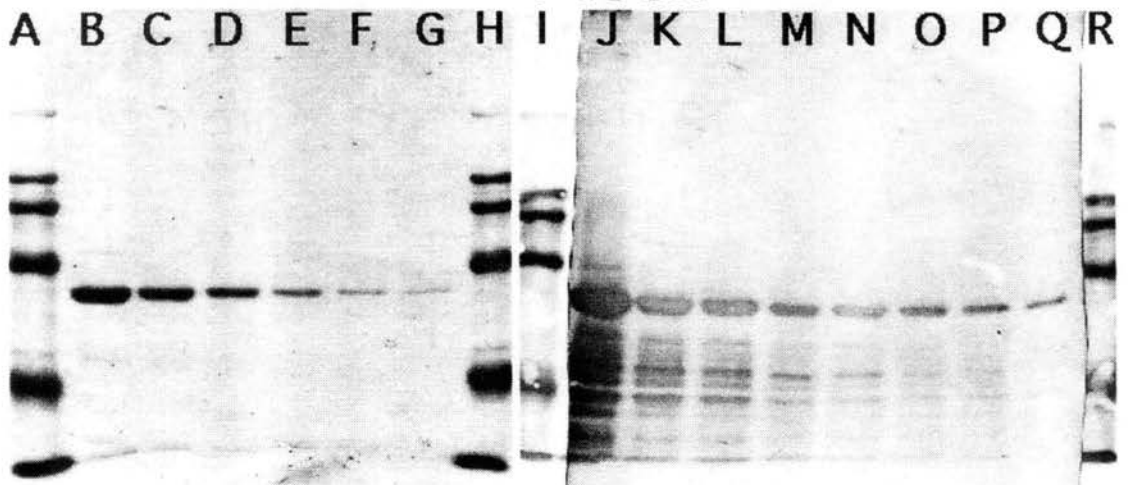
K236Q



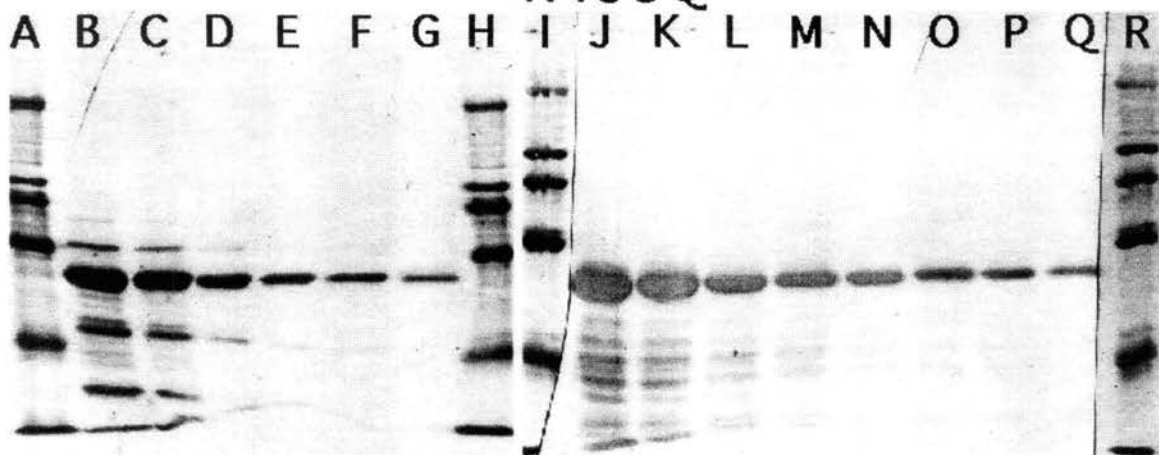
K292Q



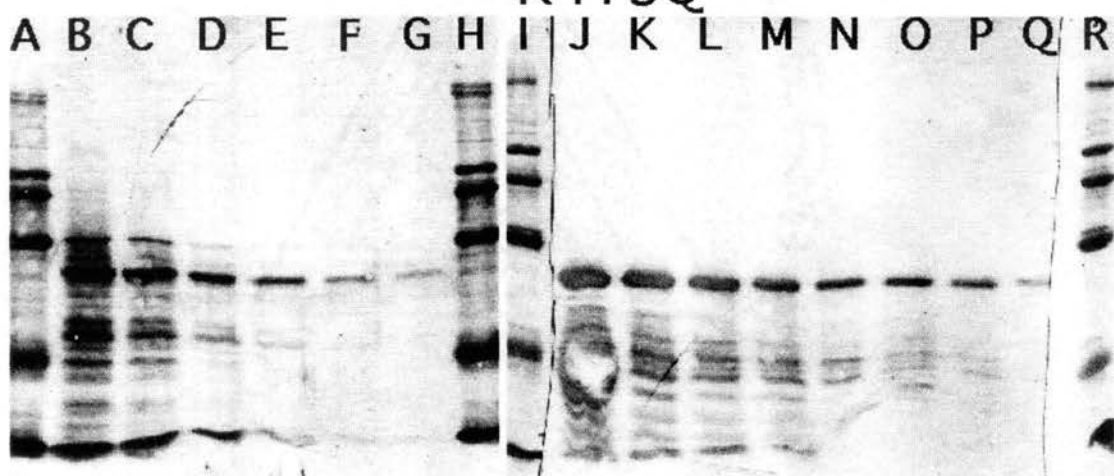
T406R



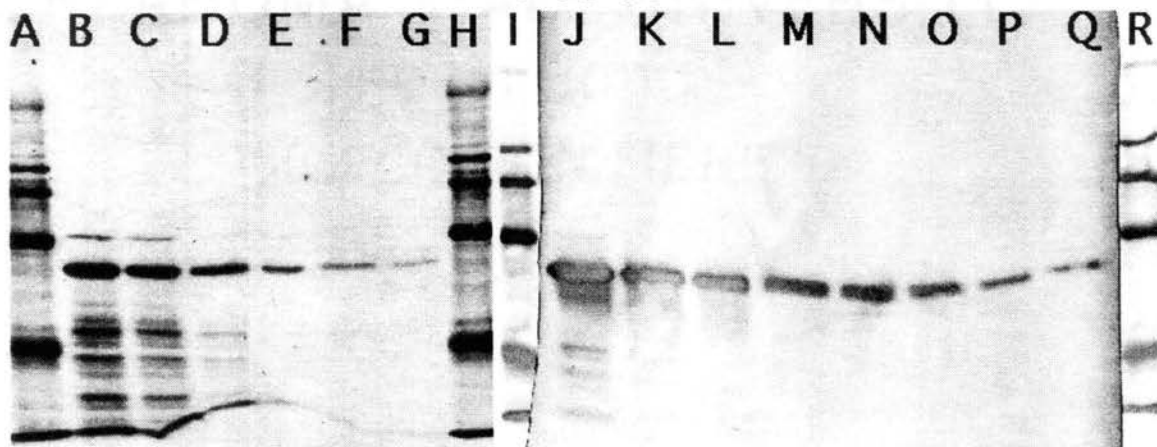
R409Q



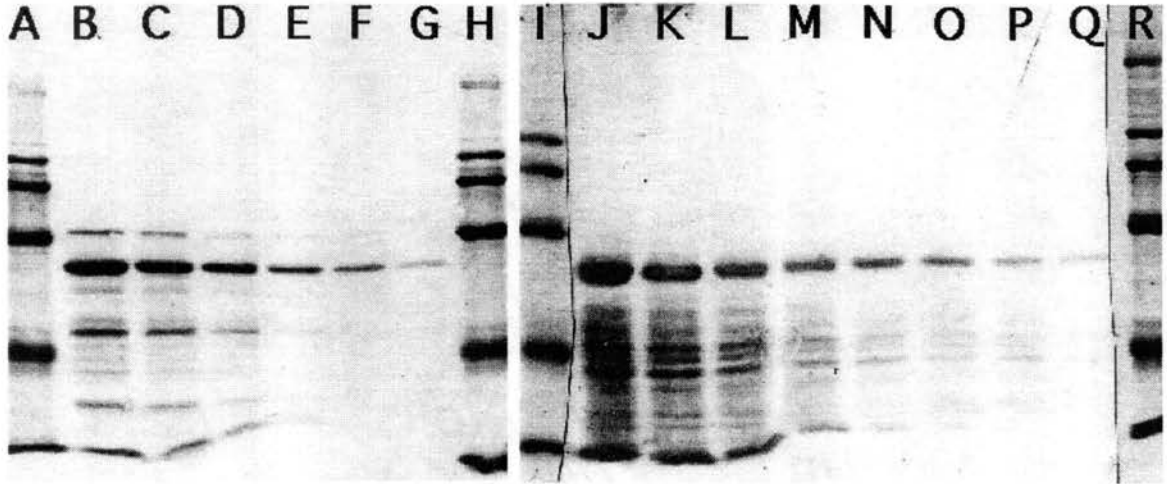
K413Q



Y436F



Y436S



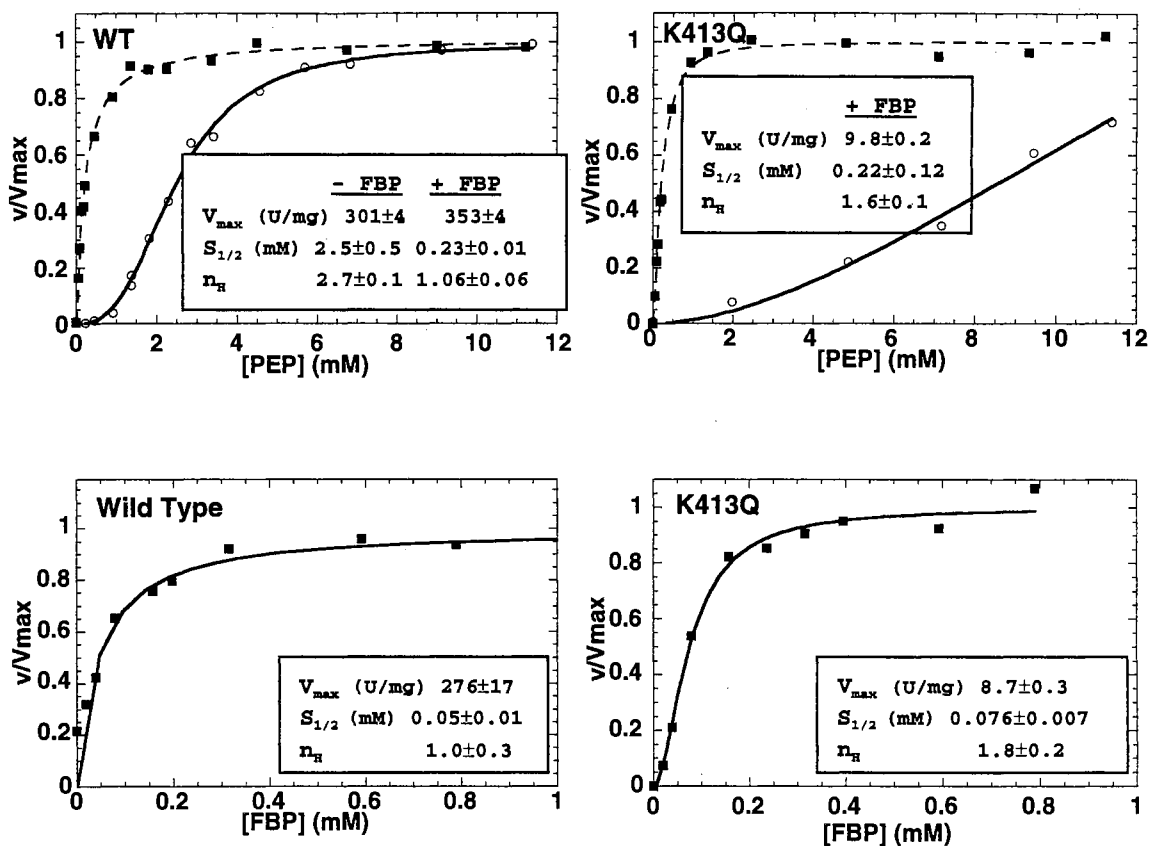


Figure 23. Kinetic Properties of Wild Type and K413Q. The catalytic activity (v) of purified wild type PK was measured at varying concentrations of PEP and FBP as described in Figure 11 and Materials and Methods using desalted protein preparations. Data presented is relative velocity (v/V_{max}) to normalize presentation of the results. Varying concentrations of PEP are without (O) or with 2.4 mM FBP (■). FBP activation of wild type and K413Q were in the presence of 1.9 mM and 3.5 mM PEP, respectively. Kinetic parameters determined by fitting the results to the Hill equation are presented in the inserts.

Table 7. Kinetic Parameters for Wild Type and Mutations of Positive Residues of the Tyr 436 Pocket.

<u>Kinetic Property</u>	<u>Enzyme Source</u>			
	<u>Wild Type</u>	<u>K292Q</u>	<u>R409Q</u>	<u>K236Q</u>
<u>PEP(-FBP)</u>				
V_{max} (U/mg)	301±4	140±5	168±4	393±12
$PEP_{1/2}$ (mM)	2.5±0.5	3.6±0.2	4.1±0.1	1.6±0.1
n_H	2.7±0.1	2.6±0.2	2.4±0.2	2.1±0.2
<u>PEP(+FBP)</u>				
V_{max} (U/mg)	353±4	172±3	185±2	399±9
$PEP_{1/2}$ (mM)	0.23±0.01	0.25±0.08	0.29±0.02	0.33±0.03
n_H	1.1±0.1	0.97±0.07	1.2±0.1	0.75±0.04
<u>FBP</u>				
V_{max} (U/mg)	276±17	119±5	158±5	269±13
$FBP_{1/2}$ (mM)	0.05±0.01	0.090±0.008	0.15±0.01	0.16±0.02
n_H	1.0±0.3	1.8±0.2	1.6±0.2	1.5±0.1

The kinetic properties of various yeast PK's were determined as described in Figure 11 and in the Materials and Methods using desalted protein preparations. FBP activation of wild type, K292Q, R409Q, and K236Q were in the presence of 1.9 mM, 1.4 mM, 1.6 mM, and 0.46 mM PEP, respectively.

Table 8. Kinetic Parameters for Wild Type and Mutations of Non-Positive Residues of the Tyr 436 Pocket.

Kinetic Property	Enzyme Source			
	Wild Type	T406R	Y436F	Y436S
PEP (-FBP)				
V_{max} (U/mg)	301±4	334±6	117±3	219±5
$PEP_{1/2}$ (mM)	2.5±0.5	2.2±0.1	3.0±0.1	1.3±0.1
n_H	2.7±0.1	2.0±0.1	2.3±0.2	2.1±0.2
PEP (+FBP)				
V_{max} (U/mg)	353±4	333±8	122±4	223±3
$PEP_{1/2}$ (mM)	0.23±0.01	0.27±0.03	0.21±0.03	0.22±0.01
n_H	1.1±0.1	0.87±0.08	0.83±0.10	1.0±0.1
FBP				
V_{max} (U/mg)	276±17	200±4	90±3	117±5
$FBP_{1/2}$ (mM)	0.05±0.01	0.049±0.004	0.064±0.006	0.076±0.009
n_H	1.0±0.3	1.1±0.1	1.4±0.2	1.8±0.3

The kinetic properties of various yeast PK's were determined as described in Figure 11 and in the Materials and Methods using desalted protein preparations. FBP activation of wild type, T406R, Y436F, and Y436S were in the presence of 1.9 mM, 1.4 mM, 1.4 mM, and 0.46 mM PEP, respectively.

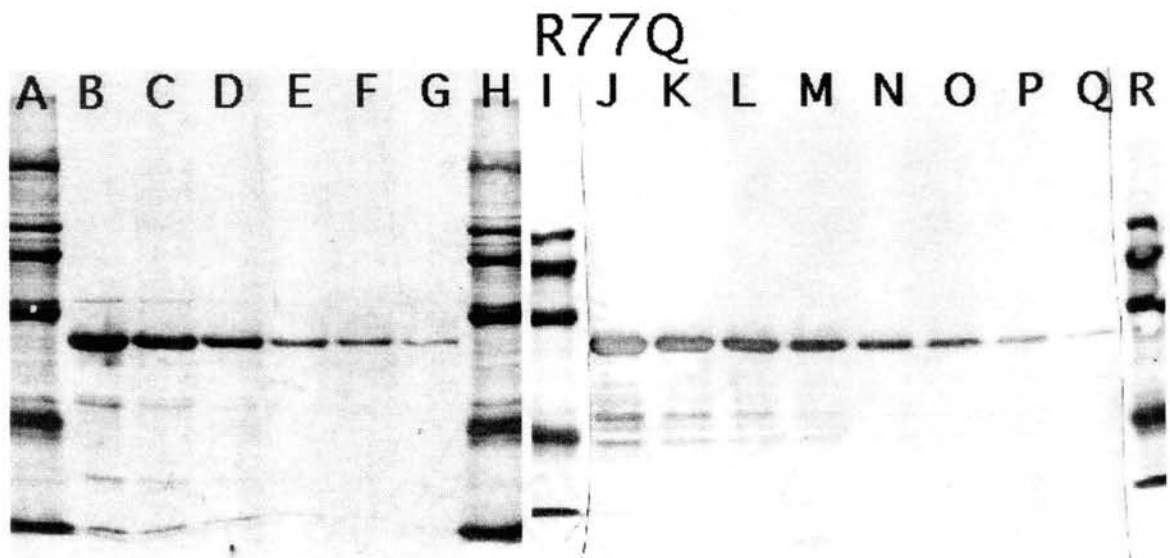


Figure 24. SDS PAGE Gel Electrophoresis of R77Q. Lanes B-G and J-Q represent serial 1:1 dilutions of purified protein. Protein concentrations in lanes B and J are 3.1 $\mu\text{g}/\text{lane}$. Lanes A-H, R, and I are stained with G-250 Coomassie blue. Lanes J-Q are Western. Lanes A, H, R, and I are protein molecular weight standards: Carbonic Anhydrase MW=29,000; Egg Albumin MW=45,000; Bovine Albumin MW=66,000; Phosphorylase b MW=97,400; β -Galactosidase MW=116,000; Myosin MW=205,000.

Table 9. Kinetic Parameters for Wild Type and R77Q.

<u>Kinetic Property</u>	<u>Enzyme Source</u>	
	<u>Wild Type</u>	<u>R77Q</u>
<u>PEP(-FBP)</u>		
V_{\max} (U/mg)	301±4	256±5
$PEP_{1/2}$ (mM)	2.5±0.5	3.5±0.1
n_H	2.7±0.1	2.4±0.1
<u>PEP(+FBP)</u>		
V_{\max} (U/mg)	353±4	292±3
$PEP_{1/2}$ (mM)	0.23±0.01	0.28±0.01
n_H	1.1±0.1	0.86±0.04
<u>FBP</u>		
V_{\max} (U/mg)	276±17	254±8
$FBP_{1/2}$ (mM)	0.05±0.01	0.048±0.006
n_H	1.0±0.3	1.1±0.1

The kinetic properties of wild type and R77Q yeast PK were determined as described in Figure 11 and in the Materials and Methods using desalted protein preparations. FBP activation of wild type and R77Q were in the presence of 1.9 mM PEP.

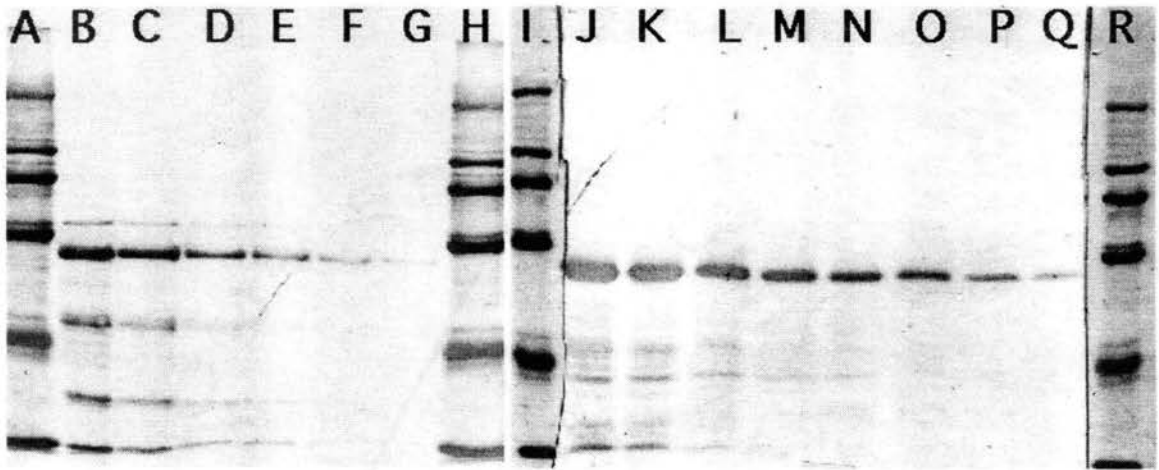
communication has been altered. Since only one PEP binding site is present per monomer, communication between binding sites must involve subunit contacts. Subunit interfaces are therefore important to allosteric regulation of PK by FBP. Yeast PK has two types of subunit interfaces. One or both types of interfaces may be important in allosteric regulation.

Studies previously reported in the literature for PK from several species were considered in order to select C-C interface residues to probe in the yeast enzyme. Mutation of alanine (at a position equivalent to yeast 369) in rat M1 PK to arginine shifts the hyperbolic PEP kinetic response to a sigmoidal response (77). Mutation of a cysteine (at a position equivalent to yeast 394) in rat M2 PK to leucine shifts the sigmoidal normal kinetic response to varying PEP concentrations to a hyperbolic response (76). The yeast residue 394 is not conserved with the equivalent residue of mammalian M1 or M2 PK's. However, upon examination of the region immediately adjacent to 394, a glutamic acid residue (position #392) which appears to interact with the neighboring subunit was identified. Jurica *et al.* (20) and Friesen *et al.* (111) have both noted the involvement of residues equivalent to 392 in hydrogen bonds across the C-C subunit interface in yeast and mammalian isozymes, respectively. Based on the work with the M1 and M2 isozymes, two sites within the C-C interface were selected for probing this interface in the yeast PK. Mutations R369A and E392A were created as probes at these sites.

R369A was successfully purified (Figure 25). However, this mutation causes the protein to lose stability when desalted. Therefore, this mutation's kinetic parameters were determined using protein diluted in saturated $(\text{NH}_4)_2\text{SO}_4$ (Table 10). R369A has a V_{max} one third that of wild type PK. The level of contaminating proteins in purified R369A as revealed by SDS-PAGE (Figure 25) does not support that the lowered V_{max} is due to contaminating proteins. The decreased V_{max} may be due in part to the reduced stability of this mutant. R369A's $S_{1/2}$ for FBP activation is triple that of wild type PK. The R369A mutation may provide more detail about allosteric regulation in the future. However the effects of R369A

Figure 25. SDS PAGE Gel Electrophoresis of R369A and E392A. Lanes B-G and J-Q represent serial 1:1 dilutions of purified proteins. Protein concentrations in lanes B and J of R369A and E392A are 6.1 and 3.7 $\mu\text{g}/\text{lane}$, respectively. Lanes A-H, R, and I are stained with G-250 Coomassie blue. Lanes J-Q are Western blotted. Lanes A, H, R, and I are protein molecular weight standards: Carbonic Anhydrase MW=29,000; Egg Albumin MW=45,000; Bovine Albumin MW=66,000; Phosphorylase b MW=97,400; β -Galactosidase MW=116,000; Myosin MW=205,000.

R369A



E392A

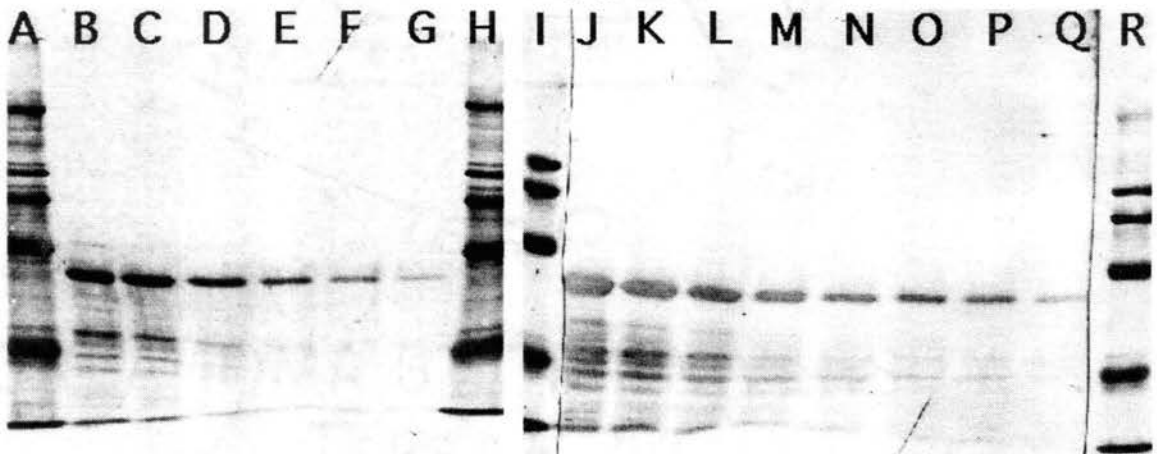


Table 10. Kinetic Parameters for Wild Type and R369A.

<u>Kinetic Property</u>	<u>Enzyme Source</u>	
	<u>Wild Type</u>	<u>R369A</u>
<u>PEP(-FBP)</u>		
V_{max} (U/mg)	113±3	39±0.6
$PEP_{1/2}$ (mM)	1.4±0.1	2.6±0.1
n_H	1.8±0.1	3.7±0.1
<u>PEP(+FBP)</u>		
V_{max} (U/mg)	122±2	38±3
$PEP_{1/2}$ (mM)	0.12±0.01	0.12±0.03
n_H	1.0±0.1	1.3±0.5
<u>FBP</u>		
V_{max} (U/mg)	89±2	41±2
$FBP_{1/2}$ (mM)	0.039±0.002	0.13±0.02
n_H	1.5±0.1	1.1±0.1

The kinetic properties of wild type and R369A yeast PK were determined as described in Figure 11 and in the Materials and Methods using enzyme preparations stored in saturated ammonium sulfate. FBP activation of wild type and R369A were in the presence of 1.9 mM and 1.2 mM PEP, respectively.

on allosteric regulation by FBP was relatively small and therefore further studies with this mutation was not pursued in this investigation.

The E392A mutant was successfully purified (Figure 25). E392A causes the sigmoidal PEP dependent kinetic response ($n_H=2.7\pm 0.1$; wild type) to become hyperbolic ($n_H=1.25\pm 0.03$; E392A) (Figure 26). E392A's $S_{1/2}$ for PEP in the absence of FBP is similar to wild type's $S_{1/2}$ for PEP in the presence of FBP. The E392A mutant is totally unresponsive to FBP. FBP binding was determined for E392A by the fluorescence quench titration described in Materials and Methods (Figure 27). The fluorescence response to FBP both with and without PEP is hyperbolic. The $[FBP]_{1/2}$ of E392A is unresponsive to PEP.

A-A Interface Interactions

As with C-C interface interactions, observations from the literature were used to select A-A interface residues, which might be important to allosteric regulation of yeast PK. A glutamine to asparagine mutation in PK of *Bacillus stearothermophilus*, at a position equivalent to yeast PK 299, alters activation by ribose-5-phosphate (59). Recreating a hemolytic anemia mutation (PK Tokyo; threonine to methionine at a position equivalent to yeast PK 311) in the mammalian M2 isozyme was reported to cause a loss of sensitivity to allosteric activation by FBP and allosteric inhibition by phenylalanine (79,80). In the present study, Q299N and T311M mutants of yeast PK were generated to probe the A-A domain contacts role in FBP regulation of yeast PK.

Both Q299N and T311M were unstable through the standard purification procedure. Therefore, crude extracts were used to screen kinetic parameters of these mutants. After enzymatic yeast lysis and separation of cell debris as described for the protein purification, a 65% ammonium sulfate precipitation of proteins was used as the only purification step. Purity of crude extracts of Q299N and T311M was not characterized by SDS-PAGE.

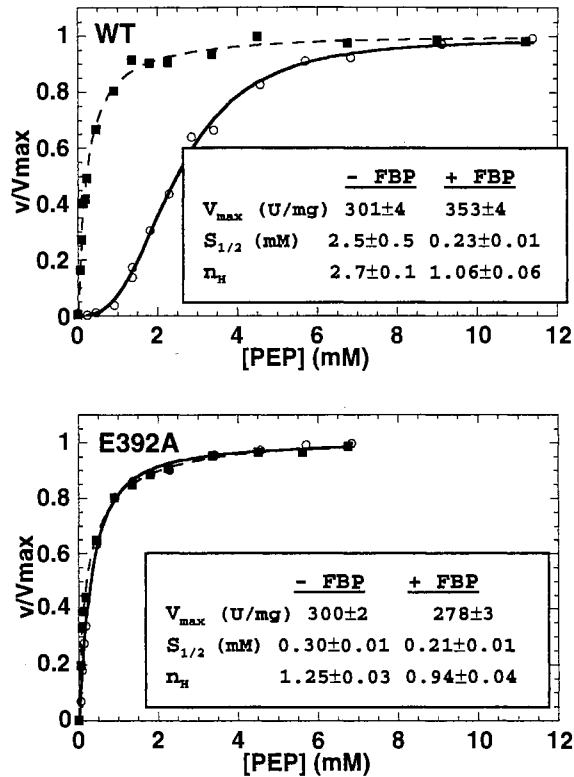
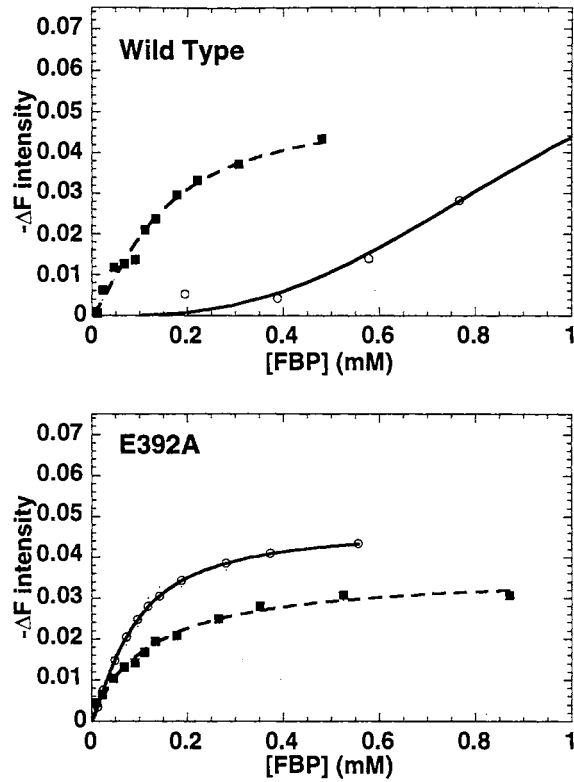


Figure 26. Kinetic Properties of Wild Type and E392A. The catalytic activity (v) of purified wild type and E392A was measured at varying concentrations of PEP as described in Figure 11 and Materials and Methods using desalted protein preparations. Data presented is relative velocity (v/V_{max}) to normalize presentation of the results. Varying concentrations of PEP are without (○) or with 2.4 mM FBP (■). Kinetic parameters determined by fitting the results to the Hill equation are presented in the inserts.



	Wild Type (- PEP)	Wild Type (+ PEP)	E392A (- PEP)	E392A (- PEP)
$-\Delta F_{\max}$	0.085	0.050	0.048	0.037
$FBP_{1/2}$ (mM)	0.98 ± 0.03	0.14 ± 0.01	0.09 ± 0.01	0.12 ± 0.02
n_H	2.9 ± 0.2	1.4 ± 0.1	1.3 ± 0.2	1.0 ± 0.1

Figure 27. Fluorescence Quench Titration Curves for Wild Type and E392A. Fluorescence emission responses were determined at varying concentrations of FBP in the absence (○) and presence (■) of 15 mM PEP as described in Figure 14. $-\Delta F$ values are per $\mu\text{g/ml}$ protein. Binding parameters obtained by fitting the fluorescence data to the Hill equation are presented in the insert.

Since a crude extract of Q299N was used to determine kinetic parameters (Figure 28), a turnover number could not be calculated. The $S_{1/2}$ for PEP in the absence of FBP, the $S_{1/2}$ for FBP activation, and the $S_{1/2}$ for ADP in the presence of FBP are three times the corresponding parameters of wild type PK. The $S_{1/2}$ for ADP is responsive to FBP in contrast to the unresponsive wild type. Haeckel *et al.* has previously reported altered ADP kinetics when PEP concentrations are less than saturating (41). To insure the FBP response of the ADP dependent kinetic curve is not due to less than saturating PEP, ADP curves were also determined in the presence of 22 mM PEP (Table 11). Increasing PEP does not have any significant effects. Even though this mutation causes very interesting changes in kinetic parameters, instability of the protein has hindered efforts for its purification, which will be needed for further study.

Crude extracts of T311M also show changes in a large number of kinetic parameters. Therefore, further efforts to purify T311M were pursued. The pH of the DEAE cellulose batch binding was decreased to 6.8. With all other purification steps unchanged from the protocol described in Materials and Methods, a purified protein was obtained (Figure 29).

Kinetic parameters for desalted purified T311M were determined (Figure 30). No activity is observed for this mutation in the absence of FBP under the standard assay conditions. In the presence of FBP, the V_{max} for T311M PK is less than one-half that of wild type PK. The level of contaminating proteins in purified T311M as revealed by SDS-PAGE (Figure 29) does not support that the lowered V_{max} is due to contaminating proteins. The $S_{1/2}$ for PEP with FBP and the $S_{1/2}$ for FBP activation are increased compared to wild type PK. In the presence of 2.4 mM FBP, T311M's kinetic response to varying concentrations of ADP and PEP are sigmoidal. The kinetic response to increasing FBP concentrations is also sigmoidal.

Figure 28. Kinetic Properties of Wild Type and Crude Extracts of Q299N. The catalytic activity (v) of purified wild type PK was measured at varying concentrations of substrates (PEP and ADP) and allosteric activator (FBP) as described in Figure 11 and Materials and Methods using enzyme preparations stored in saturated ammonium sulfate. Data presented is relative velocity (v/V_{\max} or $v/\text{MaxVelocity}$) to normalize presentation of the results. MaxVelocity of the Q299N is the maximum velocity obtained/ μl of crude extract. Varying concentrations of PEP and ADP are without (○) or with 2.4 mM FBP (■). To obtain ADP response curves ADP was varied at constant 12 mM PEP. FBP activation of wild type and Q299N were in the presence of 0.67 mM and 2.3mM PEP, respectively. Kinetic parameters determined by fitting the results to the Hill equation are presented in the inserts.

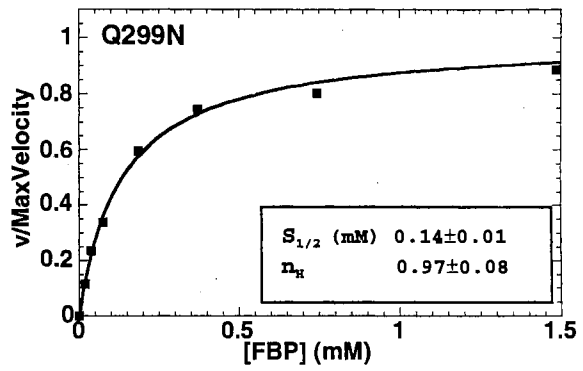
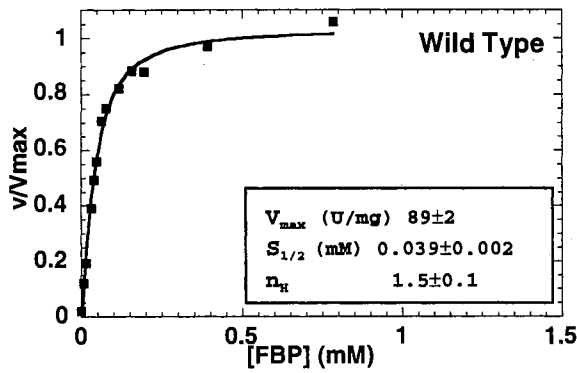
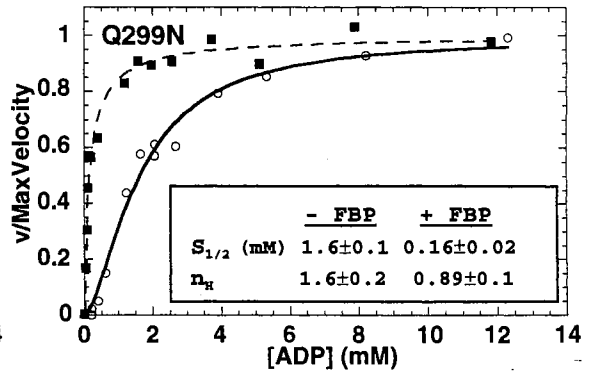
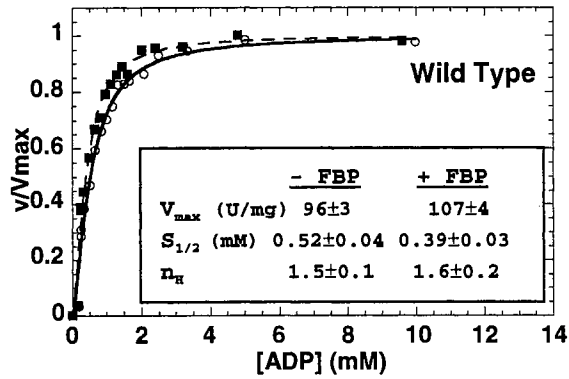
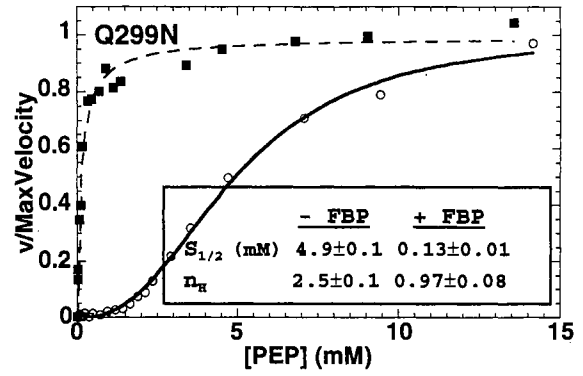
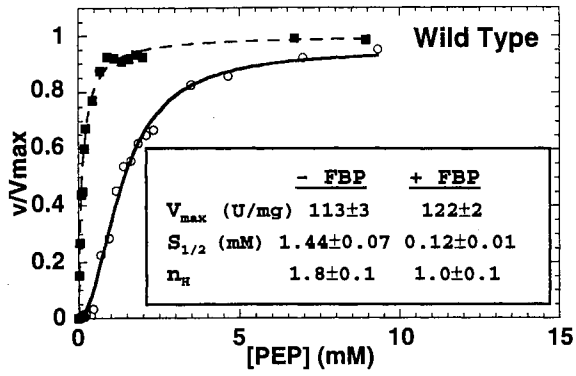


Table 11. ADP Kinetic Parameters for Wild Type and Crude Extracts of Q299N.

<u>Kinetic Property</u>	<u>FBP</u>	<u>Enzyme Source</u>		
		<u>Wild Type</u>	<u>Q299N (12mM PEP)</u>	<u>Q299N (22mM PEP)</u>
$S_{i/2}$ ADP (mM)	-	0.52±0.04	1.6±0.1	1.6±0.1
n_H ADP	-	1.5±0.1	1.6±0.2	1.6±0.1
$S_{i/2}$ ADP (mM)	+	0.39±0.03	0.16±0.02	0.22±0.04
n_H ADP	+	1.6±0.2	0.89±0.1	0.92±0.15

ADP dependent kinetic properties of wild type and crude extracts of Q299N were determined as described in Figure 11 and in the Materials and Methods using enzyme preparations stored in saturated ammonium sulfate. Wild Type PK was assayed in the presence of 12 mM PEP. Q299N was assayed in the presence of 12 mM and 22 mM PEP, as shown.

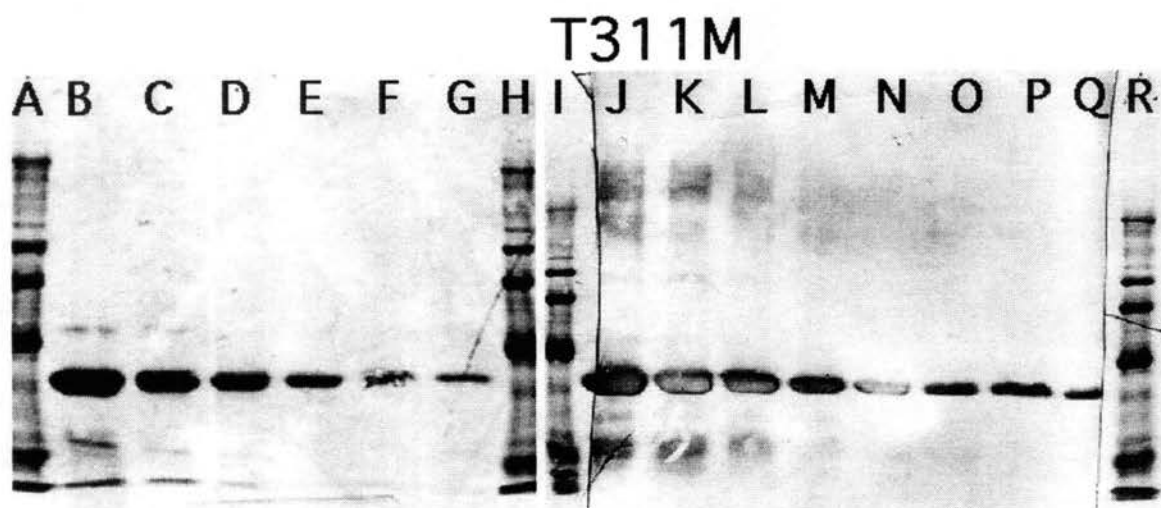
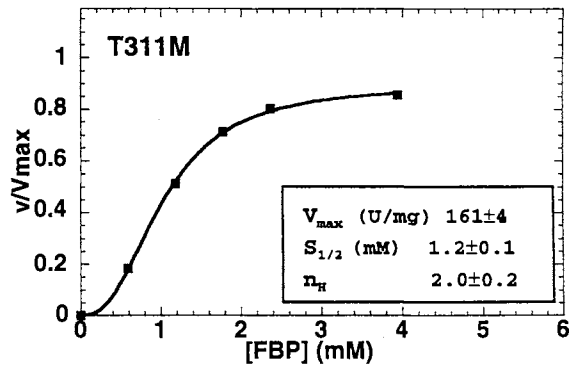
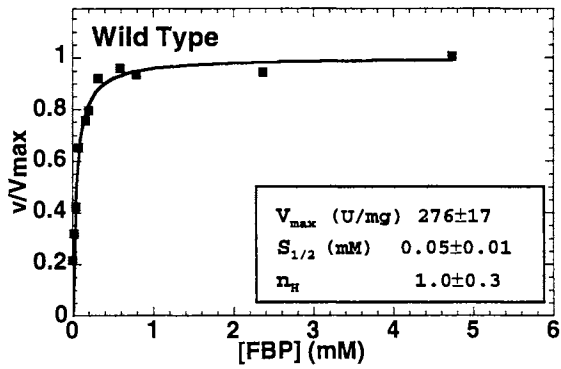
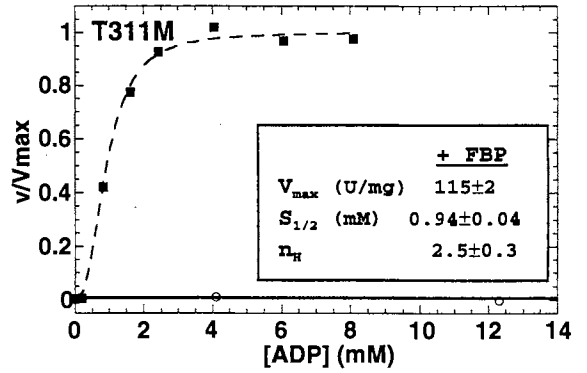
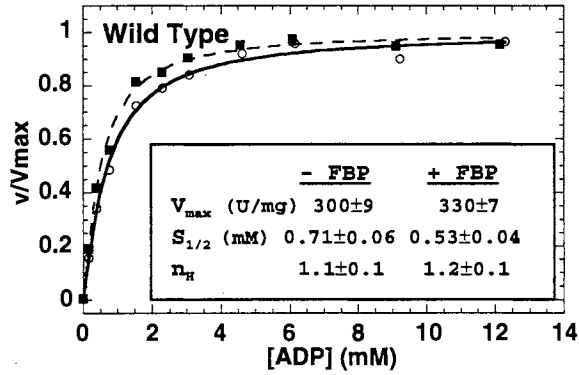
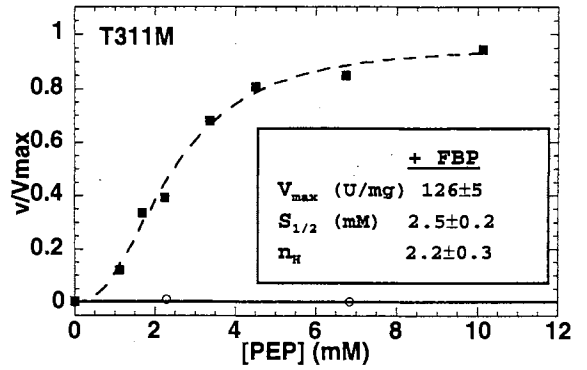
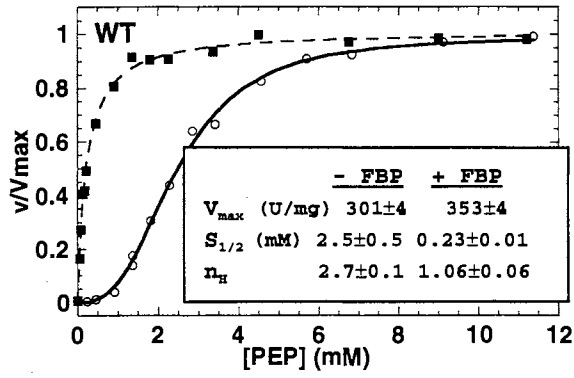


Figure 29. SDS PAGE Gel Electrophoresis Pattern of T311M. To purify T311M DEAE-cellulose was preformed at pH 6.8. All other purification steps for T311M were as described in Materials and Methods. Lanes B-G and J-Q represent serial 1:1 dilutions of purified protein. Protein concentrations in lanes B and J are 13 $\mu\text{g}/\text{lane}$. Lanes A-H, R, and I are stained with G-250 Coomassie blue. Lanes J-Q are Western blotted. Lanes A, H, R, and I are protein molecular weight standards: Carbonic Anhydrase MW=29,000; Egg Albumin MW=45,000; Bovine Albumin MW=66,000; Phosphorylase b MW=97,400; β -Galactosidase MW=116,000; Myosin MW=205,000.

Figure 30. Kinetic Properties of Wild Type and Purified T311M. The catalytic activity (v) of wild type and T311M was measured at varying concentrations of substrates (PEP and ADP) and allosteric activator (FBP) as described in Figure 11 and Materials and Methods using desalted protein preparations. Data presented is relative velocity (v/V_{\max}) to normalize presentation of the results. Varying concentrations of PEP and ADP are without (○) or with 2.4 mM FBP (■). To obtain ADP response curves ADP was varied at constant 12 mM PEP. FBP activation of wild type and T311M were in the presence of 1.9 mM and 21 mM PEP, respectively. Kinetic parameters determined by fitting the results to the Hill equation are presented in the inserts.



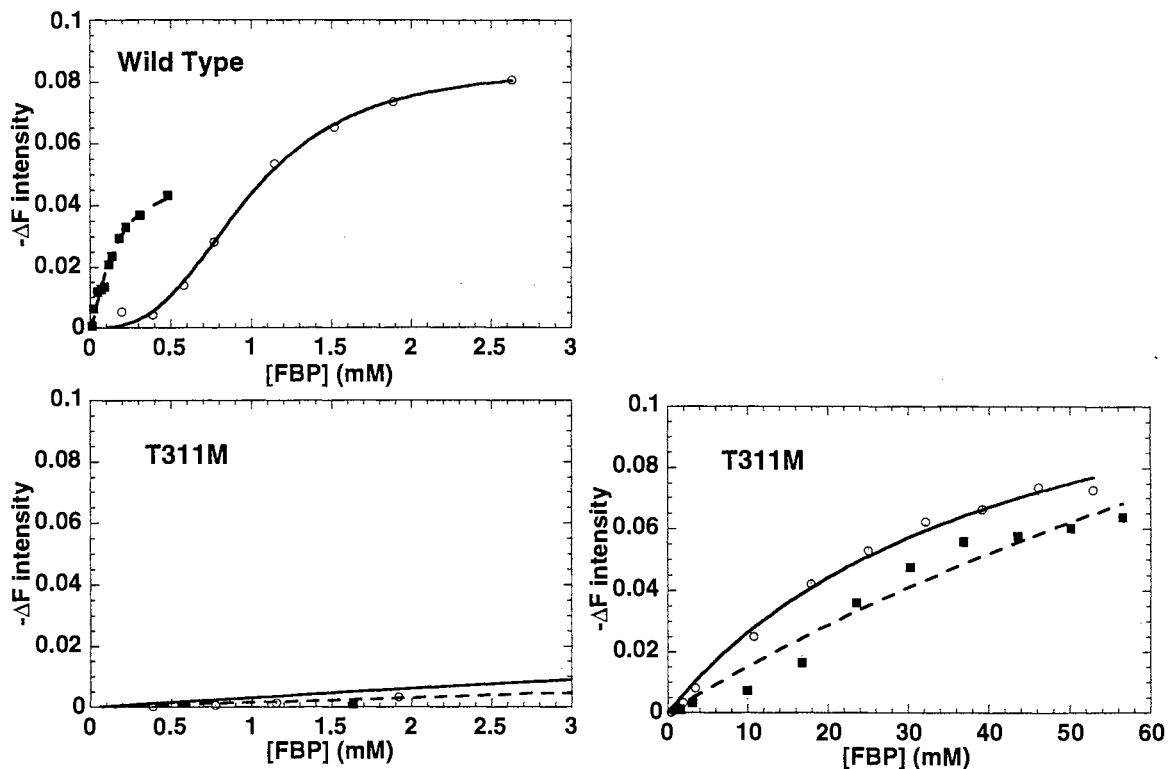


Figure 31. Fluorescence Quench Titration Curves for Wild Type and T311M. Fluorescence emission responses were determined at varying concentrations of FBP in the absence (○) and presence (■) of 15 mM PEP as described in Figure 14. $-\Delta F$ values are per $\mu\text{g/ml}$ protein. Lines on graphs of T311M data are to show general pattern of data. The fluorescence emission response of T311M is shown on two scales.

FBP binding was determined for T311M by the fluorescence quench titration described in Materials and Methods (Figure 31). Maximum binding was not obtained and the data was not fit to the Hill equation for this study.

Fructose-1,6-Bisphosphate Binding Site Mutants

Probing the FBP binding site of PK can provide insight into the mechanism by which FBP triggers an allosteric response. After the initiation of this study, the FBP binding site was identified by co-crystallization of FBP with yeast PK (20). Analysis of the electron density shows the 6'-phosphate of FBP is bound by a loop through hydrogen bond interactions (Figure 32). In yeast PK, serine 402, serine 404, and threonine 407 from the flexible loop are all involved in this interaction. The 1'-phosphate group of FBP is bound to arginine 459 through a strong electrostatic interaction (20).

Sequence differences in the 6'-phosphate binding loop may be responsible for different affinities of various isozymes for FBP reported in the literature. Sequence comparisons show that the threonine 403 position corresponds to the final residue of differences between mammalian M1 and M2 isozymes. Rat M2 has a lysine at this site, while rat M1 has a glutamic acid. A potential ionic bond between a positive charged amino acid at position 403 and the 6'-phosphate of FBP may increase yeast PK's affinity for the activator. A negative charge at position 403 could potentially mimic the effect of FBP. The possibility of a negative charge at 403 activating PK in the absence of FBP has also been proposed by Jurica *et al.*(20). To test the effects of positive and negative charges residues at the 403 position, two mutations were created: substitution by lysine to mimic rat M2 PK, and substitution by glutamic acid to mimic rat M1 PK.

Chemical modification studies previously predicted that a lysine in *E. coli* PK, at a position equivalent to yeast PK threonine 406, is involved in FBP binding (72,73). A potential ionic bond between a positive charged amino acid at position 406 and the 6'-phosphate of FBP may increase yeast PK affinity for the activator. T406R was created to test this possibility.

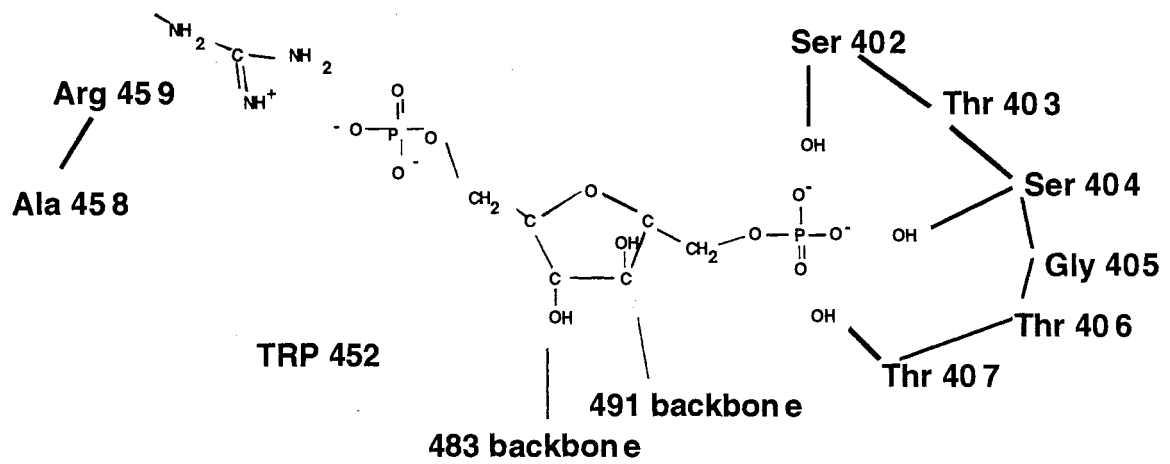


Figure 32. The FBP Binding Site as Resolved by Co-Crystallization to Yeast PK.

Recreated from Jurica *et al.* (20).

The 1'-phosphate group of FBP is bound to arginine 459 through a strong electrostatic interaction as shown by X-ray crystallography (20). Since arginine 459 is not conserved in all FBP regulated species, a central role of arginine 459 in FBP's regulation of PK activity has been questioned (20). To test the role of the positive charge of arginine 459 in the allosteric activation of yeast PK by FBP, the mutation R459Q was created.

Rat liver PK has a positive residue at a position equivalent to yeast PK 458. The crystal structure would not predict that an arginine at this position would interact in the FBP binding site (20). However, the chemical nature of the side chain may influence the peptide conformation at the FBP binding site. Thus, an additional charge at position 458 might enhance PK's affinity for FBP. To test a possible role of a positive charge at position 458, A458K was created.

The mutant PK proteins T403E, T403K, T406R, A458K, and R459Q were all successfully generated and purified (Figure 33). Kinetic parameters for these mutants determined using desalted proteins are presented in Figure 34 and Table 12. The effects of T403K, T406R, and A458R on kinetic properties of yeast PK appear to be minimal (Table 12), although the A458R mutation may have a slightly increased V_{max} . These mutants were not further studied.

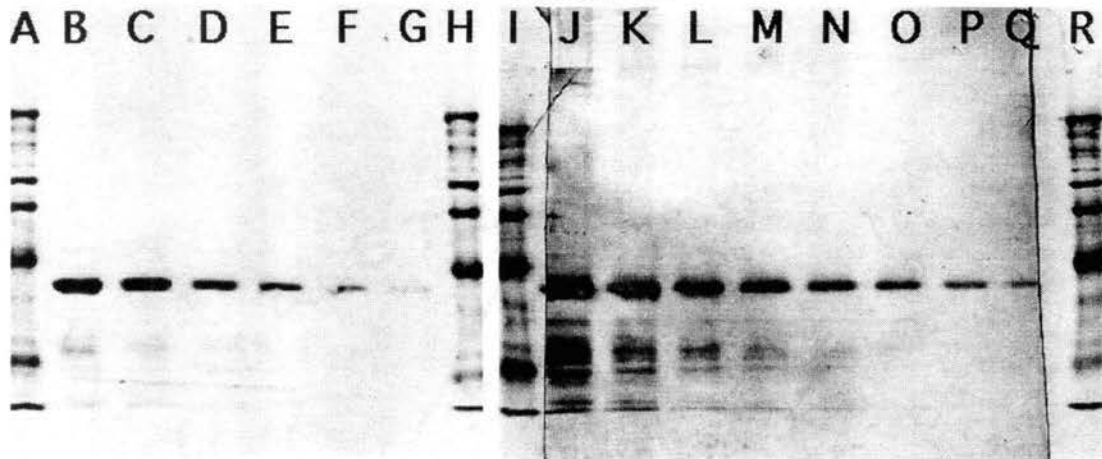
Interestingly, the T403E and R459Q mutant PK's do not respond to FBP. However, the kinetic response of T403E and R459Q to increasing concentrations of PEP is quite similar to that of the wild type enzyme (Figure 34). Fluorescence quench titrations for both T403E and A459Q indicate that the affinity of these mutant PK's for FBP is greatly reduced (Figure 35). A maximum change in fluorescence was not obtained for either mutation at high FBP concentrations and complete binding analysis was not computed.

Fructose-1,6-Bisphosphate Analogs

Mutational studies detailed above indicate that arginine 459 is important for allosteric activation by FBP. FBP analogs were used to further probe regions of the activator important to allosteric regulation. If interactions between arginine 459 and the

Figure 33. SDS PAGE Gel Electrophoresis of T403E, T403K, T406R, A458K, and R459Q. Lanes B-G and J-Q represent serial 1:1 dilutions of purified proteins. Protein concentrations in lanes B and J of T403E, T403K, T406R, A458K, and R459Q are 9.1, 6.4, 3.0, 9.7, and 5.0 $\mu\text{g}/\text{lane}$, respectively. Lanes A-H, R, and I are stained with G-250 Coomassie blue. Lanes J-Q are Western blotted. Lanes A, H, R, and I are protein molecular weight standards: Carbonic Anhydrase MW=29,000; Egg Albumin MW=45,000; Bovine Albumin MW=66,000; Phosphorylase b MW=97,400; β -Galactosidase MW=116,000; Myosin MW=205,000.

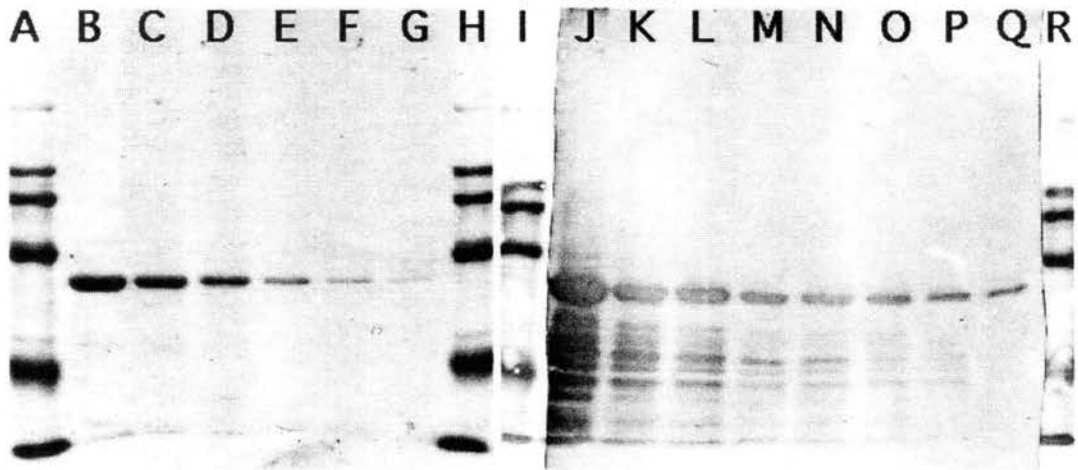
T403E



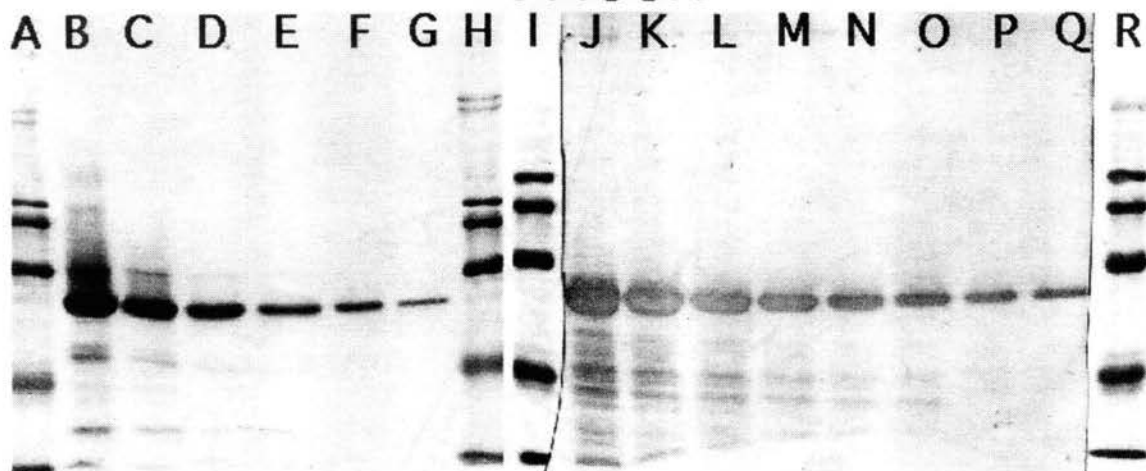
T403K



T406R



A458K



R459Q

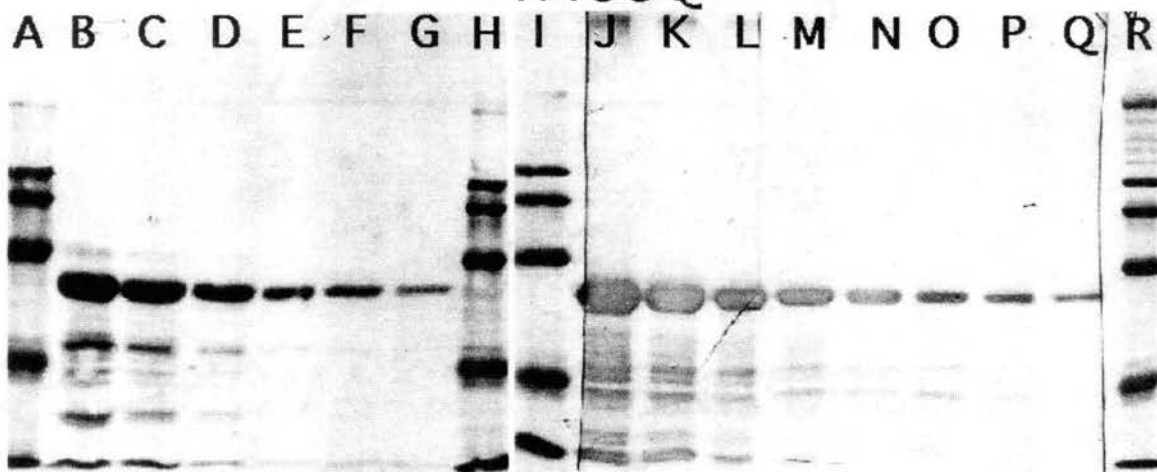


Table 12. Kinetic Parameters for Wild Type, T403K, T406R, and A458K.

<u>Kinetic Property</u>	<u>Enzyme Source</u>			
	<u>Wild Type</u>	<u>T403K</u>	<u>T406R</u>	<u>A458K</u>
<u>PEP(-FBP)</u>				
V_{max} (U/mg)	301±4	305±5	334±6	432±8
PEP _{1/2} (mM)	2.5±0.5	2.7±0.1	2.2±0.1	2.5±0.1
n_H	2.7±0.1	2.5±0.1	2.0±0.1	2.7±0.2
<u>PEP(+FBP)</u>				
V_{max} (U/mg)	353±4	311±5	333±8	444±8
PEP _{1/2} (mM)	0.23±0.01	0.28±0.02	0.27±0.03	0.22±0.01
n_H	1.1±0.1	1.0±0.1	0.87±0.08	1.0±0.1
<u>FBP</u>				
V_{max} (U/mg)	276±17	229±5	200±4	229±5
FBP _{1/2} (mM)	0.05±0.01	0.093±0.005	0.049±0.004	0.093±0.005
n_H	1.0±0.3	1.3±0.1	1.1±0.1	1.3±0.1

The kinetic properties of various yeast PK's were determined as described in Figure 11 and in the Materials and Methods using desalted protein preparations. FBP activation of wild type, T403K, T406R, and A458K were in the presence of 1.9 mM, 1.4 mM, 1.4 mM, and 1.4 mM PEP, respectively.

Figure 34. Kinetic Properties of Wild Type, T403E, and R459Q. The catalytic activity (v) of purified wild type, T403E, and R459Q was measured at varying concentrations of PEP without (○) or with 2.4 mM FBP (■) as described in Figure 11 and Materials and Methods using desalted protein preparations. Data presented is relative velocity (v/V_{\max}) to normalize presentation of the results. Kinetic parameters determined by fitting the results to the Hill equation are presented in the inserts.

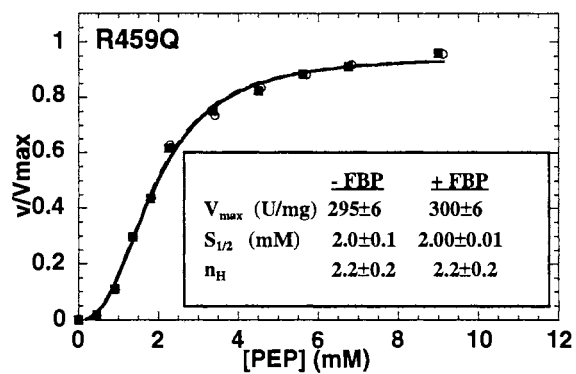
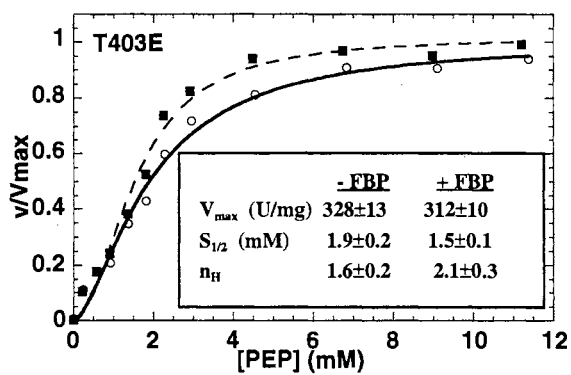
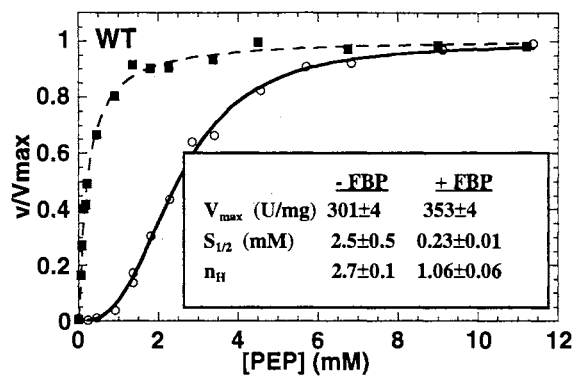
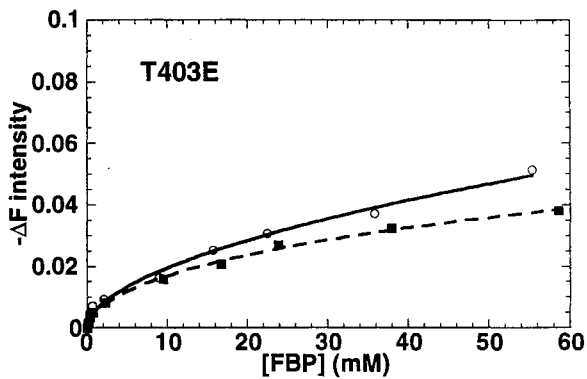
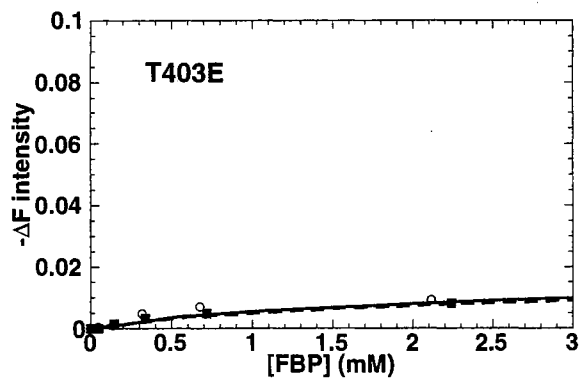
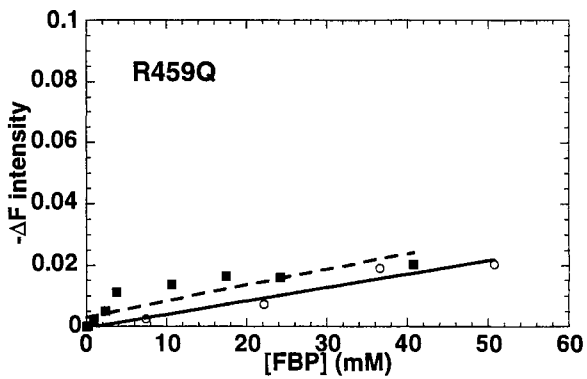
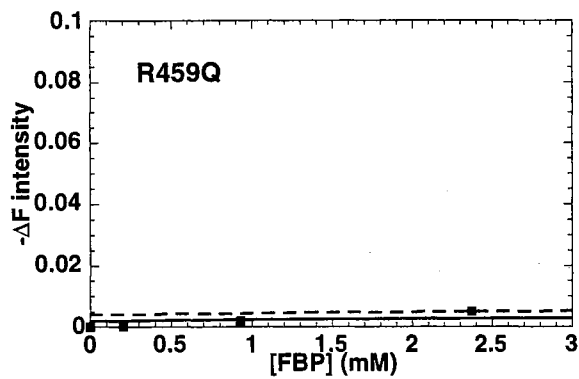
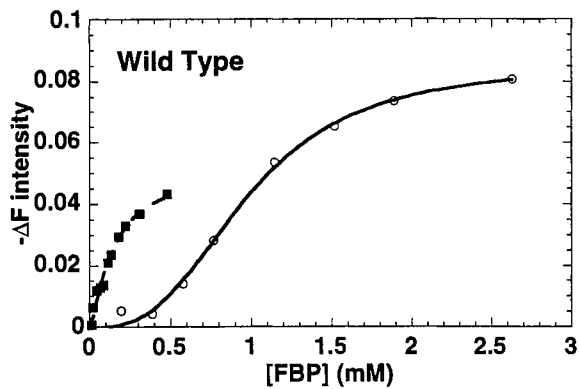
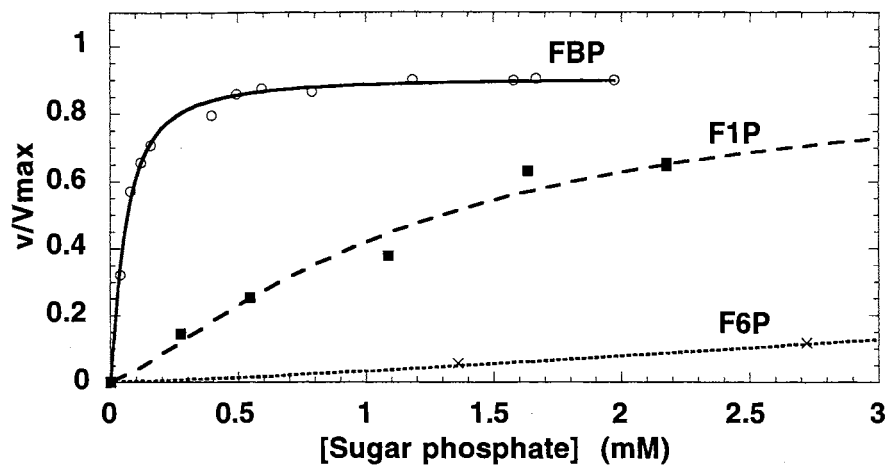


Figure 35. Fluorescence Quench Titration Curves for Wild Type, T403E, and A459Q. Fluorescence emission responses were determined at varying concentrations of FBP in the absence (○) and presence (■) of 15 mM PEP as described in Figure 14. $-\Delta F$ values are per $\mu\text{g/ml}$ protein. Lines on graphs of T403E and A459Q data are to show general pattern of data. The fluorescence emission response of T403E and A459Q is shown on two scales.



1'-phosphate group of fructose-1,6-bisphosphate are the major trigger in allosteric activation, then fructose-1-phosphate (F1P) should also be able to activate the enzyme. Fructose-6-phosphate (F6P) should bind to PK but would not be predicted to activate the enzyme by the FBP binding site model of Jurica *et al.* (Figure 32) (20). Both F1P and F6P were predicted to bind with lower affinities than FBP due to fewer interactions with phosphate groups. F1P and F6P have previously been used as FBP analogs in the study of *E. coli* type I PK and yeast PK (41,69).

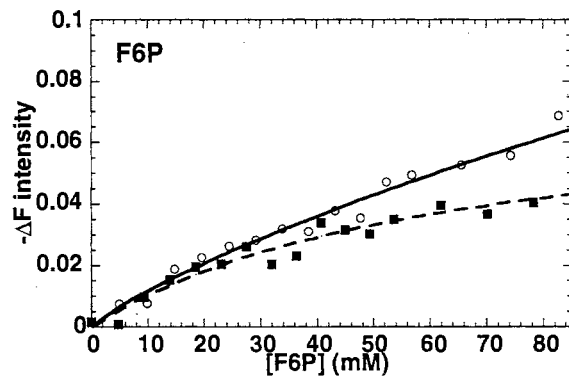
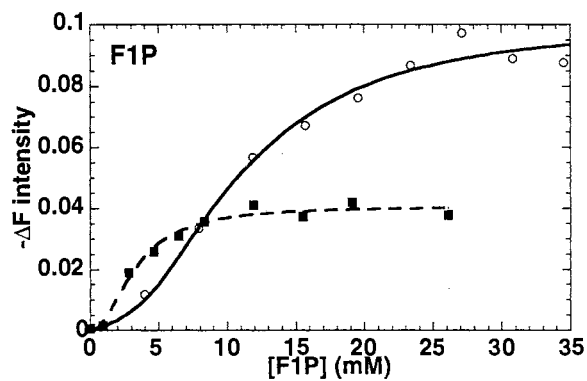
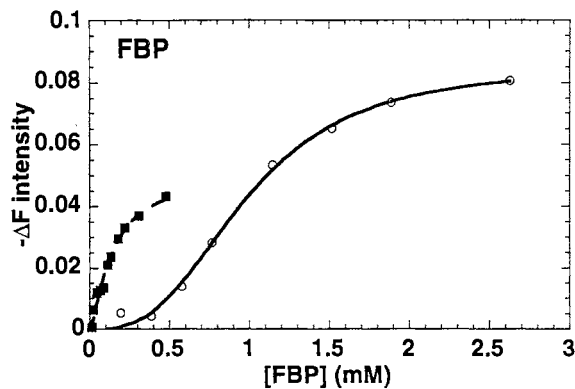
In this study, FBP, F1P, and F6P all activated wild type PK (Figure 36). The $S_{1/2}$ of F1P activation is 24 times greater than the $S_{1/2}$ for activation by FBP. The $S_{1/2}$ of F6P activation is greater than 100 times the $S_{1/2}$ for activation by FBP. Fluorescence quench titration for F1P and F6P were also monitored (Figure 37). In the absence of PEP, wild type PK binds F1P with a $[\text{sugar-phosphate}]_{1/2}$ 10 times greater than the $[\text{sugar-phosphate}]_{1/2}$ for FBP. In the presence of PEP, the $[\text{sugar-phosphate}]_{1/2}$ for F1P is 23 times greater than the $[\text{sugar-phosphate}]_{1/2}$ for FBP. No maximum was reached for titrations with F6P in the absence or presence of PEP, and therefore the binding constants for F6P were not computed.



	FBP	F1P	F6P
V_{\max} (U/mg)	276 ± 17	259 ± 15	204 ± 7
$S_{1/2}$ (mM)	0.05 ± 0.01	1.2 ± 0.1	9.4 ± 6.6
n_H	1.0 ± 0.3	1.3 ± 0.2	1.4 ± 0.1

Figure 36. FBP, F1P, and F6P Dependent Activations of Wild Type PK. The catalytic activity (v) of purified wild type PK was measured at varying concentrations of FBP (○), F1P (■), or F6P (×) using desalted protein preparations. Catalytic activity is presented as a fraction of the V_{\max} of FBP activation ($276 \mu\text{moles}/\text{min.}/\text{mg}$) to normalize presentation of the results. Kinetic parameters determined by fitting the results to the Hill equation are presented in the insert.

Figure 37. FBP, F1P, and F6P Dependent Fluorescence Quench Titration Curves for Wild Type PK. Fluorescence emission responses were determined at varying concentrations of sugar-phosphates in the absence (○) and presence (■) of 15 mM PEP as described in Figure 14. $-\Delta F$ values are per $\mu\text{g/ml}$ protein. Lines on graphs of F6P are to show general pattern of data. Concentration scales of sugar-phosphate activators are not equivalent. Binding parameters for FBP and F1P obtained by fitting the fluorescence data to the Hill equation are presented in the insert.



	FBP activation (- PEP)	FBP activation (+ PEP)	F1P activation (- PEP)	F1P activation (+ PEP)
$-\Delta F_{\max}$	0.085	0.050	0.095	0.043
$FBP_{1/2}$ (mM)	0.98 ± 0.03	0.14 ± 0.01	10 ± 1	3.3 ± 0.4
n_H	2.9 ± 0.2	1.4 ± 0.1	2.2 ± 0.5	2.0 ± 0.5

DISCUSSION

Sites of Pyruvate Kinase in Allosteric Regulation

Pyruvate kinase (PK) is a key regulating enzyme of carbohydrate metabolism in virtually every living organism. PK catalyzes the final step of glycolysis with the production of pyruvate and ATP. A common regulating feature of PK from many species is feed-forward activation by fructose-1,6-bisphosphate (FBP). Most known PK isozymes are tetramers and exhibit heterotropic and homotropic cooperativity.

Past studies of PK have utilized PK protein from many different species. Even though PK isozymes from various species share structural and regulation features, sequence differences hinder direct comparison of data from different PK isozymes. In order to allow direct comparison, a model system for studying PK is needed. This study has used yeast PK as a model system.

The purpose of this study was to contribute to our understanding of allosteric regulation of PK by FBP using yeast PK as a model system. Due to the lack of molecular characterization of the fructose-1,6-bisphosphate (FBP) binding site, the initial goal was to predict and then experimentally locate the FBP binding site. Surface charge mapping of a yeast PK molecular model identified the Tyr 436 pocket and the Arg 42 pocket as highly positively charged (Figures 17 and 18). Due to FBP's strong negative charges, these two pockets were considered as potential FBP binding sites. During the course of this study, the FBP binding site was actually identified outside of the Tyr 436 and Arg 42 pockets (20). Since the highly charged Tyr 436 and Arg 42 pockets are conserved in many PK isozymes (Figure 19) and previous studies had indicated the importance of these sites in

allosteric regulation, these regions were further explored in this investigation. In addition to the Tyr 436 and Arg 42 pockets, amino acid residues of the FBP binding site identified by Jurica *et al.* (20), the A-A subunit contacts, and the C-C subunit contacts also represent important regions for understanding allosteric regulation of PK. These regions were examined for their possible roles in allosteric regulation using site-directed mutagenesis as the major experimental approach.

Non-expressing Yeast Pyruvate Kinase Mutations

During the course of this work 22 amino acid substitutions were constructed to probe the five sites of interest (Tyr 436 pocket, Arg 42 pocket, A-A subunit contact, C-C subunit contact, and FBP binding site). Five of the 22 mutations were not expressed after multiple transformations (minimum of five attempts). R19Q, K236E, K292E, R409E, and R415Q mutated yeast PK's were not expressed. These mutations all lie between the A and C domains, at the end of the A domain β -barrel structure, and at residues with highly conserved positive amino acids. K236E, K292E, R409E, and R415Q are in the Tyr 436 pocket, while R19Q is located in the Arg 42 pocket. Since PK activity is required for growth of yeast on glucose, growth of the transformed knockout yeast on glucose only selects for kinetically active PK mutants. One can, therefore, conclude that PK activity of the non-expressed mutations is below a basal level required for yeast survival.

K236E, K292E, and R409E introduce a negative charge into the Tyr 436 pocket. A negative charge introduced into the Tyr 436 pocket might interact with positive charges across the Tyr 436 pocket (Figure 38). Such an ionic bond might pull the backbone out of the properly folded position. In addition altering a charged residue could cause rearrangement of other charged groups. R415Q removes a positive residue predicted to be in a salt bridge (34). Interruption of a salt bridge could also cause backbone misfolding and charge rearrangements. Residues in the A-C domain contacts are near the β -barrel structure of the A domain (Figure 39). The active site lies at the opposite end of the β -barrel.

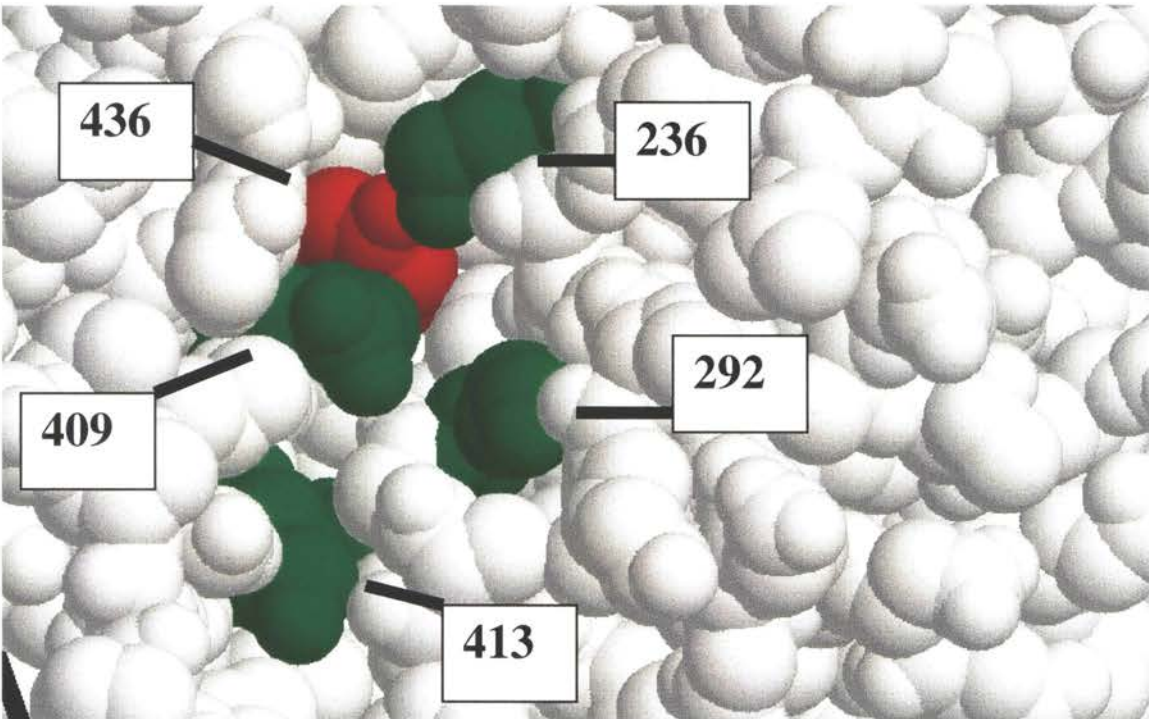


Figure 38. Location of Mutated residues of the Tyr 436 Pocket. Positively charged residues of the Tyr 436 pocket that were mutated in this study are in green. Tyrosine 436 is in colored in red for location reference. The 415 position is not visible from this view. A negative charge introduced into the Tyr 436 pocket might interact with positive charges across the Tyr 436 pocket.

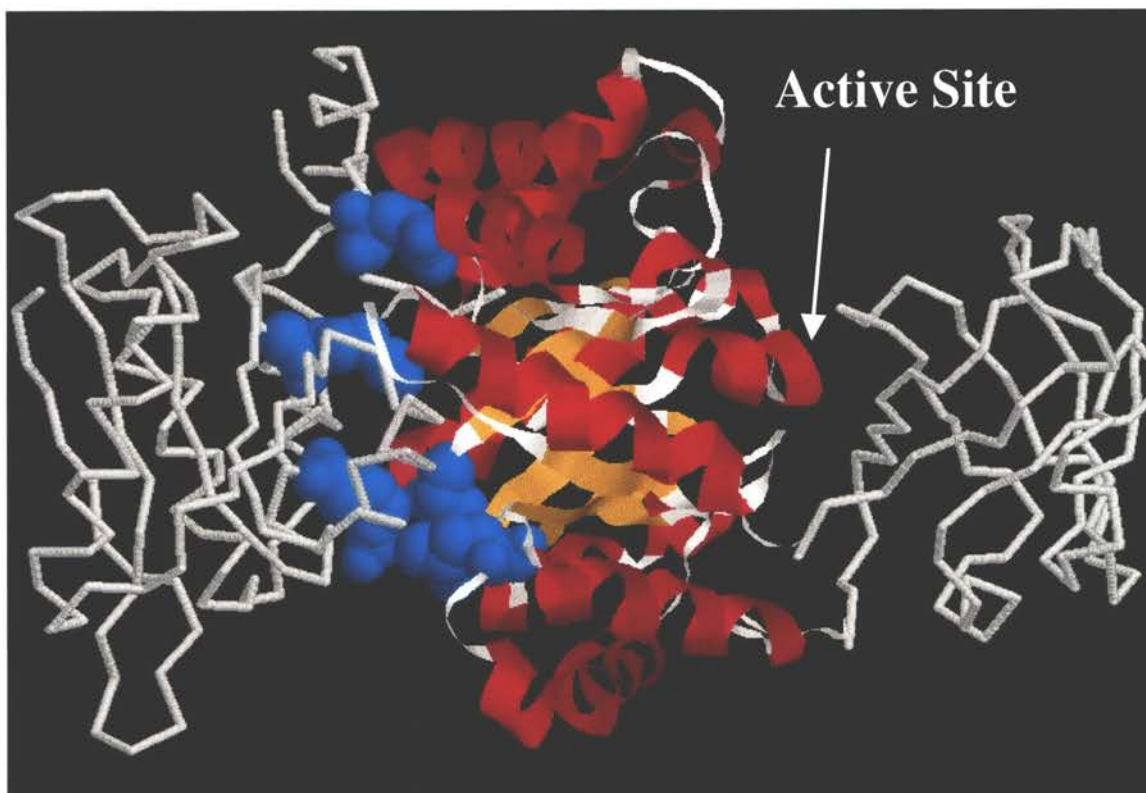


Figure 39. Location of Non-expressing Mutations with Respect to the β -barrel. A yeast PK subunit as resolved by Jurica *et al.* (20) is shown with β -barrel helices shown in magna and β -barrel sheets shown in orange. The locations of mutations that did not express are shown in cyan spacefill.

Improper folding or altered charge alignments due to mutation in the A-C domain contacts might affect the β -barrel, which in turn could alter active site structure.

Based on the lack of expression of R19Q, K236E, K292E, R409E, and R415Q, one might be tempted to predict that positive charges in the A-C domain contacts are important for proper PK structure and/or kinetic function. The high conservation of positive charges in the Tyr 436 and Arg 42 pockets would support this predication. Positive charges at the 19 and 415 positions may be important for proper PK structure and/or kinetic function. However, several A-C domain interface mutations, K292Q, R409Q, K236Q, and R77Q, were expressed and found to have normal kinetic properties (Tables 7 and 9). These mutations show that positive residues can be removed without influencing PK activity. Therefore, even though specific positive charges such as arginine 19 and arginine 415 may be important, all positive charges at the A-C domain interface are probably not important for proper PK structure and/or kinetic function.

Yeast Pyruvate Kinase Mutations with Small Kinetic Effects

All the mutations in this study were designed to probe residues for their possible roles in FBP's allosteric regulation of yeast PK. However, the R77Q, K292Q, K413E, T406R, Y436F, Y436S, T403K, and A458K mutant yeast PK's all caused changes in $S_{1/2}$'s for PEP or FBP that were less than three-fold changes from those of wild type PK (Tables 6, 7, 8, 9, and 12). In addition, R409Q, K236Q, and R369A had $S_{1/2}$'s for FBP only three times that of wild type PK (Tables 7 and 10). The R369A mutation also increased n_H for PEP dependent activation in the absence of FBP (Table 10). K413Q increased the $S_{1/2}$ for PEP in the absence of FBP without influencing other monitored kinetic properties (Figure 23). Therefore, even though all the mutations were proposed to have major effects on allosteric regulation, many mutations do not greatly alter allosteric regulation of yeast PK by FBP. With the exception of R77Q and R369A, all of the expressed mutations that caused no or small changes in kinetic properties are located in the Tyr 436 positively charged pockets and FBP binding site as identified by Jurica *et al.* (20). The FBP binding site

identified by Jurica *et al.* neighbors the Tyr 436 pocket (Figure 40) (20). Therefore, the lack of large kinetic effects of mutations in the Tyr 436 pocket and FBP binding site support that amino acids very close to the allosteric effector binding site may not be important in mediating the allosteric regulation by FBP (Figure 41).

A-C Domain Contacts in Allosteric Regulation

Even though the Tyr 436 and Arg 42 pockets were originally considered as possible FBP binding sites in this study, the FBP binding site was identified outside of the Tyr 436 and Arg 42 pockets (20). The highly charged Tyr 436 and Arg 42 pockets are conserved in many PK isozymes. In addition, the Tyr 436 pocket corresponds to the site identified as a possible FBP/ADP binding site by chemical labeling/protection studies (72,73). The Tyr 436 pocket has also been identified as a potential ATP binding site by affinity labeling of *E. coli* type I PK (74). The Arg 42 site has been predicted to be the allosteric inhibitor, ATP, binding site, since ADP co-crystallizes in this site of cat M1 PK (70). It is important to note that the allosteric inhibition by ATP seen in mammalian PK isozymes has not been demonstrated in yeast PK (31,41). Many references in the literature have assumed that all allosteric modifiers, including FBP, bind in the Arg 42 pocket (34,71,72). Mutagenesis of residues in the Arg 42 pocket in PK of *T. bruci* further supports involvement of this site in allosteric regulation by FBP (71). Therefore, both the Tyr 436 and Arg 42 pockets identified in this study as highly positively charge pockets have been suggested to be important to allosteric regulation even though the true FBP binding site is distinct from both pockets (Figure 40). This may imply that the Tyr 436 and Arg 42 pockets are important in transmitting an allosteric signal.

Mattevi *et al.* (21,81) attempted to characterize changes in conformational state of PK by comparing the crystal structures of the cat and rabbit muscle PK's with the *E. coli* PK type I isozyme. They assigned the M1 PK's as an R-state of the enzyme and the *E. coli* PK as the T-conformation of the two-state model of Monod *et al.* (54). Based on their studies, Mattevi *et al.* (21,81) predicted that very little conformational changes occur within

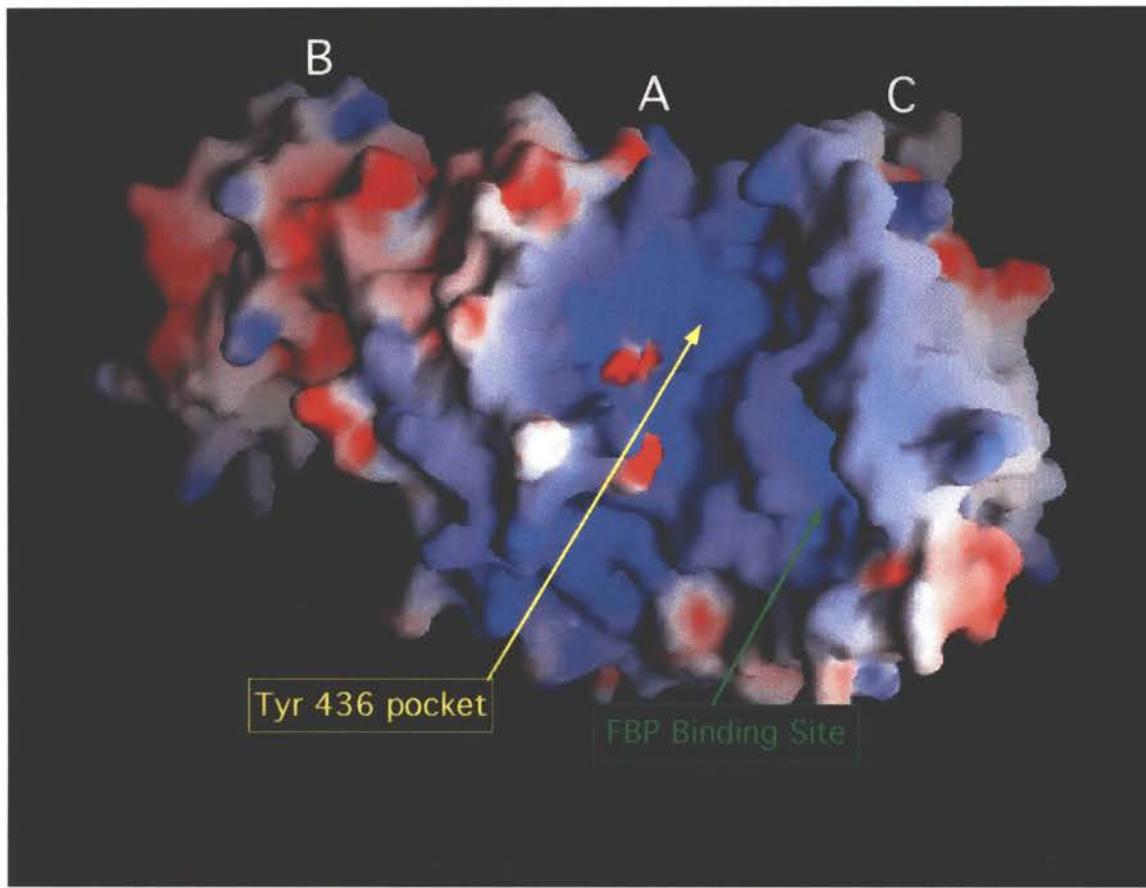


Figure 40. Location of the FBP Binding Site on the Surface Charge Map of the Yeast PK Model Developed in this Study. The FBP binding site was identified by Jurica *et al.* (20).

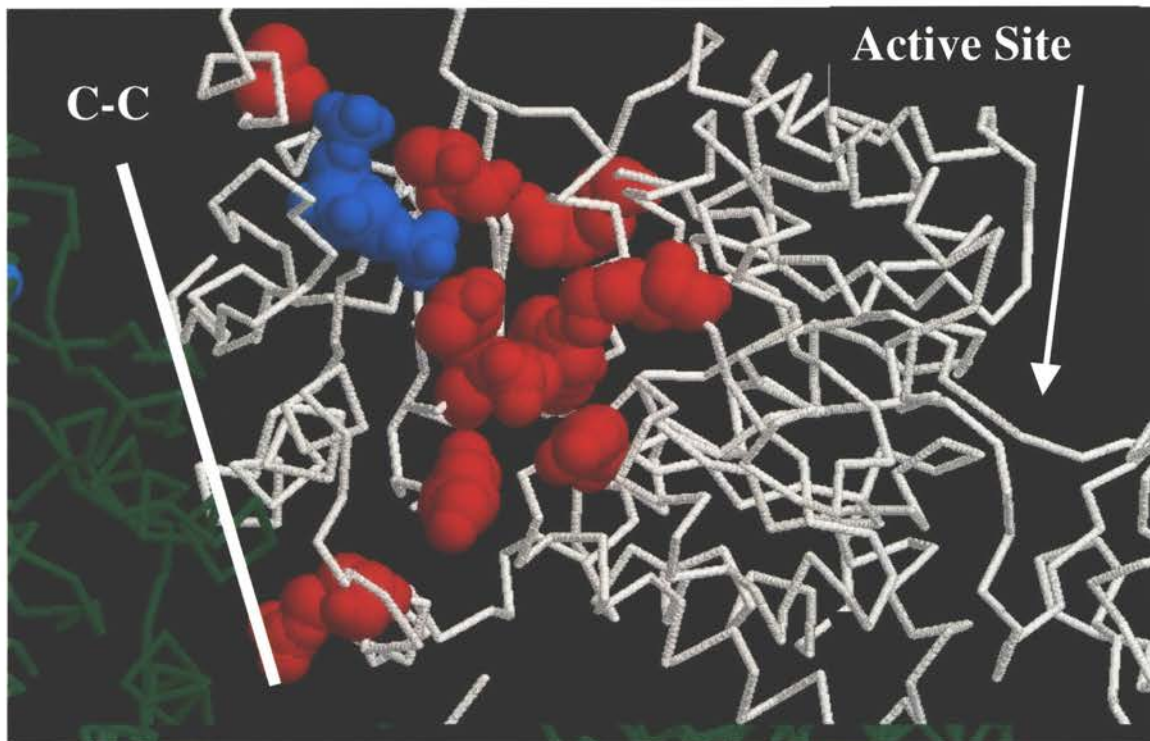


Figure 41. Location of Mutations with Little or No Effects on Monitored Kinetic Properties. A yeast PK subunit as resolved by Jurica *et al.* is shown in white while neighboring subunits are in green (20). Amino acid residues, which have been mutated with little consequence on kinetic parameters, are shown in red spacefill. FBP is shown in cyan spacefill.

domains of PK when the two activity states are interconverted. Instead, they suggest that domains within each subunit rotate with respect to each other in allosteric and cooperative transition. Unfortunately, their conclusions are based on enzymes from different species and not transition states of the same enzyme. However, light scattering and crystallography studies of rabbit muscle PK support rotations of the B domain with respect to the A domain during the transformation between active and inactive forms (18,66). Fluorescent studies of *B. stearothermophilus* PK also support movement of the C domain with respect to the A domain during allosteric transition (34). Assuming that all activity states of PK have equivalent domain structures, allosteric communications may occur by side chain interactions on the surfaces of domains and/or subunits. Salt bridges between the A and C domains and A and B domains have previously been predicted to be important for regulation of rabbit M1 PK (79) and of *B. stearothermophilus* PK (34), respectively. Based on the structural comparison of Mattevi *et al.* (21,81), A-C domain contacts may be predicted to be important in mediating allosteric regulation.

Since the conserved positive residues of both the Tyr 436 and Arg 42 pockets were between the A and C domains, the mutations created in these sites probe A-C domain interactions. In this study, the relatively small effects of expressed mutations of the Tyr 436 and Arg 42 pockets (Figures 23 and Tables 6, 7, 8, and 9) do not support the involvement of A-C domain interactions in the Tyr 436 and Arg 42 pockets in allosteric regulation.

R369A: A C-C Subunit Interface Mutation

Cooperative substrate binding and allosteric regulation of PK require communications between multiple subunits of the protein. X-ray crystallography studies have shown that PK is a dimer of dimers (56). Therefore, PK has two distinct subunit interface types that have been identified and may be involved in allosteric regulation.

The M1 and M2 isozymes of mammalian PK present an interesting model to explore the importance of interface interactions of PK. These mammalian isozymes are coded by the same gene with alternative splice sites giving rise to a small number of amino

acid differences (22 amino acid differences) in the C-C interfaces (25). M1 PK shows classic hyperbolic substrate kinetics whereas the M2 PK exhibits sigmoidal kinetics (26). However both isozymes are subject to allosteric activation by FBP under appropriate conditions (26). Point mutations at the C-C interfaces of rat M1, rat M2, yeast, and *B. stearotherophilus* isozymes are reported to alter cooperative and/or allosteric regulation of these enzymes, supporting the role of this interface in regulation (59,76-78). In addition, the lack of conserved residues at the C-C interface of the non-regulated, dimeric pyruvate kinase from *Z. mobilis* suggests that loss of regulation may be due to changes in the C-C subunit interface (36,37).

Mutation analysis in rat M1 PK has previously suggested a role of an arginine (equivalent to the yeast PK 369 position) in allosteric regulation (77). In the present study, R369A was created to examine the possible role of arginine 369 in allosteric regulation of yeast PK by FBP (Figure 42). R369A has a V_{max} one third that of wild type PK which could not be fully accounted for by contamination with other proteins (Figure 25). A link between V_{max} and the C-C interface has previously been identified (44). The R369A mutation did not greatly influence allosteric regulation of yeast PK by FBP (Table 10). R369A's $S_{1/2}$ for FBP activation is triple that of wild type PK (Table 10). Replacement of an arginine with an alanine at an equivalent site to yeast PK's 369 position in M2 PK also has little effect on FBP activation (76). Replacing alanine with arginine at an equivalent site in M1 PK shifts hyperbolic shaped PEP dependent kinetic curves to sigmoidal shaped (77). Based on the alanine to arginine mutation in mammalian M1 PK, Ikeda *et al.* has suggested that arginines at residue positions equivalent to yeast PK 369 may stabilize the T-state (77). One may conclude that since no effects were seen in arginine to alanine mutations of yeast PK, that complete stabilization of the T-state in yeast PK cannot be attributed to arginine 369.

Ikeda *et al.* have also suggested that interactions between arginines equivalent to yeast PK 369 and 362 may attribute to the high cooperativity found in mammalian L and R

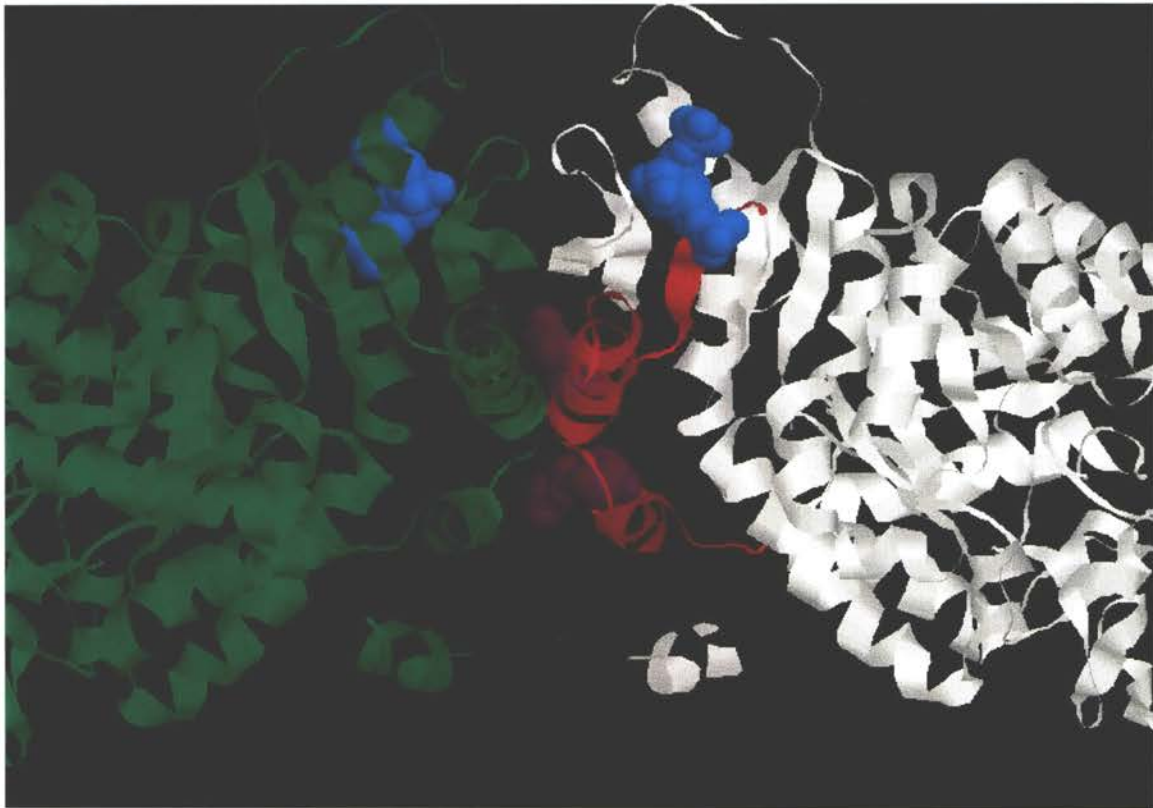


Figure 42. Location of C-C Subunit Interface Mutations. A yeast PK subunit as resolved by Jurica *et al.* (20) is shown in green and a second subunit is in white. The mammalian M1 PK which has a hyperbolic response to PEP and the mammalian M2 PK which has a sigmoidal response to PEP have a difference of 22 amino acids. Positions of the 22 amino acid differences are within a 45 amino acid sequence. The yeast PK sequence equivalent to this 45 amino acid sequence is shown in red for one subunit. FBP is shown in cyan spacefill. The yeast positions 369 and 392 of one subunit are shown in purple spacefill.

isozymes (77). The 362 position in yeast PK is a leucine and is less likely to enhance the cooperativity of this isozyme due to the lack of charge interactions. However, aspartic acid 366 and asparagine 370 of the same subunit and arginine 369 and aspartic acid 366 of the neighboring subunit all may interact with arginine 369 in yeast PK. Mutation probing of mammalian isozymes by Ikeda *et al.* (76,77) and yeast PK in this study are not inconsistent with the hypothesis of Friesen *et al.* (111) that different isozymes may use different salt-bridge interactions to mediate allosteric activation.

E392A: A C-C Subunit Interface Mutation

Mutation of a cysteine (at a position equivalent to yeast 394) in rat M2 PK to leucine shifted the normal sigmoidal kinetic response to varying PEP concentrations to a hyperbolic response (76). The yeast residue 394 is not a cysteine residue; however, a glutamic acid residue at position 392 interacts with the neighboring subunit in the yeast PK molecular model (Figure 42). Jurica *et al.* (20) and Friesen *et al.* (111) have both noted the involvement of residues equivalent to 392 in hydrogen bonds across the C-C subunit interface in yeast and mammalian isozymes, respectively. The E392A yeast PK mutant was created in this study to investigate the role of glutamic acid 392 in the allosteric regulation of yeast PK by FBP.

In this study, hyperbolic PEP dependent activation (Figure 26) and hyperbolic FBP dependent fluorescence quench curves (Figure 27) both suggest that the E392A mutation converts yeast PK to a high activity state (R-state), uncoupling communications between subunits. Furthermore, since the apparent affinities of E392A for PEP and FBP are similar to those of the activated wild type PK, the mutation does not appear to influence binding of PEP or FBP. Therefore the glutamic acid 392 of yeast PK may stabilize a low activity state of yeast PK (T- state).

Uncoupling caused by the E392A mutation may be due to disruption of communication at the interface and/or dissociation of subunits. Active dimers or monomers of yeast PK have not been reported (65). However, Kuczynski and Suelter showed that loss

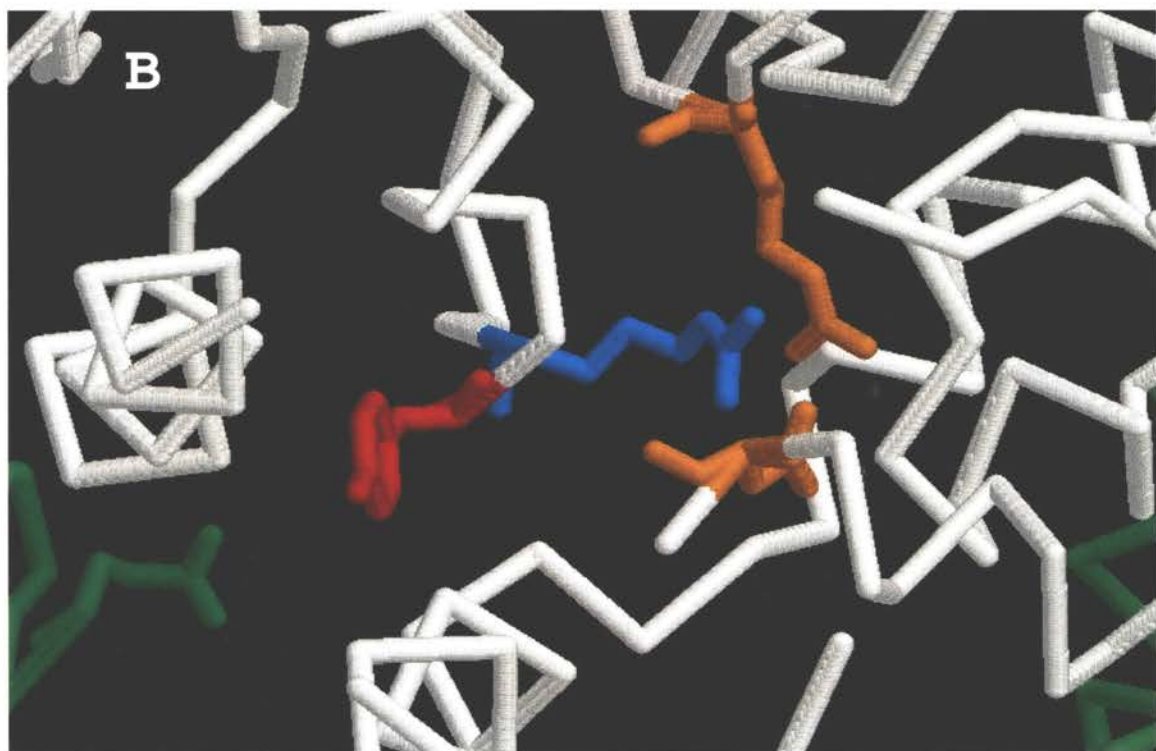
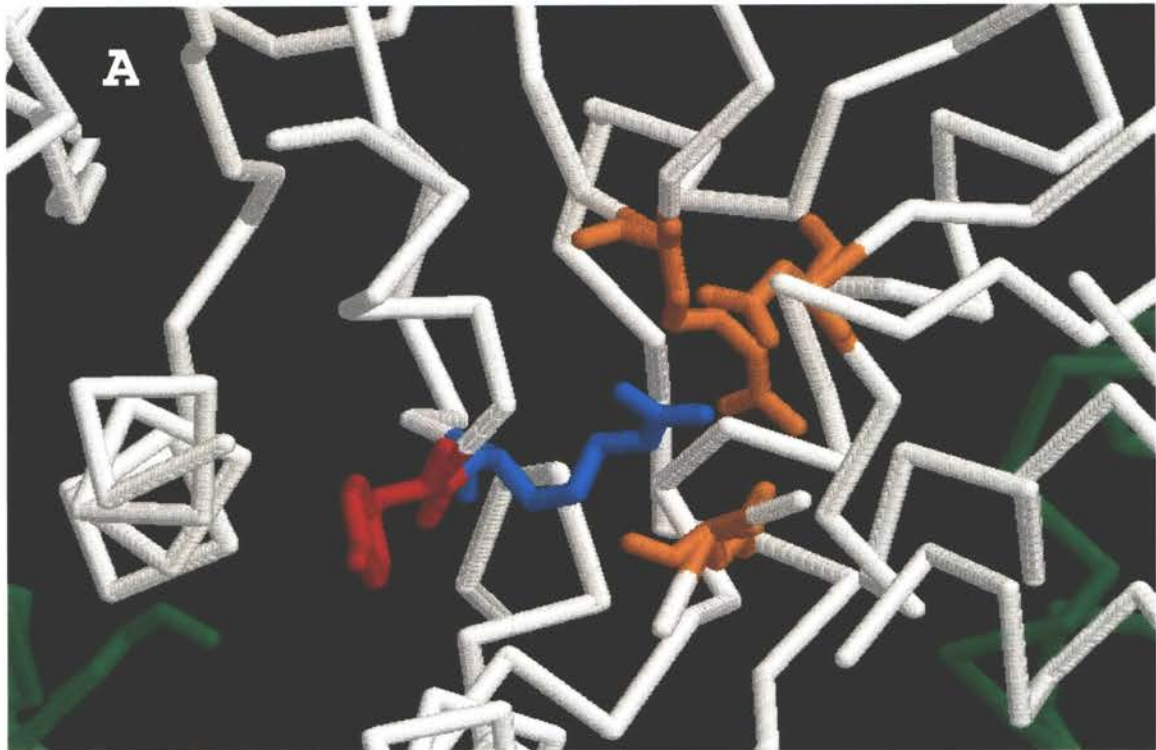
of activity of yeast PK follows a two step inactivation. This two step inactivation corresponding to dissociation of tetramers first into dimers, with half of the activity of the native isozyme, and then inactive subunits (108). Since the E392A mutation does not cause a decrease in activity (Figure 26), the multimeric conformation of this mutation is not predicted to be different from that of wild type PK.

Even though the 392 equivalent residue position in mammalian isozymes is a lysine (Figure A1) with a positive charge instead of the negatively charged glutamic acid of yeast PK 392, both appear to be in hydrogen bonds with a tyrosine residue, 414 in yeast PK, of the neighboring subunit. Friesen *et al.* (111) has proposed that the tyrosine residue is part of a hydrogen bonding network which transmits an allosteric signal from the C-C subunit interface to the active site. In the hypothesis of Friesen *et al.* (111), the tyrosine (equivalent to 414 in yeast PK) would interact with an alanine. However, PK isozymes have a highly conserved tyrosine-arginine sequence equivalent to yeast PK 414-415. The *B. stearothermophilus* arginine equivalent to yeast PK 415 has previously been predicted to be in a salt bridge that is important to allosteric regulation (34). In crystal structures of both mammalian M1 (17-19) and yeast (20) isozymes, this arginine is orientated towards charged groups across the A-C domain interface (Figure 42). Therefore, in contrast to the predictions of Friesen *et al.* (111), the yeast PK arginine 415 may be involved in relaying the allosteric signal to the active site. Unfortunately, the R415Q mutation designed in the current study was not expressed, preventing further study of this possibility.

Q299N: An A-A Subunit Interface Mutation

A glutamine to asparagine mutation in PK of *B. stearothermophilus*, at a position equivalent to yeast PK 299, decreased the enzyme's kinetic responsiveness to its allosteric activator, ribose-5-phosphate (59). However, the *Bacillus* enzyme's affinity for PEP followed by fluorescent quench techniques is still responsive to the activator (59). To investigate the role of glutamine 299 in the allosteric regulation of yeast PK by FBP, the Q299N yeast PK mutation was created.

Figure 43. Location of Amino Acids of a Possible Relay Involved in Allosteric Regulation. Panel A shows rabbit M1 PK (17-19) and panel B shows yeast PK (20). In both structures, the subunit of interest is shown in white and the neighboring subunits green. The yeast PK equivalent positions of 392, 414, 415 are shown in green, red, cyan, respectively. In addition, charged A-domain amino acids orientated towards the 415 equivalent residue are orange.



In contrast to the *B. stearothermophilus* mutant PK, the Q299N yeast PK mutant's $S_{1/2}$ for PEP was responsive to the allosteric activator, FBP. The Q299N yeast PK mutant has an increased $S_{1/2}$ for PEP in the absence of FBP and increased $S_{1/2}$ for FBP activation. These results might support that the Q299N mutation reduces ligand affinities of the T-state without affecting ligand affinity of the R-state. The Q299N mutation may also stabilize the low activity state of yeast PK (T- state), evidenced by the increased n_H for varying PEP in the absence of FBP. Due to the lack of purification, FBP binding could not be followed with the fluorescent technique.

In this study, the kinetic response of Q299N yeast PK to varying concentrations of ADP supports that FBP regulates apparent ADP affinity (Figure 28). However, even though the 12 mM PEP concentration used while varying ADP is saturating for wild type PK, this PEP concentration may be below saturating conditions for Q299N (Figure 28). At PEP concentrations below saturating, FBP's ability to shift the $S_{1/2}$ for ADP may be due to FBP's affect on PEP affinity. Increasing the PEP concentration to 22 mM while varying ADP had no effect on ADP dependent parameters (Table 11). Therefore, in this study, the Q299N mutant exhibits an observable FBP regulation of ADP affinity in contrast to wild type enzyme. A similar regulation of ADP affinity by FBP has been seen in another A-A subunit interface yeast PK mutant (T311M) studied by Bollenbach (109).

Dr. Thomas Nowak has shown that even though the kinetic dependent response of yeast PK for ADP is hyperbolic, ADP binding curves are sigmoidal (110). Mesecar observed that high concentrations of free ADP increase the $S_{1/2}$ for PEP. Competition between PEP and ADP with ADP acting as a dead-end inhibitor as suggested by Mesecar (24) may explain these observations. However, Haeckel *et al.* reported that the n_H of yeast PK's ADP-dependent kinetic curves is dependent on PEP concentration (41). A dead-end inhibitor complex caused by ADP binding does not easily explain this observation. However, a coupling between ADP and PEP binding is supported. The 299 residue is adjacent to threonine 298 of the PEP binding site (20). Lovell *et al.* has proposed that the

glutamine 299 equivalent of *B. stearothermophilus* is important in coupling PEP binding with cooperative and allosteric functions (59). Altered coupling of PEP binding may allow the apparent ADP affinity to become responsive to FBP. This hypothesis is consistent with the report of Kuczynski and Suelter, who used fluorescent techniques to show coupling between the binding of ADP and FBP to yeast PK (44).

T311M: An A-A Subunit Interface Mutation

Recreating a hemolytic anemia mutation (PK Tokyo; threonine to methionine at a position equivalent to yeast PK 311) in the mammalian M2 isozyme is reported to cause a loss of sensitivity to allosteric activation by FBP and loss of allosteric inhibition by phenylalanine (79,80). To examine the role of yeast PK's threonine 311 in allosteric regulation, T311M was created in this study.

The T311M yeast PK mutant has an increased $S_{1/2}$ for PEP and FBP, a decreased affinity for FBP as indirectly evidenced by fluorescent quench titration curves, and is absolutely dependent on FBP for catalytic activity under standard assay conditions used in this study (Figures 30 and 31). Since T311M had reduced affinity for FBP, the enzyme may not have been fully activated by standard assay conditions in the presence of FBP. Therefore the activity response to varying ADP and PEP are both sigmoidal in the presence of FBP. Since T311M has an increased $S_{1/2}$ for PEP and FBP and a decreased affinity for FBP, the main effect of the T311M yeast PK mutation may be to stabilize the low activity state of yeast PK (T- state).

During the course of this study, the T311M mutation in yeast PK was also created by Bollenbach (109). Regulation of apparent ADP affinity of T311M by FBP is reported (109). Bollenbach demonstrated that the largest shift in ligand affinity caused by the T311M mutation was for the divalent cation, Mg^{+2} or Mn^{+2} (109). The current study did not monitor effects of mutations on divalent cation affinity and therefore the T311M yeast PK mutant's apparent dependence on FBP for catalytic activity observed in this study may be due to the lowered divalent cation affinity reported by Bollenbach (109). Binding of

divalent ion to yeast PK is coupled to both FBP and PEP binding (60,61). Therefore, T311M yeast PK mutation may stabilize the low activity state of yeast PK (T- state) by reducing divalent cation affinity as reported by Bollenbach (109). Since the role of the divalent ion in coupling PEP binding with binding of FBP has been reported, altered coupling of PEP binding to binding of other ligands may allow apparent ADP affinity to become responsive to FBP.

Friesen *et al.* has suggested that the T311M equivalent mutation in mammalian PK isozymes may interrupt a salt bridge between the A and B domains (79). In the proposal of Friesen *et al.*, the T311M mutation might cause the helix, containing both the yeast PK 311 and 312 positions, to reorientate. This helix reorientation could interrupt a salt bridge found between arginine 312 and aspartic acid 147 equivalent positions in the rabbit muscle PK crystal structure (79).

The Fructose-1,6-Bisphosphate Binding Site

The true FBP binding site identified by co-crystallization of FBP with yeast PK shows that the FBP binding site is not highly positive as was proposed early in this study (20). Instead only one ionic bond is involved in binding FBP to yeast PK (Figure 32). The 1'-phosphate group of FBP is bound to arginine 459 through a strong electrostatic interaction (20). In contrast to predictions in the current study, hydrogen bonds play an important role in FBP docking. Analysis of the electron density shows the 6'-phosphate of FBP is bound by a loop (402-407 loop) through hydrogen bond interactions (Figure 32). Serine 402, serine 404, and threonine 407 of the loop in yeast PK are all involved in this interaction.

Site directed mutagenesis was used to probe residues of the FBP binding site that are predicted to be important to allosteric regulation. In the FBP binding site, T406R, T403K, and A458K do not cause large changes in kinetic parameters (Table 12). However, R459Q causes a lack of kinetic activation by FBP (Figure 34) and greatly decreases affinity for FBP as indirectly evidenced by fluorescence titration curves (Figure 35). Reduced FBP

affinity in the R459Q mutation was predicted due to removal of ionic bonding capabilities. R459Q has a sigmoidal PEP activation curve indicating that even though the mutation reduces FBP affinity it does not affect the activity state of the enzyme or the ability of PEP to activate the enzyme (cooperative regulation) (Figure 34). Since the R459Q mutation greatly reduces yeast PK's affinity for FBP, this mutation does not support that the 459 arginine is responsible for triggering an allosteric transition. However, positively charged mutants at positions in the FBP binding site, other than the 459 position, did not alter allosteric regulation by FBP. Therefore, the ionic bond formed between arginine 459 and the 1'-phosphate of FBP may be a key residue in allosteric regulation.

FBP analogs were used to probe regions of the activator important to triggering the allosteric response. F1P was able to activate wild type PK (Figure 36), supporting F1P's ability to cause allosteric activation of PK. F1P affinity indirectly monitored by fluorescence quench titrations is responsive to allosteric regulation by PEP in a manner similar to that of FBP (Figure 37). Very high concentrations of F6P were also able to activate PK activity (Figure 36). Due to the very low affinity of yeast PK for F6P indirectly monitored by fluorescence quench titrations, the influence of PEP on F6P affinity could not be determined (Figure 37). The use of F1P and F6P as FBP analogs supports FBP's 1'-phosphate as important for mediating the allosteric activation of yeast PK.

Haeckel *et al.* reported no activation by 10 mM and 7.5 mM of fructose-1-phosphate and fructose-6-phosphate, respectively (41). However Haeckel *et al.* assayed for activation in the presence of low levels of PEP, ADP, and Mg ions (41). Since, binding of divalent ion to yeast PK is coupled to both FBP and PEP binding (60,61), reduced divalent cation levels in the activation assay of Haeckel *et al.* (41) may have caused reduced affinity for FBP and FBP analogs. Since the 5 mM FBP used by Haeckel *et al.* to test FBP activation were well in excess of saturating FBP concentrations (Figure 36), a reduced FBP affinity due to low divalent cation concentrations may not have been detected (41). Ten mM and 7.5 mM concentrations of fructose-1-phosphate and fructose-6-phosphate, respectively,

used by Haeckel *et al.* are not saturating concentrations for these activators (Figure 36). Therefore the F1P and F6P activation in the current study are not inconsistent with those reported by Haeckel *et al.* (41).

Mutational probing into the FBP binding site and FBP analogs studies in the current work is consistent with a hypothesis that FBP is anchored to PK through 6'-phosphate and sugar ring interactions. Interactions with the 1'-phosphate of FBP may be responsible for triggering allosteric transition. Sequence alignments show all FBP activated PK's do not have an amino acid sequence that conserves an arginine at a position equivalent to yeast PK 459 (20). The structures of two PK isozymes, *E. coli* and *Leishmania* have been solved by crystallography (21,22). These crystallized isozymes do not have an amino acid sequence that conserves an arginine at a position equivalent to yeast PK 459 (Figure A1). However, when the structures of *E. coli* and *Leishmania* are examined, two arginines are in likely locations to function similarly to the yeast arginine 459 (Figure 44) (21,22). Therefore, even though the yeast PK arginine 459 may not be conserved in the amino acid sequence of other PK isozymes, the arginine may be conserved in the structures of other PK isozymes.

Yeast PK arginine 459 is located on a helix structure (H17 helix) that also contains the single tryptophan per subunit (tryptophan 452). When FBP binds interactions between arginine 459 and the 1'-phosphate may shift the H17 helix. This is consistent with fluorescence changes caused by FBP binding to yeast PK (Figure 15). Allosteric regulation between FBP and PEP must link specific changes in the FBP binding site to specific changes in the PEP binding site. FBP's allosteric regulation of PEP apparent affinity (Figure 12) and PEP's allosteric regulation of FBP affinity (Figure 15) support this assertion. Therefore, activation of PK by PEP must induce a change in the FBP binding site. This is supported by the fluorescence quench caused by PEP binding even though the single tryptophan residue is in the FBP binding site (Figure 15). Fluorescence quench caused by FBP binding in addition to that caused by PEP binding may be due to direct

Alignment A

481	waed vd lrvn l amnv g kar	rabbit M1
481	waed vd lrvn l amnv g kar	cat M1
452	wtd d vea r in f gie k ake f	yeast
427	ddfy- r lgkelalqs	<i>E. coli</i>
453	ke h -- r vaagvefak s k	<i>Leishmanic</i>

Alignment B

481	waed vd lrvn l amnv g kar	rabbit M1
481	waed vd lrvn l amnv g kar	cat M1
452	wtd d vea r in f gie k ake f	yeast
427	ddfyrl g kelalqs	<i>E. coli</i>
453	ke-- h rvaagvefak s k	<i>Leishmanic</i>

Figure 44. Hand Alignment of Amino Acids of Crystallized PK Isozymes in the Arginine 459 Helix. Alignment A shows sequences aligned to the sequence of yeast PK based on *E. coli's* arginine 431 being equivalent to yeast's arginine 459 (21). Alignment B shows sequences aligned to the sequence of yeast PK based on *Leishmania's* arginine 456 being equivalent to yeast's arginine 459 (22). Conserved residues that may correspond to yeast 459 and 455 are in bold.

interactions of FBP with tryptophan 452 and not due to further protein structural changes around the tryptophan. This further supports that a shift of the H17 helix may be intermediary to communications between the FBP binding site and the active site.

The amino acids that interact with the sugar ring (402-407 loop) and 6'-phosphate of FBP in yeast PK (20) are not conserved between species (Figure A1). Therefore the bonds responsible for anchoring FBP may vary between PK isozymes. One might predict that the residues that mediate allosteric activation are highly conserved in allosteric activated PK isozymes. The lack of conservation of residues of the 402-407 loop also supports that the residues of this loop are probably not key residues in mediating allosteric activation.

The structure of the 402-407 loop in crystallized yeast PK is responsive to the presence of FBP (20), even though the yeast PK structures both in the presence and absence of FBP were activated by substrate analogs (20). Yeast PK's affinity for FBP is under allosteric regulated by PEP (Figure 15). Therefore, activation of the yeast PK isozyme by substrate, or substrate analogs, causes a change in the FBP binding site that affects FBP affinity. Since the structure of the 402-407 hydrogen-bonding loop of substrate activated yeast PK is responsive to FBP binding (20), this loop may not be part of the structural changes in the FBP binding site caused by substrate activation. In crystallized yeast PK structures, the responsiveness of the 402-407 hydrogen-bonding loop to FBP binding (20) is consistent with the mechanism of FBP allosteric activation proposed here.

As discussed earlier, the M1 isozyme has a hyperbolic response to varying concentrations of PEP in the absence of allosteric effectors, while the response of the M2 isozyme is sigmoidal (26). There are 22 amino acid differences between these two isozymes (25). The position of the last residue that differs between the mammalian M1 and M2 PK's is at a position equivalent to yeast PK 403 (threonine in yeast), and is part of the 402-407 hydrogen-bonding loop which binds the 6'-phosphate of FBP (20). In the M1 isozyme the position equivalent to yeast PK 403 is a glutamic acid. The same equivalent position in the M2 isozyme is a lysine. In the current study the threonine 403 of yeast PK

was mutated to mimic that of the M1 isozyme (T403E) and that of the M2 isozyme (T403K). Since 403 is in a position to interact with the 6'-phosphate of FBP, T403E was predicted to repel negatively charged FBP, while T403K was predicted to increase the yeast PK's affinity for FBP. The M1 isozyme exists in an activated state in the absence of FBP, therefore, the presence of a negative charge in the FBP binding site was considered as a possible activator of PK. Activation of the T403E yeast PK mutation in the absence of FBP was considered possible. As predicted the T403E yeast PK mutation was less sensitive to activation by FBP (Figure 34) and had a decreased affinity for FBP as indirectly evidenced by fluorescence titration curves (Figure 35). However, the sigmoidal kinetic response of T403E to varying PEP concentrations (Figure 34) does not support activation of the enzyme caused by introducing a negative charge into the FBP binding site. Surprisingly, the T403K mutation had a $S_{1/2}$ for FBP activation very similar to that of wild type PK (Table 12). Therefore, the 403 position is not predicted to be a key residue in mediating allosteric activation of yeast PK. This further supports that specific interactions between yeast PK and FBP are responsible for binding FBP and for activating the allosteric response of yeast PK. Therefore, an overall positive charge in the FBP binding site does not appear to mediate allosteric regulation through charge-charge interactions.

Pyruvate Kinase Regulation Speculation

As discussed in the introduction, allosteric effectors may shift the equilibrium between activity states independently of the substrate effects. Due to the possible ties between cooperative and allosteric regulation, discussing cooperative regulation may be useful to understand allosteric regulation. In order for PK to have cooperative regulation by PEP, then the ligation state of a PEP binding site must be communicated to one or both of the subunit interfaces and then to the other PEP binding sites. Communication of the PEP ligation to a subunit interface must be through the amino acids of PK.

There are several lines of evidence that support that communication at the C-C subunit interface is responsible for cooperative regulation. 1) The 22 amino acid

differences between the mammalian M1 and M2 isozymes occur in a 45 amino acid stretch which is largely located in the C-C interface (25). As a reminder, the mammalian M1 isozyme has a hyperbolic response to varying concentration of PEP and M2 has a sigmoidal response (26). 2) Mutating specific amino acids of the C-C interface has greatly altered cooperativity in mammalian M1, mammalian M2, yeast, and *B. stearthermophils* PK isozymes (59,76-78, this study). 3) Comparison of the amino acid sequence of the non-cooperative, dimeric PK isozyme from *Z. mobilis* (36,37) with amino acid sequence of cooperative, tetrameric PK isozymes suggests that loss of cooperativity may be the consequence of changes in the C-C subunit interface. 4) In the present study a single mutation, E392A, in the C-C interface causes the sigmoidal response to varying concentrations of PEP to become hyperbolic.

Within the C-C interface, a hydrogen bond between glutamic acid 392 of one subunit and tyrosine 414 of the neighboring subunit may mediate allosteric regulation. In this study, the E392A mutation completely removed cooperative regulation. Binding of PEP at the active site may be coupled to interactions between the glutamic acid 392 and tyrosine 414. Friesen *et al.* proposed that in mammalian muscle PK such a coupling between the C-C interface and the active site might involve hydrogen bonding between the tyrosine equivalent to yeast PK tyrosine 414 and an alanine at the 290 equivalent position (111). Mutagenesis of the 414 equivalent residue of rabbit muscle PK supports this possibility (111). Friesen *et al.* suggested that the 392 to 414 hydrogen-bond could be linked to the active site through the H10 helix (111).

Based on the crystal structure of yeast PK (20), a second possible regulation pathways might be proposed for coupling the 392-414 interactions with the active site (Figure 45). PK isozymes have a highly conserved tyrosine-arginine sequence equivalent to yeast PK 414-415. The *B. stearothermophilus* PK arginine equivalent to yeast PK 415 has previously been suggested to be in a salt bridge with the equivalent to yeast PK aspartic acid 327. This salt bridge has been suggested to be important to allosteric regulation, based on

mutation studies (34). In crystal structures of both mammalian M1 (17-19) and yeast (20) isozymes, this arginine is orientated towards charged groups across the A-C domain interface (Figure 42). A salt bridge across the A-C domain interface between arginine 415 and aspartic acid 327 may be part of a communication relay between the C-C interface and the active site. The aspartic acid 327 in yeast PK is in a loop at one end of S17 β -sheet while serine 332 is at the other end. The S17 β -sheet extends the A domain as part of the β -barrel structure. Serine 332 residue is in the active site. Therefore, the ligation state of PEP may be communicated from the active site through the S17 β -sheet to the salt bridge between aspartic acid 327 and arginine 415 and finally to the interactions between tyrosine 414 and glutamic acid 392. Unfortunately, the R415Q mutation designed in the current study was not expressed.

A third pathway can be proposed (Figure 45). The loop containing aspartic acid 327 is connected to the H11 helix. The H11 helix is part of the A-A interface. The H11 helix contains aspartic acid 317, which is in a salt bridge with arginine 264. Arginine 264, in turn, is covalently linked to aspartic acid 266, which is involved in coordinating the divalent cation in the active site. In this possible pathway, the ligation state of PEP may be communicated from the active site through the divalent cation to the 317 to 264 salt bridge, through the H11 helix, across the 327 to 415 salt bridge and to the interactions between tyrosine 414 and glutamic acid 392.

One might consider if cooperative regulation occurs by a ligand's ability to destabilize subunit interfaces or if a specific regulation relay pathway exists across a subunit interface. At the C-C subunit interface interruption of the interactions between glutamic acid 392 of one subunit and tyrosine 414 of the neighboring subunit may destabilize the subunit interface. The interactions at the interface may adjust to more favorable interactions. This rearrangement may be related to the T to R conformational switch assumed in both the concerted and sequential models of cooperative regulation (53,54). If cooperativity is due to a ligand's ability to destabilize a subunit interface, then any mutation that alters the stability

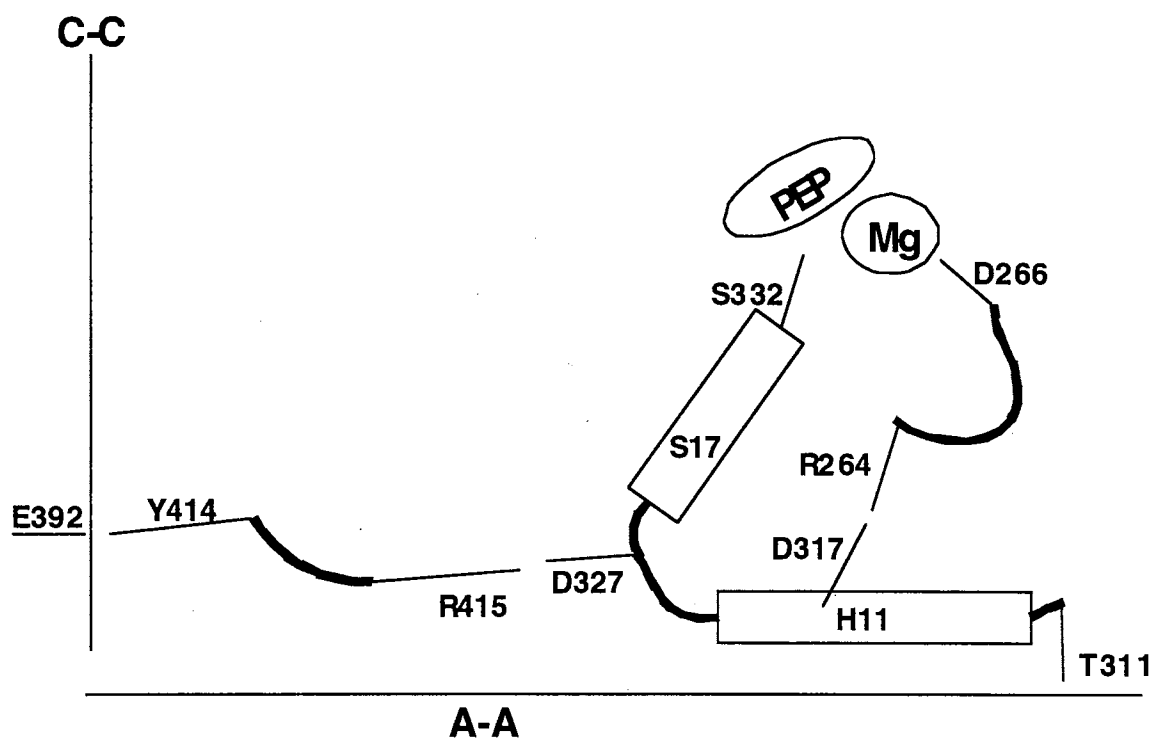


Figure 45. Possible Communication Pathways Linking the PEP Binding Site With the C-C Subunit Interface.

of the subunit interface would affect cooperativity. Therefore, an effect of a single mutation will be influenced by what other stabilizing interactions are already present. Such an explanation may explain the effects seen by adding an arginine at the 369 yeast PK equivalent position in the mammalian muscle PK isozyme. However, removing the arginine 369 equivalent residue in yeast PK, in the current study, as well as the mammalian M2 PK isozyme did not alter allosteric regulation.

Instead of a general destabilization of the C-C subunit interface, a molecular relay across the C-C interface may allow for active sites to communicate. Most likely is that a molecular relay across the C-C interface would connect two identical pathways, one in each subunit. If the 392 to 414 interaction is part of a molecular relay, then the two 392 to 414 contacts of a single C-C subunit interface might be coupled. Within a single subunit, the yeast PK structure (20) indicates that arginine 413 is in a salt bridge with glutamic acid 380 (Figure 46). Since arginine 413 is covalently linked to tyrosine 414 and glutamic acid 380 is located on the same helix (H14 helix) as glutamic acid 392, this 413 to 380 salt bridge might be involved in coupling the two 392 to 414 interactions of a C-C subunit interface. However, both R413Q and R413E did not greatly alter kinetic properties. This does not support that the 380 to 413 interactions are involved in coupling the two 392-414 interactions of a C-C subunit interface.

Next, one might consider if there is direct communication between a FBP binding site and a PEP binding site, or only communication of the two types of binding sites with the subunit interface? The E392A mutant yeast PK has a hyperbolic kinetic response to varying concentrations of PEP and a hyperbolic fluorescence quench response to varying concentrations of FBP (Figures 26 and 27). This suggests that this single mutation has interrupted the communication between PEP binding sites as well as between FBP binding sites. In addition, the PEP dependent kinetic activation curve of E392A was not responsive to FBP, nor the FBP dependent fluorescence quench titration curve of E392A responsive to PEP (Figures 26 and 27). Therefore the communication between the FBP binding site and

the PEP binding site has been disrupted by a C-C interface mutation. The 392 position is likely to play a major role in allosteric activation.

Glutamic acid 392 is located near the S18 β -sheet that extends the hydrophobic core of the C domain (Figure 47). The hydrogen-bonding loop responsible for binding the 6'-phosphate of FBP is located at the other end of the S18 β -sheet. After the backbone forms the hydrogen-bonding loop in the FBP binding pocket, it forms the H15 helix. Arginine 413, tyrosine 414, and arginine 415 are at the end of the H15 helix. The backbone then makes a β -sheet (S19 β -sheet) which again passes through the hydrophobic core of the C-domain. At the end of the S19 β -sheet arginine 425 interacts with aspartic acid 455 of the H17 helix. As a reminder, H17 contains arginine 459, which forms an ionic bond with the 1'-phosphate of FBP. Therefore the S18 β -sheet, the H15 helix and the S19 β -sheet may all be involved in relaying the ligation state of the FBP binding site to the E392-Y414-R415 pathway already proposed in PEP cooperative regulation (Figure 47).

The molecular interactions of the FBP binding site in yeast PK have already been discussed. Data in the current study are constant with the importance of a specific amino acid residue involvement in allosteric regulation, in contrast to an overall charge effect introduced by FBP binding. Mutagenesis of amino acids in the hydrogen binding loop that interact with the 6'-phosphate of FBP do not support the involvement of these amino acids communicating a regulation "signal". Therefore, the link between the hydrogen bonding loop of the FBP binding site with glutamic acid 392 through the S18 β -sheet helix may not be important in communicating the ligation state of the FBP binding site to the proposed E392-Y414-R415 cooperativity communication pathway. The same may be true of the link between the hydrogen-bonding loop with tyrosine 414 through the H15 helix.

If the formation of the ionic bond between arginine 459 and the 1'-phosphate of FBP causes the H17 helix to shift, then ionic interactions between aspartic acid 455 and arginine 425 may be disrupted (Figure 48). This altered interaction may be communicated through the S19 β -sheet to arginine 415. The ligation state of the FBP binding site may

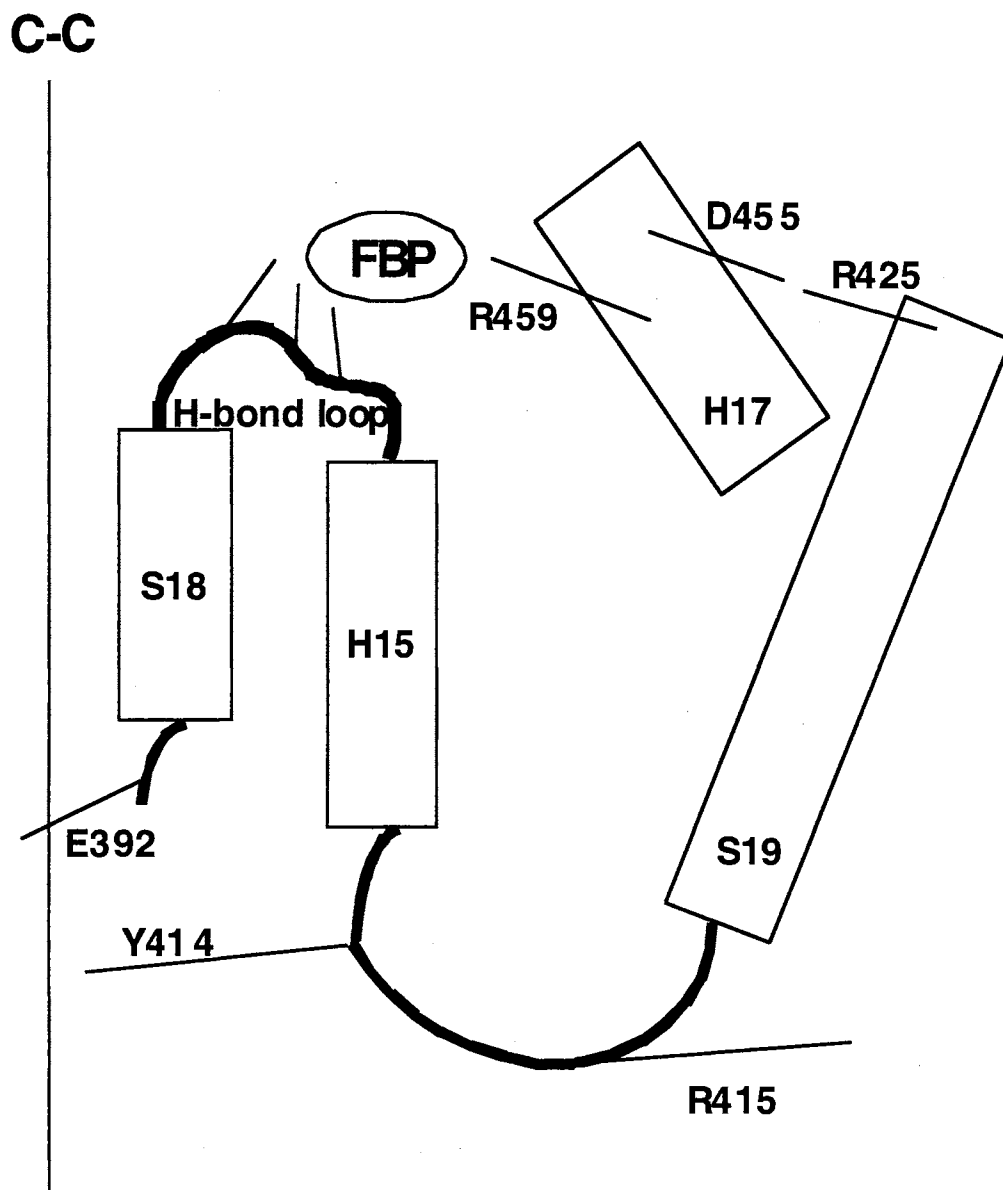


Figure 47. Possible Communication Pathways Linking the FBP Binding Site With the C-C Subunit Interface.

influence the E392-Y414-R415 cooperativity communication pathway. Therefore FBP ligation might affect both the C-C subunit interface and the active site. This possible communication pathway may also be used to explain the cooperative regulation of FBP apparent affinity.

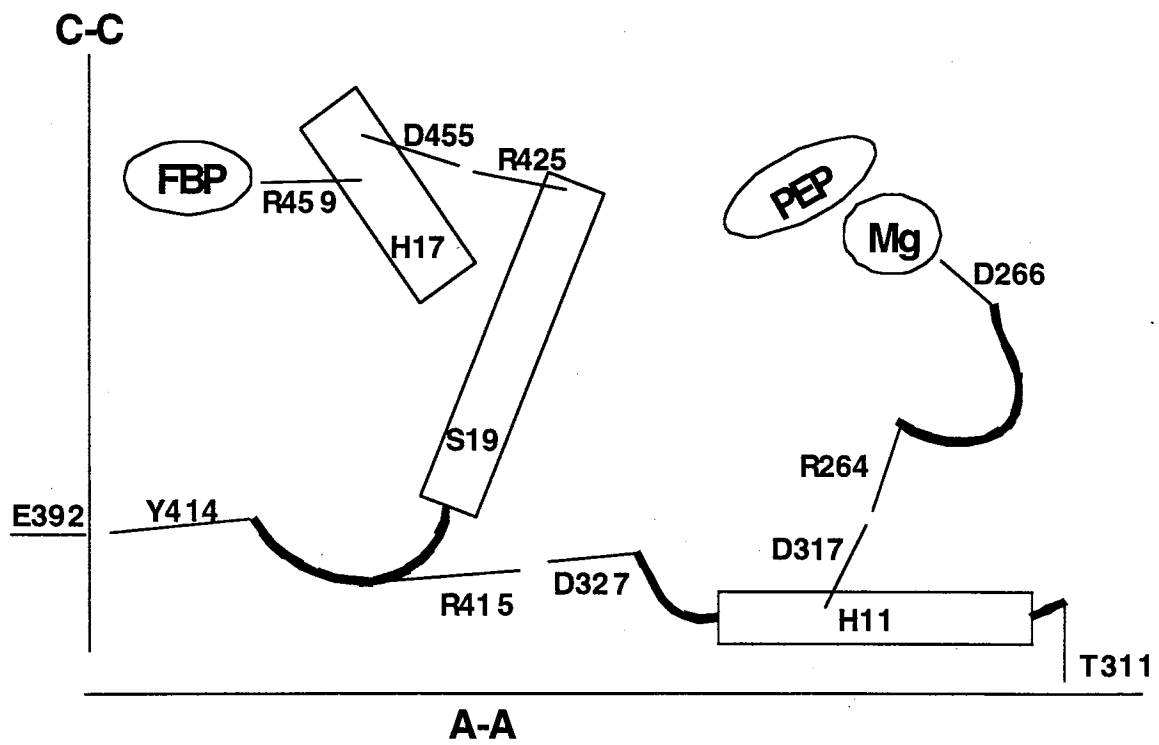
A possible communication pathway through the S17 β -sheet, as discussed earlier, does not account for the central role of the divalent cation in coupling binding of FBP to binding of PEP as has been reported by Mesecar *et al.* (60,61). However, the proposed pathway through the H11 helix incorporates a role of the divalent cation in coupling FBP binding and PEP binding. Furthermore, the H11 helix is connected to the 311 position of the T311M mutation, which in this study affects both PEP and FBP apparent affinities. Therefore the communication pathway(s) most consistent with data of this study and that reported in the literature is summarized in Figure 48.

Future Studies

In the regulation pathway(s) proposed above (Figure 48) there are a few residues that might be predicted to be key elements of the pathway(s). Mutagenesis of these key residues might be used to probe the accuracy of the proposed regulation pathway(s). The ionic bond between arginine 425 and aspartic acid 455 is central in FBP communication in the proposed model. Therefore, mutagenesis of arginine 425 and aspartic acid 455 to alter charges and side chain lengths might be useful to testing the model. The ionic bond between arginine 264 and aspartic acid 317 is central in PEP communication in the model. Mutagenesis of arginine 264 and aspartic acid 317 to alter charges and side chain lengths might be useful to testing the model. In addition the model predicts that the ionic bond between arginine 415 and aspartic acid 327 is important in all channels of communication. Therefore, further mutagenesis of arginine 415 and aspartic acid 327 to alter charges and side chain length might be useful to testing the model.

Mutations created in the current study might be useful in a number of new investigations into allosteric regulation of PK. The E392A mutation is locked in the

Figure 48. Proposed Communication Pathways. Formation of the ionic bond between the 1'-phosphate of FBP and arginine 459 might cause a rearrangement of the H17 helix. This rearrangement might disrupt the interactions of aspartic acid 455 and arginine 425. The "signal" might be passed from arginine 425 through the S19 β -sheet to a salt bridge between the A and C domains involving arginine 415 and aspartic acid 327. Changes in the 415 to 327 salt bridge might cause the H11 helix to rearrange, which might in turn effect a salt bridge between aspartic acid 317 and arginine 264. Changes in the 317 to 264 salt bridge might then cause changes in the interaction between aspartic acid 266 and the divalent cation. These changes might be responsible for altered $S_{1/2}$ for PEP associated with allosteric regulation by FBP. The "signal" passed through the S19 β -sheet might also affect the C-C subunit interface. A hydrogen bond across the C-C subunit interface involving tyrosine 414 and glutamic acid 392 of the neighboring subunit might be one important subunit contact involved in regulation. Interactions across the C-C interface may give rise to the cooperativity in FBP binding. The same pathways, which communicate the PEP binding site with the C-C subunit interface, might be used to explain the cooperativity of PEP apparent binding. In like manner, the pathway linking the PEP binding site with the FBP binding site might be used to explain allosteric regulation of FBP binding by PEP.



activated state (R-state) and therefore comparison of free energies of E392A PK ligation with those of wild type PK ligation can be used to derive stoichiometric free energy components of FBP cooperativity for yeast PK. R459Q disrupts FBP binding and therefore if mixed tetramers of this mutation with wild type PK are generated, the stepwise ligation of yeast PK with FBP could be determined. Similar approaches have been used to determine stoichiometric free energy components and stepwise ligation of hemoglobin (55).

Summary

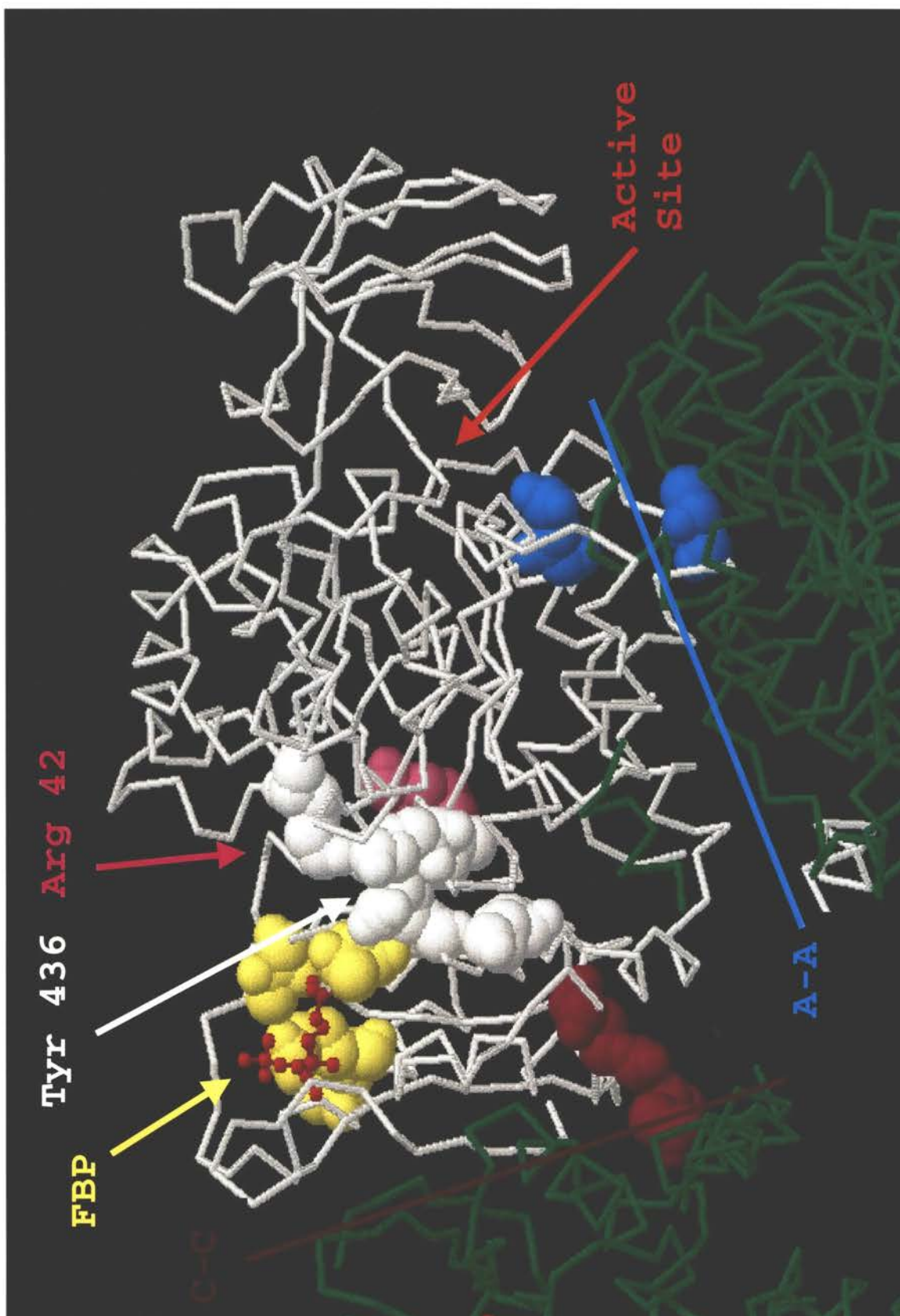
Yeast pyruvate kinase (PK), the tetrameric regulating enzyme of carbohydrate metabolism, catalyzes the final step of glycolysis and is regulated by several mechanisms including feed forward activation by fructose-1,6-bisphosphate (FBP). This study used site directed mutagenesis as the major experimental approach to gain understanding of the mechanism of allosteric regulation of yeast PK by FBP. Two positively charged A-C domain interface pockets (Tyr 436 pocket and Arg 42 pocket), the C-C subunit interface, the A-A subunit interface, and the FBP binding site were probed to understand their roles in allosteric regulation of PK by FBP (Figure 49).

Interrupting a specific hydrogen bond in the C-C interface disrupts cooperative binding of both PEP and FBP. Even though a number of roles for residues in the A-C domain contacts have been proposed, little evidence has supported these theories. However, specific interactions in the A-C domain contacts, which may include yeast PK arginine 415, may be in an allosteric signal pathway between the C-C subunit interface and the active site. Altered energy constraints due to changes at C-C subunit interface is also possible.

The role of the A-A interface in cooperative and allosteric regulation has not been well studied. A-A interface residues that play a role in allosteric regulation do not abolish cooperativity. In addition, mutagenesis of the A-A interface residues causes the ADP apparent affinity to become regulated by FBP. Current evidence suggests that both the active site and FBP binding site are sensitive to the perturbations at the A-A interface.

Several possible pathways of communication between the subunit interfaces, the active site, and the FBP binding site are discussed. A molecular network of communication may link the FBP binding site, the PEP binding site, and the C-C subunit interface.

Figure 49. Locations of Expressed Mutations. A yeast PK subunit as resolved by Jurica *et al.* (20) is shown in white. Neighboring subunits are shown in green. FBP is shown in the FBP binding site as a red ball-and-stick structure. Mutations in the A-A subunit contacts (A-A) are in cyan spacefill. Mutations in the C-C subunit contacts (C-C) are in purple spacefill. Mutations in the FBP binding site (FBP) are in yellow spacefill. Expressed mutations in the Tyr 436 pocket (Tyr 436) are in white spacefill. R77Q of the Arg 42 pocket (Arg 42) is shown in pink spacefill and appears on the back site of the structure.



BIBLIOGRAPHY

1. Valentine, W. N., Tanaka, K. R., and Miwa, S. (1961) *Trans. Assn. Am. Physicians* **74**, 100-110
2. Lakomek, M., and Winkler, H. (1997) *Biophys. Chem.* **66**, 269-284
3. Jacobasch, G., and Rapoport, S. M. (1996) *Mol. Aspects Med.* **17**, 143-170
4. Tanaka, K. R., and Paglia, D. E. (1995) in *The Metabolic and Molecular Bases of Inherited Diseases* (Scriver C. R. et. al., ed), pp. 3485-3511 McGraw-Hill, New York
5. Miwa, S., Kanno, H., and Fujii, H. (1993) *Am. J. Hematol.* **42**, 31-35
6. Chapman, B. L., and Giger, U. (1990) *J. Small Anim. Pract.* **31**, 610-616
7. Whitney, K. M., Goodman, S. A., Bailey, E. M., and Lothrop, C. D., Jr. (1994) *Exp. Hematol.* **22**, 866-874
8. Searcy, G. P., Miller, D. R., and Tasker, J. B. (1971) *Can. J. Comp. Med. Vet. Sci.* **35**, 67-70
9. Prasse, K. W., Crouser, D., Beutler, E., Walker, M., and Schall, W. D. (1975) *J. Am. Vet. Med. Assoc.* **166**, 1170-1175
10. Kanno, H., Morimoto, M., Fujii, H., Tsujimura, T., Asai, H., Noguchi, T., Kitamura, Y., and Miwa, S. (1995) *Blood* **86**, 3205-3210
11. Nwagwu, M., and Opperdoes, F. R. (1982) *Acta. Trop.* **39**, 61-72
12. Cazzulo, J. J. (1992) *FASEB J.* **6**, 3153-3161
13. Cronin, C. N., and Tipton, K. F. (1985) *Biochem. J.* **227**, 113-124
14. Opperdoes, F. R. (1987) *Annu. Rev. Microbiol.* **41**, 127-151
15. Van Schaftingen, E., Opperdoes, F. R., and Hers, H.-G. (1985) *Eur. J. Biochem.* **166**, 653-661
16. Stuart, D. I., Levine, M., Muirhead, H., and Stammers, D. K. (1979) *J. Mol. Biol.* **134**, 109-142
17. Larsen, T. M., Laughlin, L. T., Holden, H. M., Rayment, I., and Reed, G. H. (1994) *Biochemistry* **33**, 6301-6309
18. Larsen, T. M., Benning, M. M., Wesenberg, G. E., Rayment, I., and Reed, G. H. (1997) *Arch. Biochem. Biophys.* **345**, 119-206
19. Larsen, T. M., Benning, M. M., Rayment, I., and Reed, G. H. (1998) *Biochemistry* **37**, 6247-6255
20. Jurica, M. S., Mesecar, A., Heath, P. J., Shi, W., Nowak, T., and Stoddard, B. L. (1998) *Structure* **15**, 195-210
21. Mattevi, A., Valentini, G., Rizzi, M., Speranza, M. L., Bolognesi, M., and Coda, A. (1995) *Structure* **3**, 729-741
22. Rigden, D. J., Phillips, S. E. V., Michels, P. A. M., and Fothergill-Gilmore, L. A. (1998) *Unpublished*
23. Muirhead, H. (1983) *TIBS* **8**, 326-330
24. Mesecar, A. D. (1995) Ph.D. Dissertation, University of Notre Dame
25. Noguchi, T., Inoue, H., and Tanaka, T. (1986) *J. Biol. Chem.* **261**, 13807- 13812

26. Consler, T. G., Woodard, S. H., and Lee, J. C. (1989) *Biochemistry* **28**, 8756-8764
27. Pogson, C. I. (1968) *Biochem. J.* **110**, 67-77
28. Schering, B., Eigenbrodt, E., Linder, D., and Schoner, W. (1982) *Biochim. Biophys. Acta* **717**(2), 337-347
29. VanBerkel, T. J. C. (1974) *Biochim. Biophys. Acta* **370**, 140-152
30. Noguchi, T., Yamada, K., Inoue, H., Matsuda, T., and Tanaka, T. (1987) *J. Biol. Chem.* **262**, 14366-14371
31. Blair, J. B. (1980) in *The Regulation on Carbohydrate Formation and Utilization in Mammals* (Veneziale, C. M., ed), pp. 121-151, University Park Press, Baltimore
32. Boivin, P., Galand, C., and Estrada, M. (1980) *Experientia* **36**, 900-901
33. Sakai, H., and Ohta, T. (1987) *J. Biochem.* **101**, 633-642
34. Walker, D., Chia, W. N., and Muirhead, H. (1992) *J. Mol. Biol.* **228**, 265-276
35. Malcovati, M., and Valentini, G. (1982) *Methods Enzymol.* **90**, 170-179
36. Steiner, P., Fussenegger, M., Bailey, J. E., and Sauer, U. (1998) *Gene* **220**, 31-38
37. Pawluk, A., Scopes, R. K., and Griffiths-Smith, K. (1986) *Biochem. J.* **238**, 275-281
38. Podesta, F. E., and Plaxton, W. C. (1991) *Biochem. J.* **279**, 495-501
39. Kinderlerer, J., Ainsworth, S., Morris, C. N., and Rhodes, N. (1986) *Biochem. J.* **234**, 699-703
40. Hess, B., Haeckel, R., and Brand, K. (1966) *Biochem. Biophys. Res. Commun.* **24**, 824-831
41. Haeckel, R., Hess, B., Lauterborn, W., and Wuster, K. H. (1968) *Hoppe Seylers Z. Physiol. Chem.* **349**, 699-714
42. Blair, J. B., and Harman, D. L. (1986) *Feder. Proc.* **45**, 1657
43. Brazill, D. T., Thorner, J., and Martin, G. S. (1997) *J. Bacteriol.* **179**, 4415-4418
44. Kuczenski, R. T., and Suelter, C. H. (1971) *Biochemistry* **10**, 2862-2866
45. Wieker, H. J., and Hess, B. (1971) *Biochemistry* **10**, 1243-1248
46. Macfarlane, N., and Ainsworth, S. (1972) *Biochem. J.* **129**, 1035-1047
47. Rhodes, N., Morris, C. N., Ainsworth, S., and Kinderlerer, J. (1986) *Biochem. J.* **234**, 705-715
48. Hunsley, J. R., and Suelter, C. H. (1969) *J. Biol. Chem.* **244**, 4815-4818
49. Hunsley, J. R., and Suelter, C. H. (1969) *J. Biol. Chem.* **244**, 4819-4822
50. Yun, S. L., Aust, A. E., and Suelter, C. H. (1976) *J. Biol. Chem.* **251**, 124-128
51. Morris, C. N., Ainsworth, S., and Kinderlerer, J. (1986) *Biochem. J.* **234**, 691-698
52. Murcott, T. H. L. (1990) Ph.D. Dissertation, University of Bristol
53. Koshland, D. E. J., Nemethy, G., and Filmer, D. (1966) *Biochemistry* **5**, 365-385
54. Monod, J., Wyman, J., and Changeux, J.-P. (1965) *J. Mol. Biol. Chem.* **12**, 88-118
55. Ackers, G. K. (1998) *Adv. Protein Chem.* **51**, 185-253
56. Muirhead, H., Clayden, D. A., Barford, D., Lorimer, C. G., Fothergill-Gilmore, L. A., Schiltz, E., and Schmitt, W. (1986) *EMBO J.* **5**, 475-481
57. Dyson, R. D., and Cardenas, J. M. (1973) *J. Biol. Chem.* **248**, 8482-8488
58. Johannes, K.-J., and Hess, B. (1973) *J. Mol. Biol.* **76**, 181-205
59. Lovell, S. C., Mullick, A. H., and Muirhead, H. (1998) *J. Mol. Biol.* **276**, 839-851
60. Mesecar, A. D., and Nowak, T. (1997) *Biochemistry* **36**, 6803-6813
61. Mesecar, A. D., and Nowak, T. (1997) *Biochemistry* **36**, 6792-6802
62. Nowak, T. (1978) *J. Biol. Chem.* **253**, 1998-2004
63. Raushel, F. M., and Villafranca, J. J. (1980) *Biochemistry* **19**, 5481-5485
64. Loria, J. P., and Nowak, T. (1998) *Biochemistry* **37**, 6967-6974
65. Loria, J. P. (1997) Ph.D. Dissertation, University of Notre Dame
66. Consler, T. G., Uberbacher, E. C., Bunick, G. J., Liebman, M. N., and Lee, J. C. (1988) *J. Biol. Chem.* **263**, 2794-801
67. Wurster, B., and Hess, B. (1976) *FEBS Lett.* **63**, 17-21
68. Fishbein, R., Benkovic, P. A., and Benkovic, S. J. (1975) *Biochemistry* **14**, 4060-4063

69. Speranza, M. L., Valentini, G., and Malcovati, M. (1990) *Eur. J. Biochem.* **191**, 701-704
70. Stammers, D. K., and Muirhead, H. (1975) *J. Mol. Biol.* **95**, 213-25
71. Ernest, I., Callens, M., Uttaro, A. D., Chevalier, N., Opperdoes, F. R., Muirhead, H., and Michels, P. A. (1998) *Protein Expr. Purif.* **13**, 373-382
72. Speranza, M. L., Valentini, G., Iadarola, P., Stoppini, M., Malcovati, M., and Ferri, G. (1989) *Biol. Chem. Hoppe Seyler* **370**, 211-216
73. Valentini, G., Speranza, M. L., Iadarola, P., Ferri, G., and Malcovati, M. (1988) *Biol. Chem. Hoppe Seyler* **369**, 1219-1226
74. Valentini, G., Iadarola, P., Ferri, G., and Speranza, M. L. (1995) *Biol. Chem. Hoppe Seyler* **376**, 231-235
75. Blair, J. B., and Walker, R. G. (1984) *Arch. Biochem. Biophys.* **232**, 202-213
76. Ikeda, Y., and Noguchi, T. (1998) *J. Biol. Chem.* **273**, 12227-12233
77. Ikeda, Y., Tanaka, T., and Noguchi, T. (1997) *J. Biol. Chem.* **272**, 20495-20501
78. Collins, R. A., McNally, T., Fothergill-Gilmore, L. A., and Muirhead, H. (1995) *Biochem. J.* **310**, 117-123
79. Friesen, R. H. E., and Lee, J. C. (1998) *J. Biol. Chem.* **273**, 14772-14779
80. Cheng, X., Friesen, R. H., and Lee, J. C. (1996) *J. Biol. Chem.* **271**, 6313-6321
81. Mattevi, A., Bolognesi, M., and Valentini, G. (1996) *FEBS Let.* **389**, 15-19
82. Demina, A., Varughese, K. I., Forman, L., Beutler, E., Lakomek, M., and Winkler, H. (1997) *Blood* **90**, 1199-1199
83. Cohen-Solal, M., Prehu, C., Wajeman, H., Poyart, C., Bardakdjian-Michau, J., Kister, J., Prome, D., Valentin, C., Bachir, D., and Galacteros, F. (1998) *Br. J. Haematol.* **103**, 950-956
84. Kanno, H., Fujii, H., Wei, D. C., Chan, L. C., Hirono, A., Tsukimoto, I., and Miwa, S. (1997) *Blood* **89**, 4213-4218
85. Baronciani, L., Bianchi, P., and Zanella, A. (1996) *Blood Cells Mol. Dis.* **22**, 259-264
86. Beutler, E., and Baronciani, L. (1996) *Hum. Mutat.* **7**, 1-6
87. Lakomek, M., Neubauer, B., von der Luhe, A., Hoch, G., Winkler, H., and Schroter, W. (1992) *Eur. J. Haematol.* **49**, 82-92
88. Park, S. (1998) M.S. Thesis, Oklahoma State University
89. Maitra, P. K., and Lobo, Z. (1977) *Molec. Gen. Genet.* **152**, 193-200
90. Maitra, P. K., and Lobo, Z. (1977) *Eur. J. Biochem.* **78**, 353-360
91. Gillies, R. J., and Benoit, A. G. (1983) *Biochim. Biophys. Acta* **762**, 466-470
92. Hartwell, L. H., Culotti, J., and Reid, B. (1970) *Proc. Natl. Acad. Sci. U.S.A.* **66**, 352-359
93. Beutler, E., Westwood, B., van Zwieten, R., and Roos, D. (1997) *Hum. Mutat.* **9**, 282-285
94. Sambrook, J., Fritsch, E. F., and Maniatis, T. (1989) *Molecular Cloning: A Laboratory Manual*, 2 Ed., Cold Spring Harbor Laboratory Press, Cold Spring Harbor
95. Burke, R. L., Tekamp-Olson, P., and Najarian, R. (1983) *J. Biol. Chem.* **258**, 2193-2201
96. Beuken, E., Vink, C., and Bruggeman, C. A. (1998) *BioTechniques* **24**, 748-750
97. Gietz, R. D., and Schiestl, R. H. (1995) in *Methods in Molecular and Cellular Biology* Vol. 5, pp. 255-269
98. Boles, E., Schulte, F., Miosga, T., Freidel, D., Schluter, E., Zimmermann, F. K., Hollenberg, C. P., and Heinisch, J. J. (1997) *J. Bacteriol.* **179**, 2987-2993
99. Bucher, T., and Pfeleiderer, G. (1955) in *Methods Enzymol.* (Colowick, S. P. and Kaplan, N. O., ed) Vol. 1, pp. 435-440, Academic Press, Inc., New York
100. Michal, G., and Beutler, H.-O. (1974) in *Methods of Enzymatic Analysis* (Bergmeyer, H. U., ed) Vol. 3, pp. 1314-1319, Academic Press, Inc., New York

101. Czok, R., and Lamprecht, W. (1974) in *Methods of Enzymatic Analysis* (Bergmeyer, H. U., ed) Vol. 3, pp. 1446-1451, Academic Press, Inc., New York
102. Lehoux, E. A., Svedruzic, Z., Backer, S. M., and Spivey, H. O. (1999) *unpublished*
103. Murcott, T. H., Gutfreund, H., and Muirhead, H. (1992) *EMBO J.* **11**, 3811-3814
104. Hill, A. V. (1910) *J. Physiol.* **40**, 190-224
105. Chandler, J. P., Hill, D. E., and Spivey, H. O. (1972) *Comput. and Biomed. Res.* **5**, 515-534
106. Perkins, J., and Gadd, G. M. (1996) *Mycol. Res.* **100**, 449-454
107. Sober, H. A. (1970) *CRC Handbook of Biochemistry: Selected Data for Molecular Biology*, 2 Ed., The Chemical Rubber Co., Cleveland
108. Kuczenski, R. T., and Suelter, C. H. (1971) *Biochemistry* **10**, 2867-2872
109. Bollenbach, T. (1999) Ph.D. Dissertation, University of Notre Dame
110. Nowak, T. (1999), personal communication
111. Friesen, R. H. E., Castellani, R. J., Lee, J. C., and Braun, W. (1998) *Biochemistry* **37**, 15266-15276
112. Boles, E. (1997) in *Yeast Sugar Metabolism* (Zimmermann, F. K., and Entian, K.-D., eds), pp. 171-186, Technomic Publishing Co., Inc., Lancaster
113. Kanno, H., Fujii, H., Hirono, A., and Miwa, S. (1991) *Proc. Natl. Acad. Sci. USA* **88**, 8218-8221
114. Tani, K., Fujii, H., Tsutsumi, H., Sukegawa, J., Toyoshima, K., Yoshida, M. C., Noguchi, T., Tanaka, T., and Miwa, S. (1987) *Biochem. Biophys. Res. Commun.* **143**, 431-438
115. Izumi, S., Manabe, A., Tomoyasu, A., Kihara-Negishi, F., and Ariga, H. (1995) *Biochim. Biophys. Acta* **1267**, 135-138
116. Takenaka, M., Noguchi, T., Sadahiro, S., Hirai, H., Yamada, K., Matsuda, T., Imai, E., and Tanaka, T. (1991) *Eur. J. Biochem.* **198**, 101-106
117. Shi, Y. B., Liang, V. C. T., Parkison, C., and Cheng, S. Y. (1994) *FEBS Lett.* **355**, 61-64
118. Lonberg, N., and Gilbert, W. (1985) *Cell* **40**(1), 81-90
119. McNally, T., Purvis, I. J., Fothergill-Gilmore, L. A., and Brown, A. J. (1989) *FEBS Lett.* **247**, 312-316
120. Goffeau, A., and Purnelle, B. (1996) *unpublished*
121. Strick, C. A., James, L. C., O'Donnell, M. M., Gollaher, M. G., and Franke, A. E. (1992) *Gene* **118**, 65-72
122. de Graaff, L., and Visser, J. (1988) *Curr. Genet.* **14**, 553-560
123. de Graaff, L., van den Broeck, H., and Visser, J. (1992) *Curr. Genet.* **22**, 21-27
124. Schindler, M., Mach, R. L., Vollenhofer, S. K., Hodits, R., Gruber, F., Visser, J., De Graaff, L., and Kubicek, C. P. (1993) *Gene* **130**, 271-275
125. Allert, S., Ernest, I., Poliszczak, A., Opperdoes, F. R., and Michels, P. A. M. (1991) *Eur. J. Biochem.* **200**, 19-27
126. Ernest, I., Opperdoes, F. R., and Michels, P. A. M. (1994) *Biochem. Biophys. Res. Commun.* **201**, 727-732
127. Cole, K. P., Blakeley, S. D., and Dennis, D. T. (1992) *Gene* **122**, 255-261
128. Gottlob-Mchugh, S. G., Blakeley, S. D., Knowles, V., Plaxton, W. C., Miki, B. G., and Dennis, D. T. (1994) *unpublished*
129. Kunst, F., Ogasawara, N., Moszer, I., Albertini, A. M., Alloni, G., Azevedo, V., Bertero, M. G., Bessieres, P., Bolotin, A., Borchert, S., Boriss, R., Boursier, L., Brans, A., Braun, M., Brignell, S. C., Bron, S., Brouillet, S., Bruschi, C. V., Caldwell, B., Capuano, V., Carter, N. M., Choi, S. K., Codani, J. J., Connerton, I. F., Cummings, N. J., Daniel, R. A., Denizot, F., Devine, K. M., Duesterhoeft, A., Ehrlich, S. D., Emmerson, P. T., Entian, K. D., Errington, J., Fabret, C., Ferrari, E., Foulger, D., Fritz, C., Fujita, M., Fujita, Y., Fuma, S., Galizzi, A., Galleron, N., Ghim, S. Y., Glaser, P., Goffeau, A., Golightly, E. J., Grandi, G., Guiseppi, G., Guy, B. J., Haga, K., Haiech, J., Harwood, C. R., Henaut, A., Hilbert, H., Holsappel, S., Hosono,

- S., Hullo, M. F., Itaya, M., Jones, L., Joris, B., Karamata, D., Kasahara, Y., Klaerr-Blanchard, M., Klein, C., Kobayashi, Y., Koetter, P., Koningstein, G., Krogh, S., Kumano, M., Kurita, K., Lapidus, A., Lardinois, S., Lauber, J., Lazarevic, V., Lee, S. M., Levine, A., Liu, H., Masuda, S., Mauel, C., Medigue, C., Medina, N., Mellado, R. P., Mizuno, M., Moestl, D., Nakai, S., Noback, M., Noone, D., O'Reilly, M., Ogawa, K., Ogiwara, A., Oudega, B., Park, S. H., Parro, V., Pohl, T. M., Portetelle, D., Porwollik, S., Prescott, A. M., Presecan, E., Pujic, P., Purnelle, B., et al. (1997) *Nature* **390**, 249-256
130. Tanaka, K., Sakai, H., Ohta, T., and Matsuzawa, H. (1995) *Biosci. Biotechnol. Biochem.* **59**, 1536-1542
131. Sakai, H., and Ohta, T. (1993) *Eur. J. Biochem.* **211**, 851-859
132. Blattner, F. R., Plunkett III, G., Bloch, C. A., Perna, N. T., Burland, V., Riley, M., Collado-Vides, J., Glasner, J. D., Rode, C. K., Mayhew, G. F., Gregor, J., Davis, N. W., Kirkpatrick, H. A., Goeden, M. A., Rose, D. J., Mau, B., and Shao, Y. (1997) *Science* **277**, 1453-1462
133. Kaneko, T., Sato, S., Kotani, H., Tanaka, A., Asamizu, E., Nakamura, Y., Miyajima, N., Hirosawa, M., Sugiura, M., Sasamoto, S., Kimura, T., Hosouchi, T., Matsuno, A., Muraki, A., Nakazaki, N., Naruo, K., Okumura, S., Shimpo, S., Takeuchi, C., Wada, T., Watanabe, A., Yamada, M., Yasuda, M., and Tabata, S. (1996) *DNA Res.* **3**, 109-136
134. Llanos, R. M., Harris, C. J., Hillier, A. J., and Davidson, B. E. (1993) *J. Bacteriol.* **175**, 2541-2551
135. Fraser, C. M., Casjens, S., Huang, W. M., Sutton, G. G., Clayton, R., Lathigra, R., White, O., Ketchum, K. A., Dodson, R., Hickey, E. K., Gwinn, M., Dougherty, B., Tomb, J. F., Fleischmann, R. D., Richardson, D., Peterson, J., Kerlavage, A. R., Quackenbush, J., Salzberg, S., Hanson, M., Vugt, R. V., Palmer, N., Adams, M. D., Gocayne, J., Weidman, J., Utterback, T., Wathley, L., McDonald, L., Artiach, P., Bowman, C., Garland, S., Fujii, C., Cotton, M. D., Horst, K., Roberts, K., Hatch, B., Smith, H. O., and Venter, J. C. (1997) *Nature* **390**, 580-586
136. Blakeley, S., Gottlob-McHugh, S., Wan, J., Crews, L., Miki, B., Ko, K., and Dennis, D. (1993) *unpublished*
137. Blakeley, S., Gottlob-McHugh, S., Wan, J., Crews, L., Miki, B., Ko, K., and Dennis, D. T. (1995) *Plant Mol. Biol.* **27**, 79-89
138. Fleischmann, R. D., Adams, M. D., White, O., Clayton, R. A., Kirkness, E. F., Kerlavage, A. R., Bult, C. J., Tomb, J. F., Dougherty, B. A., Merrick, J. M., McKenney, K., Sutton, G., FitzHugh, W., Fields, C., Gocayne, J. D., Scott, J., Shirley, R., Liu, L. I., Glodek, A., Kelley, J. M., Weidman, J. F., Phillips, C. A., Spriggs, T., Hedblom, E., Cotton, M. D., Utterback, T. R., Hanna, M. C., Nguyen, D. T., Saudek, D. M., Brandon, R. C., Fine, L. D., Fritchman, J. L., Fuhrmann, J. L., Geoghagen, N. S. M., Gnehm, C. L., McDonald, L. A., Small, K. V., Fraser, C. M., Smith, H. O., and Venter, J. C. (1995) *Science* **269**, 496-512
139. Bledig, S. A., Fotheringham, I. G., and Hunter, M. G. (1991) *unpublished*
140. Cole, S. T., Brosch, R., Parkhill, J., Garnier, T., Churcher, C., Harris, D., Gordon, S. V., Eiglmeier, K., Gas, S., Barry III, C. E., Tekaiia, F., Badcock, K., Basham, D., Brown, D., Chillingworth, T., Connor, R., Davies, R., Devlin, K., Feltwell, T., Gentles, S., Hamlin, N., Holroyd, S., Hornsby, T., Jagels, K., Krogh, A., McLean, J., Moule, S., Murphy, L., Oliver, S., Osborne, J., Quail, M. A., Rajandream, M. A., Rogers, J., Rutter, S., Seeger, K., Skelton, S., Squares, S., Squires, R., Sulston, J. E., Taylor, K., Whitehead, S., and Barrell, B. G. (1998) *Nature* **393**, 537-544
141. Jetten, M. S., Gubler, M. E., Lee, S. H., and Sinskey, A. J. (1994) *Appl. Environ. Microbiol.* **60**, 2501-2507
142. Laughlin, L. T., and Reed, G. H. (1997) *Arch. Biochem. Biophys.* **348**, 262-267

143. Bollenbach, T. J., Mesecar, A. D., and Nowak, T. (1999) *Biochemistry* **38**, 9137-9145
144. Friesen, R. H. E., Chin, A. J., Ledman, D. W., and Lee, J. C. (1998) *Biochemistry* **37**, 2949-2960
145. Lenzner, C., Nurnberg, P., Jacobasch, G., Gerth, C., and Thiele, B. J. (1997) *Blood* **89**, 1793-1799

APPENDIX

Figure A1. Sequence Alignment for Many PK Isozymes. The positions of residues with single amino acid replacements in red blood cell deficiency are highlighted. These residues are listed in Table 1. Mutations listed in Table 2 are denoted by (^). Mutations listed in Table 3 are denoted by (*). Structural assignments are based on the rabbit muscle PK structure (17).

Label:	PK isozyme:	Reference:
HumanR	Human red blood cell	(113)
HumanL	Human liver	(114)
RatR	Rat red blood cell	(30)
RatL	Rat Liver	(30)
MouseM2	Mouse M2	(115)
RatM2	Rat M2	(25)
HumanM2	Human M2	(116)
HumanM1	Human muscle	(116)
CatM1	Cat muscle	(56)
RabbitM1	Rabbit muscle	(17)
RatM1	Rat muscle	(25)
FrogMuscle	Clawed frog muscle	(117)
ChickenMuscle	Chicken muscle	(118)
S. cerevisiae1	<i>Saccharomyces cerevisiae</i> pyk1	(119)
S. cerevisiae2	<i>Saccharomyces cerevisiae</i> pyk2	(120)
Yarrowia	<i>Yarrowia lipolytica</i>	(121)
Emericella	<i>Emericella nidulans</i>	(122)
Aspergillus	<i>Aspergillus niger</i>	(123)
Trichoderma	<i>Trichoderma reesei</i>	(124)
T. brucei	<i>Trypanosoma brucei</i>	(125)
T. borelli	<i>Trypanoplasma borelli</i>	(126)
PotatoCytosolic	Potato cytosolic	(127)
TobaccoCytosolc	Tobacco cytosolic	(128)
B. subtilis	<i>Bacillus subtilis</i>	(129)
B. licheniforms	<i>Bacillus licheniformis</i>	(130)
B. stearotherm.	<i>Bacillus stearothermophilus</i>	(131)
B. psychrophils	<i>Bacillus psychrophilus</i>	(130)
E. coli TypeI	<i>Escherichia coli</i> TypeI	
	FBP activated	(132)
Synechocystis	<i>Synechocystis</i> sp.	
	(strain PCC 6803)	(133)
Lactococcus	<i>Lactococcus lactis</i>	(134)
spirochete	<i>Borrelia burgdorferi</i>	(135)
Tobaccoplastid	Tobacco plastid	(137)
TobaccoCloropt	Tobacco chloroplast	(137)
Haemophilus	<i>Haemophilus influenzae</i>	
	(strain Rd KW20)	(138)
E. coli TypeII	<i>Escherichia coli</i> TypeII	
	AMP activated	(139)
Mycobacterium	<i>Mycobacterium tuberculosis</i>	
	(strain H37RV)	(140)
Corynebacterium	<i>Corynebacterium glutamicum</i>	(141)
Zymomonas	<i>Zymomonas mobilis</i>	(36)
Leishmania	Leishmania	(22)

HumanR	-----MSIQENISSLQLRSWVSKSQRD LAKSILIGAPGGPAGYLRRASVAQLTQE	50
HumanL	-----MEGPAGYLRRASVAQLTQE	19
RatR	-----MSVQENTLPQQLWPWIFRSQKDLAKSALS GAPGGPAGYLRRASVAQLTQE	50
RatL	-----MEGPAGYLRRASVAQLTQE	19
MouseM2	-----MPKPHSE	7
RatM2	-----MPKPDSE	7
HumanM2	-----MSKPHSE	7
HumanM1	-----MSKPHSE	7
CatM1	-----SKPHSD	6
RabbitM1	-----SKSHSE	6
RatM1	-----MPKPDSE	7
FrogMuscle	-----MSE	3
ChickenMuscle	-----MSKHHD	6
S. cerevisiae1	-----	
S. cerevisiae2	-----	
Yarrowia	-----	
Emericella	-----	
Aspergillus	-----	
Trichoderma	-----MSQISR	6
T. brucei	-----	
T. borelli	-----	
PotatoCytosolic	-----	
TobaccoCytosolic	-----	
B. subtilis	-----	
B. licheniformis	-----	
B. stearotherm.	-----	
B. psychrophils	-----	
E. coli TypeI	-----	
Synechocystis	-----	
Lactococcus	-----	
spirochete	-----	
Tobaccoplastid	-----MATMNLPTGLHVAAKPASLDRLSSAKNVGDLFFSDSRHRKRVN	43
TobaccoCloroplast	MSQALNFFVSSSSRSPATFTTISRPSVFPSTGSLRLLVKKSLRTLVEASSAAASDLDEPQ	60
Haemophilus	-----	
E. coli TypeII	-----	
Mycobacterium	-----	
Corynebacterium	-----	
Zymomonas	-----	
Leishmania	-----	

*

	<H1->	<-H2->	<S1-->	
HumanR	LGTAFFQQQLPAAMADTFLEHLCLLDID	SEPVA	-----RSTSI	92
HumanL	LGTAFFQQQLPAAMADTFLEHLCLLDID	SEPVA	-----RSTSI	61
RatR	LGTAFFQQQLPAAMADTFLEHLCLLDID	SOPVA	-----RSTSI	92
RatL	LGTAFFQQQLPAAMADTFLEHLCLLDID	SOPVA	-----RSTSI	61
MouseM2	AGTAFIQTQQLHAAMADTFLEHMCRLDID	SAPITA	-----RNTGI	49
RatM2	AGTAFIQTQQLHAAMADTFLEHMCRLDID	SAPITA	-----RNTGI	49
HumanM2	AGTAFIQTQQLHAAMADTFLEHMCRLDID	SPPIA	-----RNTGI	49
HumanM1	AGTAFIQTQQLHAAMADTFLEHMCRLDID	SPPIA	-----RNTGI	49
CatM1	VGTAFIQTQQLHAAMADTFLEHMCRLDID	SPPIA	-----RNTGI	48
RabbitM1	AGSAFIQTQQLHAAMADTFLEHMCRLDID	SAPITA	-----RNTGI	48
RatM1	AGTAFIQTQQLHAAMADTFLEHMCRLDID	SAPITA	-----RNTGI	49
FrogMuscle	AGSAFIQTQQLHAAMADTFLEHMCRLDID	SEPIVA	-----RNTGI	45
ChickenMuscle	AGTAFIQTQQLHAAMADTFLEHMCRLDID	SEPTIA	-----RNTGI	48
S. cerevisiae1	-----MSRLERLTSLN	--VAGSDL	-----RRTSI	25
S. cerevisiae2	-----MPESRLQRLANLK	--ICTPQL	-----RRTSI	27
Yarrowia	-----MIYTAN	--SSPSTNL	-----QGPSTLN	20
Emericella	---MAASSSLDHLNRMKLEWHSKLNTEM	VPKKNF	-----RRTSI	39
Aspergillus	---MAASSSLDHLNRMKLEWHSKLNTEM	VPKKNF	-----RRTSI	39
Trichoderma	TQSIMATTAQEHELETGGRLNWLASLNTAF	VPARNF	-----RRTSI	48
T. brucei	-----MSQLEHNIGLSIF	EPVAKH	-----RANRIV	26
T. borelli	-----MRKSQLOFNTELRVH	EPALF	-----RSNKI	28
PotatoCytosolic	-----MANIDIAGIMKDL	ENDGRI	-----PKTKIV	26
TobaccoCytosolic	-----MAIENNNNGVNF	CVKR	-----PKTKIV	24
B. subtilis	-----	█	-----M	8
B. licheniformis	-----	█	-----M	8
B. stearotherm.	-----	█	-----MK	9
B. psychrophils	-----	█	-----M	8
E. coli TypeI	-----	█	-----M	8
Synechocystis	-----MPALINPVK	MRPLS	-----HRTKIV	22
Lactococcus	-----MNKRVKIVSTLGP	AVEIRGG	-----KFKGESG	27
spirochete	-----	█	-----MIS	10
Tobaccoplastid	TSNQIMAVQSLEHIGVNNNVYANYVNF	MPSSGYSLGQESVYLN	-----SPRKTIV	97
TobaccoCloroplast	SSPVLVSENGSGGVLSSATQEYGRNAPP	GDSSSIEVDTVTEAELKENGFRSTR	RRTKLIC	120
Haemophilus	-----	█	-----MSRRL	12
E. coli TypeII	-----	█	-----MSRRL	12
Mycobacterium	-----	█	-----MT	9
Corynebacterium	-----	█	-----MD	9
Zymomonas	-----	█	-----MTEGLFPRGRKVRVVS	16
Leishmania	-----MSQLAHNLTLSIF	EPVANY	-----RAARI	26

S1-> <--H4----> <S2-> <-----H4----->

HumanR TIG---PASRSVERLKEIKAGMNIARLNFSHGSHEYHAEISIANVREAVESFAGSPLSYR 149
HumanL TIG---PASRSVERLKEIKAGMNIARLNFSHGSHEYHAEISIANVREAVESFAGSPLSYR 118
RatR TIG---PASRSVDRLEIKAGMNIARLNFSHGSHEYHAEISIANVREAVESFAGSPLSYR 149
RatL TIG---PASRSVDRLEIKAGMNIARLNFSHGSHEYHAEISIANVREAVESFAGSPLSYR 118
MouseM2 TIG---PASRSVEMLKEIKSGMNVARLNFSHGTHEYHAEIKNVRRAATESFASDPILYR 106
RatM2 TIG---PASRSVEMLKEIKSGMNVARLNFSHGTHEYHAEIKNVRRAATESFASDPILYR 106
HumanM2 TIG---PASRSVETLKEIKSGMNVARLNFSHGTHEYHAEIKNVRTATESFASDPILYR 106
HumanM1 TIG---PASRSVETLKEIKSGMNVARLNFSHGTHEYHAEIKNVRTATESFASDPILYR 106
CatM1 TIG---PASRSVEILKEIKSGMNVARLNFSHGTHEYHAEIKNVRRAATESFASDPILYR 105
RabbitM1 TIG---PASRSVETLKEIKSGMNVARLNFSHGTHEYHAEIKNVRTATESFASDPILYR 105
RatM1 TIG---PASRSVEMLKEIKSGMNVARLNFSHGTHEYHAEIKNVRRAATESFASDPILYR 106
FrogMuscle TIG---PASRSVEMLKEIKSGMNIARLNFSHGTHEYHAEIKNVRRAATESLANSPIHYR 102
ChickenMuscle TIG---PASRSVDLKEIKSGMNVARLNFSHGTHEYHAEIKNVRRAATESFASDPITYR 105
S. cerevisiae1 TIG---PKTNNPETLVARRKAGLNVRMNFSGSYEYHQSVIDNVRKSEELYP-G----R 77
S. cerevisiae2 TIG---PKTNSCEAITARRKAGLNVRMNFSGSYEYHQSVIDNVRKSEQQFP-G----R 79
Yarrowia TDDI---PTKNYRKSSIICTIAGLNVRMNFSGSYEYHQSVIDNVRRESEQFR-G----R 73
Emergella TIG---PKTNSVEKLNARRKAGLNVRMNFSGSYEYHQSVIDNVRRAEKQAA-G----R 91
Aspergillus TIG---PKTNSVEKINSRRTAGLNVRMNFSGSYEYHQSVIDNVRRAAKTQV-G----R 91
Trichoderma TIG---PKTNSVEALNKRRDAGLNVRMNFSGSYEYHQSVIDNVRASVAHP-G----R 100
T. brucei TIG---PSTQSEALKNIMKSGMNVARLNFSHGSHEYHQTINNVRAAAELG-----L 77
T. borelli TIG---PSSQSEVLKDIRKAGLNVRMNFSGTYEYHQSVIDNVRKAASELG-----I 79
PotatoCytosolic TLG---PSSRTVPMLEKRLRAGMNVARFNFSHGTHEYHQTIDNVRKIAMQNTQ-----I 77
TobaccoCytosolic TLG---PASRSVPMLEKRLRAGMNVARFNFSHGSHDYHQTIDNVRQAMESTG-----I 75
B. subtilis TIG---PASESIEMLTQIMESGMNVARLNFSHGDFEEHGARIKNVREASKKLK-----K 59
B. licheniforms TIG---PASESVEKLTQIMEAGMNVARLNFSHGDFEEHGARIKNVREAAKGLG-----K 59
B. stearotherm. TIG---PASESVDKLVQIMEAGMNVARLNFSHGDFEEHGARIKNVREAAKRTG-----R 60
B. psychrophilis TIG---PASESPELLEQIEAGMNVARLNFSHGNHAEHKAVIDSRKVAEREK-----K 59
E. coli TypeI TIG---PKTESSEMLAKMLDAGMNVARLNFSHGDAYEHGQRIQNVRNVMKSTG-----K 59
Synechocystis TIG---PASSSVEVIRQIVDAGMNVARLNFSHGSYEDHATMVRIRSRVQEMD-----T 73
Lactococcus YWGESLDVEASAKNIAALIEGANVRRFNFSHGDPHEQGARMAVVRRAEEIAG-----H 81
spirochete TIS---DLRCEPEHIKDDHDAGVNVARLNFSHQSHEDTIRVIDNVRKISN-----57
Tobaccoplastid TIG---PSTSSREMIWKAIEAGMNVARLNFSHGDFHASHQRIIDLVRKEYNAQFED-----K 149
TobaccoChloroplast TIG---PATCGFEQLERDAEGGMNVARINMCHGTREWHRMVIERVRRLLNEEKG-----F 171
Haemophilus TMG---PSTDRDNNLEKVIAGANVRRMNFSGTTPDDHIGRAERVRSIAKKLK-----K 63
E. coli TypeII TLG---PATDRDNNLEKVIAGANVRRMNFSGSPEDHKVADRVRRIAAKLG-----R 63
Mycobacterium TLG---PATQRDDLVRALVEAGMNVARMNFSGDYDDHKVAYERVRVASDATG-----R 60
Corynebacterium TLG---PAVASADGILRIVVDGMVARRLNFSHGDFPDHEQNYKVRRAAEKTK-----R 60
Zymomonas TLG---PASSTAEQIRDRFLAGADVRRINMCHGTHDEKKVIVDNRRALEKEFN-----R 67
Leishmania TIG---PSTQSEALKGDIQSGMNVARMNFSGSHEYHQTINNVRAAAELG-----V 77

A A A A *

	<S8->	<--S9-->	<S10->	<S11->	<S12->	
HumanR	IVRVVAVGGRIYID	DGLISLVVQKIGPE	--GLVTQVENGGV	LGSG	-----RKG	VNLPGA 257
HumanL	IVRVVAVGGRIYID	DGLISLVVQKIGPE	--GLVTQVENGGV	LGSG	-----RKG	VNLPGA 226
RatR	ITRVVAVGGRIYID	DGLISLVVQKIGPE	--GLVTEVEHGGIL	LGSG	-----RKG	VNLPNT 257
RatL	ITRVVAVGGRIYID	DGLISLVVQKIGPE	--GLVTEVEHGGIL	LGSG	-----RKG	VNLPNT 226
MouseM2	ICKVVEVGSKIYV	DDGLISLQVKEK	GAD--FLVTEVEN	GGSLGS	-----KKG	VNLPGA 214
RatM2	ICKVVEVGSKIYV	DDGLISLQVKEK	GAD--YLVTEVEN	GGSLGS	-----KKG	VNLPGA 214
HumanM2	ICKVVEVGSKIYV	DDGLISLQVKEK	GAD--FLVTEVEN	GGSLGS	-----KKG	VNLPGA 214
HumanM1	ICKVVEVGSKIYV	DDGLISLQVKEK	GAD--FLVTEVEN	GGSLGS	-----KKG	VNLPGA 214
CatM1	ICKVVEVGSKIYV	DDGLISLQVKEK	GAD--FLVTEVEN	GGSLGS	-----KKG	VNLPGA 213
RabbitM1	ICKVVDVGSKVYV	DDGLISLQVKEK	GPD--FLVTEVEN	GGFLGS	-----KKG	VNLPGA 213
RatM1	ICKVVEVGSKIYV	DDGLISLQVKEK	GAD--YLVTEVEN	GGSLGS	-----KKG	VNLPGA 214
FrogMuscle	LTKVVKPGSKIYV	DDGLISLLVKEI	GPD--FCVTEIEN	GGMLGS	-----KKG	VNLPGA 210
ChickenMuscle	LIKVIDVGSKIYV	DDGLISLLVKEK	GKD--FVMTTEVEN	GGMLGS	-----KKG	VNLPGA 213
S. cerevisiae1	ITKVISAGRIYV	DDGVLSFQVLE	VDDK-TLKVKALN	AGKICS	-----HKG	VNLPGT 184
S. cerevisiae2	LTKVIVPGRFIYV	DDGLISFKVLI	QIDES-NLRVQAV	NSGYLAS	-----HKG	VNLPNT 186
Yarrowia	IVRQIDIGKIIF	VDDGVLSFKVLE	KIDGE-TLKVETL	NNGKISS	-----RKG	VNLPGT 180
Emericella	ITKVISAGKLIYV	DDGILSFEVLE	VDDK-TLRVRC	LNNGNISS	-----RKG	VNLPGT 198
Aspergillus	ITKVISPGKLIYV	DDGILSFEVLE	VDDK-TIRVRC	LNNGNISS	-----RKG	VNLPGT 198
Trichoderma	ITKVIQGRVIYV	DDGVLAFDVL	SIKDDQ-FVEVRAR	NNGFISS	-----RKG	VNLPNT 207
T. brucei	LTVAVRPGSIYV	DDGVMTLRVVS	KEDDR-TLKCHVN	NHRLTD	-----RRG	INLPGC 183
T. borelli	ITKVVAVGGHIF	VDDGGLDL-IV	VKISGK-DIECVA	QNTHTISN	-----RKG	INLPNA 184
PotatoCytosolic	LVVDLKPNTIL	CADGTTTLTVL	SCDPPSGTVRC	CENSATLGE	-----RKN	VNLPGV 183
TobaccoCytosolic	LAEDVKPQSVIL	CADGQITFTVL	SCDKENGLDR	CRCENTAVLGE	-----RKN	VNLPGV 181
B. subtilis	LVHDVEQGSTIL	LDGGLIGLEVL	DVDAKREIKTK	VLNNGTLKN	-----KKG	VNVPGV 163
B. licheniformis	LIHDVSVGSTIL	LDGGLIGLEVL	DINDKREIVTK	VMSGTLKN	-----KKG	VNVPGV 163
B. stearotherm.	LIDDVSVGAKIL	LDGGLISLEVN	AVDRQAGEIVT	TVLNGVLYKN	-----KKG	VNVPGV 164
B. psychrophils	LIEDVNEGSVIL	LDGGLIQLEVT	GKDVARGLIHT	LIINSGLSN	-----NKG	VNLPGV 163
E. coli TypeI	FTTDLVSGNTV	LVDGGLIGMEV	TAIEGNK--VICK	VLNNGDLGE	-----NKG	VNLPGV 163
Synechocystis	LATEAKVGERIL	LDGLEMVVS	IQDPE--VICEV	VTGGILKS	-----RKG	VNLPGL 176
Lactococcus	IFDDVEIGQTIL	IDDGKLGSLT	GKDAATREFE	VEAQNDGVIGK	-----QKG	VNLPNT 191
spirochete	FVKEVPQGSKV	LIDGELMTV	VAKLPDR--LICE	IKNDGQIKN	-----KKS	INTPGI 157
Tobaccoplastid	FINDVEAGDILL	VDDGMMSLAV	KSSTSD--IVK	CEVIDGGELKS	-----RRH	LNVRGK 250
TobaccoCloropt	FAEDVKVGDILL	DDGMRVFEV	IEKIGP--DVK	CLCTDPGLL	PRANLTFWR	DGKLVRR 283
Haemophilus	LPQDVVPGDILL	DDGRVQLKVL	STDGAK--VFTE	VTVGGPLSN	-----NKG	INKLGG 167
E. coli TypeII	LPADVVPGDILL	DDGRVQLKVL	EVQGMK--VFTE	VTVGGPLSN	-----NKG	INKLGG 167
Mycobacterium	LAQDAVAGDRV	LVDGKVALV	DAVEGDD--VVCT	VVEGGPVSD	-----NKG	ISLPGM 162
Corynebacterium	LAKDAKPGDRLL	VDDGKVLVCS	VSEGND--VICE	VVEGGPVSN	-----NKG	VS LPGM 162
Zymomonas	IFRALDKGHRLL	DDGKIVVRC	VESPTK--IVTR	VEVPGPLSD	-----HKG	FNVDPV 169
Leishmania	LSKVVRPGNIYI	DDGILILQV	SHED-OTLECT	VTNSTISD	-----RRG	VNLPGC 183

	<-----H5----->	<S13>	<---H6--->	<S14	
HumanR	QVDLPLSEQDVRD-LRFVEH--GVDIVFASVVRKASDVAVRAALGPE--GHGIRIIS				312
HumanL	QVDLPLSEQDVRD-LRFVEH--GVDIVFASVVRKASDVAVRAALGPE--GHGIRIIS				281
RatR	EVDLPLSEQDLLD-LRFVQH--NVDIIFASVVRKASDVAVRDALGPE--GQNIKIIS				312
RatL	EVDLPLSEQDLLD-LRFVQH--NVDIIFASVVRKASDVAVRDALGPE--GQNIKIIS				281
MouseM2	AVDLPVSEKDIQD-LKFVEQ--DVMVFASVIRKAADVHEVRKVLGEK--GKNIKIIS				269
RatM2	AVDLPVSEKDIQD-LKFVEQ--DVMVFASVIRKAADVHEVRKVLGEK--GKNIKIIS				269
HumanM2	AVDLPVSEKDIQD-LKFVEQ--DVMVFASVIRKASDVHEVRKVLGEK--GKNIKIIS				269
HumanM1	AVDLPVSEKDIQD-LKFVEQ--DVMVFASVIRKASDVHEVRKVLGEK--GKNIKIIS				269
CatM1	AVDLPVSEKDIQD-LKFVEQ--DVMVFASVIRKASDVHEVRKVLGEK--GKNIKIIS				268
RabbitM1	AVDLPVSEKDIQD-LKFVDE--DVMVFASVIRKAADVHEVRKILGEK--GKNIKIIS				268
RatM1	AVDLPVSEKDIQD-LKFVEQ--DVMVFASVIRKAADVHEVRKVLGEK--GKNIKIIS				269
FrogMuscle	AVDLPVSEKDIQD-LKFVEQ--DVMVFASVIRKAADVHEVRKVLGEK--GKNIKIIS				265
ChickenMuscle	AVDLPVSEKDIQD-LKFVEQ--NVMVFASVIRKAADVAVRKLGEK--GKHIKIIS				268
S. cerevisiae1	DVDLPLSEKDKED-LRFVKN--GVDMVFASVIRTANDVLTIREVLGEQ--GKDVKIV				239
S. cerevisiae2	DVDLPLSARMDKD-LQFVNR--GIHIVFASVIRTSEDVLSIRKALGSE--GQDIKIIS				241
Yarrowia	DVDLPLSEKDKAD-LKFVEH--GVDMIFASVIRTANDVQAIRDVLGEK--GKGIOIIS				235
Emericella	DVDLPLSEKDISD-LKFVKN--KVMVFASVIRGSDIRHIREVLGEE--GREIOITA				253
Aspergillus	DVDLPLSEKDIAD-LKFVNR--KVMVFASVIRGSDIRHIREVLGEE--GREIOITA				253
Trichoderma	DVDLPLSEKDKAD-LKFVKN--NVMVFASVIRRAQDIKDIRDVLGPE--GKQIOITA				262
T. brucei	EVDLPAVSEKDRKD-LEFVAQ--GVDMIFASVIRTAEQVREVRALGPK--GKDILIIS				238
T. borelli	DVDLPAVSEKDLMD-LQFAKN--RVDFVFASVIRNADQVNEVRQAFG----GK-IAITA				236
PotatoCytosolic	VVDLPLTEKDKEDILEWVFN--NIDMIALSVVRKGSDLVVRKALGPH--AKRIOIMS				239
TobaccoCytosolic	IVDLPALTDKDKDDILNWVFN--HIDMIALSVVRKGSDLVVRKLLGEH--AKNILIMS				237
B. subtilis	SVNLPITEKDARD-IVFIEQ--GVDFAASVRRSDVLEIRELLEHN-AQDIOIIP				219
B. licheniformis	SVNLPITEKDARD-IVFIEQ--GVDFAASVRRSDVLEIRELLEHN-AADIOIIP				219
B. stearotherm.	KVNLPITEKDRAD-ILFIRQ--GIDFAASVRRASDVLEIRELLEHD-ALHIOITA				220
B. psychrophils	SVQLPMTTEKDAED-ILFIRE--GVDFAASVRRASDVLEIRALLENNN-GSNLOIIP				219
E. coli TypeI	SIALPLAEKDKQD-LIFCEQ--GVDFAASVIRKRSDVLEIREHLKAHG-GENIHIIS				219
Synechocystis	VLTLPSMTTKDKQD-LEFELSQ--GIDMVSLSVVRKGEDITLTKQFLAERG-HPDLPIITA				232
Lactococcus	KIPFPALAEKDDAD-IRFELSQPGGINFIAISVIRTANDVKEVRRICEETG-NPHVOILA				249
spirochete	SLKLPVTEKDKGF-IEFAKY--NVDFAHSVVRHSDVQVQEILTASG-NPDVKIIS				213
Tobaccoplastid	SATLPIITEKDWD-IKFVNN--QVDFYAVSVKDAKVVHELKDYLKSC--NADIHIV				305
TobaccoChloroplast	NAMLPVSSKDWLD-IDFIAE--GVDFAVSVKSAEVIKHLKSYIQARARDSDISVITA				340
Haemophilus	GLSADLITEKDKAD-IITARI--GVDFLAVSPRSSADLYARELAQA--GLNAKIITA				222
E. coli TypeII	GLSADLITEKDKAD-IKTALI--GVDYLAVSPRCGEDLYARRLARDA--GCDAKIITA				222
Mycobacterium	NVTAPLSEKDIED-LTFALNL--GVDMVAVSVRSPADVLELVEVMDRI--GRRVPIITA				217
Corynebacterium	DISVPLSEKDIRD-LRFALKL--GVDFIASVVRSPADVLELHKIMDEE--GRRVPIITA				217
Zymomonas	VIPLALTPKDRKD-LDFALKE--KADWVALSVQRVEDVLEAKELIKG-----RAPILV				221
Leishmania	DVDLPAVSAKDRVD-LQFVEQ--GVDMIFASVIRSAEQVDVRKALGPK--GRDIMIIC				238

S14-> <-H7> <-H8--> <S15><-H9--> <-----H10-----> <S16-

HumanR KIENHEGVKR---FDEILEVSDGIMVARCDLGHEIPAEKVFLAQKMMIGRCNLAGKPVVC 369

HumanL KIENHEGVKR---FDEILEVSDGIMVARCDLGHEIPAEKVFLAQKMMIGRCNLAGKPVVC 338

RatR KIENHEGVKR---FDEILEVSDGIMVARCDLGHEIPAEKVFLAQKMMIGRCNLAGKPVVC 369

RatL KIENHEGVKR---FDEILEVSDGIMVARCDLGHEIPAEKVFLAQKMMIGRCNLAGKPVVC 338

MouseM2 KIENHEGVRR---FDEILEASDGI MVARCDLGHEIPAEKVFLAQKMMIGRCNRAKGPVVC 326

RatM2 KIENHEGVRR---FDEILEASDGI MVARCDLGHEIPAEKVFLAQKMMIGRCNRAKGPVVC 326

HumanM2 KIENHEGVRR---FDEILEASDGI MVARCDLGHEIPAEKVFLAQKMMIGRCNRAKGPVVC 326

HumanM1 KIENHEGVRR---FDEILEASDGI MVARCDLGHEIPAEKVFLAQKMMIGRCNRAKGPVVC 326

CatM1 KIENHEGVRR---FDEILEASDGI MVARCDLGHEIPAEKVFLAQKMMIGRCNRAKGPVVC 325

RabbitM1 KIENHEGVRR---FDEILEASDGI MVARCDLGHEIPAEKVFLAQKMMIGRCNRAKGPVVC 325

RatM1 KIENHEGVRR---FDEILEASDGI MVARCDLGHEIPAEKVFLAQKMMIGRCNRAKGPVVC 326

FrogMuscle KIENHEGVRR---FDEILEASDGI MVARCDLGHEIPAEKVFLAQKMMIGRCNRAKGPVVC 322

ChickenMuscle KIENHEGVRR---FDEILEASDGI MVARCDLGHEIPAEKVFLAQKMMIGRCNRAKGPVVC 325

S. cerevisiae1 KIENQQGVNN---FDEILKVTGVMVARCDLGHEIPAEKVFLAQKMLIAKSNLAGKPVVC 296

S. cerevisiae2 KIENQQGLDN---FDEILEVTDGVMVARCDLGHEIPAEKVFLAQKMLIAKSNLAGKPVVC 298

Yarrowia KIENQQGVNN---FDEILEKTDGVMVARCDLGHEIPAEKVFLAQKMLIAKSNLAGKPVVC 292

Emericella KIENQQGVNN---FDEILEETDGMVARCDLGHEIPAEKVFLAQKMLIAKSNLAGKPVVC 310

Aspergillus KIENQQGVNN---FDEILEETDGMVARCDLGHEIPAEKVFLAQKMLIAKSNLAGKPVVC 310

Trichoderma KIENRQGLNN---FAEILEETDGMVARCDLGHEIPAEKVFLAQKMLIAKSNLAGKPVVC 319

T. brucei KIENHQGVQN---IDSII EASNGIMVARCDLGHEIPAEKVFLAQKMLIAKSNLAGKPVVC 295

T. borelli KIENYQGDIN---IDAII DAADGIMVARCDLGHEIPAEKVFLAQKMLIAKSNLAGKPVVC 293

PotatoCytosolic KVENQEGVIN---FDEILRETDSFMVARCDLGHEIPAEKVFLAQKMLIAKSNLAGKAVVT 296

TobaccoCytosolic KVENQEGVAN---FDDILNSDAFMVARCDLGHEIPAEKVFLAQKMLIAKSNLAGKAVVT 294

B. subtilis KIENQEGVDN---IDAILEVSDGLMVARCDLGHEIPAEKVFLAQKMLIAKSNLAGKAVVT 276

B. licheniforms KIENQEGVDN---IDAILEVSDGLMVARCDLGHEIPAEKVFLAQKMLIAKSNLAGKAVVT 276

B. stearotherm. KIENQEGVAN---IDEILEAADGLMVARCDLGHEIPAEKVFLAQKMLIAKSNLAGKAVVT 277

B. psychrophils KIENQEGVDN---IDEILNVS DGLMVARCDLGHEIPAEKVFLAQKMLIAKSNLAGKAVVT 276

E. coli TypeI KIENQEGVNN---FDEILEASDGI MVARCDLGHEIPAEKVFLAQKMLIAKSNLAGKAVVT 276

Synechocystis KIEKPAIDN---LEEIVAVSNGIMVARCDLGHEIPAEKVFLAQKMLIAKSNLAGKAVVT 289

Lactococcus KIENQGGIEN---LDEIIEAADGIMVARCDLGHEIPAEKVFLAQKMLIAKSNLAGKAVVT 306

spirochete KIENQEGIDN---IEEIAKASVGI MVARCDLGHEIPAEKVFLAQKMLIAKSNLAGKAVVT 270

Tobaccoplastid KIESADSIPN---LHSIISASDGI MVARCDLGHEIPAEKVFLAQKMLIAKSNLAGKAVVT 362

TobaccoCloroplast KIESIDSLKN---LEEIIQASDGI MVARCDLGHEIPAEKVFLAQKMLIAKSNLAGKAVVT 397

Haemophilus KVERAETVANDEAMDDIILASDVIMVARCDLGHEIPAEKVFLAQKMLIAKSNLAGKAVVT 282

E. coli TypeII KVERAEAVCSQDAMDDIILASDVIMVARCDLGHEIPAEKVFLAQKMLIAKSNLAGKAVVT 282

Mycobacterium KIEKPEAIDN---LEAIVLAFDAVMVARCDLGHEIPAEKVFLAQKMLIAKSNLAGKAVVT 274

Corynebacterium KIEKPEAVTS---LEPIVLAFDAVMVARCDLGHEIPAEKVFLAQKMLIAKSNLAGKAVVT 274

Zymomonas KIEKPAAIEN---LESILAATDAVMVARCDLGHEIPAEKVFLAQKMLIAKSNLAGKAVVT 278

Leishmania KIENHQGVQN---IDSII EESDGI MVARCDLGHEIPAEKVFLAQKMLIAKSNLAGKAVVT 295

S16> <----H11----> <S17> <-----H12----->

HumanR ATQMLESMITKARPTRAETS DVANAVLDGADCIMLSGETARGNFPVEAVKMOHAIAREAE 429

HumanL ATQMLESMITKARPTRAETS DVANAVLDGADCIMLSGETARGNFPVEAVKMOHAIAREAE 398

RatR ATQMLESMITKARPTRAETS DVANAVLDGADCIMLSGETARGSFPPVEAVMMOHAIAREAE 429

RatL ATQMLESMITKARPTRAETS DVANAVLDGADCIMLSGETARGSFPPVEAVMMOHAIAREAE 398

MouseM2 STQMLESMIKKPRPTRAEGSDVANAVLDGADCIMLSGETARGDYPLEAVRMOHLIAREAE 386

RatM2 ATQMLESMIKKPRPTRAEGSDVANAVLDGADCIMLSGETARGDYPLEAVRMOHLIAREAE 386

HumanM2 ATQMLESMIKKPPPTRAEGSDVANAVLDGADCIMLSGETARGDYPLEAVRMOHLIAREAE 386

HumanM1 ATQMLESMIKKPPPTRAEGSDVANAVLDGADCIMLSGETARGDYPLEAVRMOHLIAREAE 386

CatM1 ATQMLESMIKKPRPTRAEGSDVANAVLDGADCIMLSGETARGDYPLEAVRMOHLIAREAE 385

RabbitM1 ATQMLESMIKKPRPTRAEGSDVANAVLDGADCIMLSGETARGDYPLEAVRMOHLIAREAE 385

RatM1 ATQMLESMIKKPRPTRAEGSDVANAVLDGADCIMLSGETARGDYPLEAVRMOHLIAREAE 386

FrogMuscle ATQMLESMIKKPRPTRAEGSDVANAVLDGADCIMLSGETARGDYPLEAVRMOHAIAREAE 382

ChickenMuscle ATQMLESMIKKPRPTRAEGSDVANAVLDGADCIMLSGETARGDYPLEAVRMOHAIAREAE 385

S. cerevisiae1 ATQMLESMITYNPRPTRAEVS DVANAVLDGADCIMLSGETARGNYPINAVTTMAETAAREAE 356

S. cerevisiae2 ATQMLDSMTHNPRPTRAEVS DVANAVLDGADCIMLSGETARGDYFVNAVNTMAATAAREAE 358

Yarrowia ATQMLDSMITYNPRPTRAEVS DVANAVLDGADCIMLSGETARGTYPIESVVMHETCAREAE 352

Emericella ATQMLESMITYNPRPTRAEVS DVANAVLDGADCIMLSGETARGNYPCAVTMMSETCAREAE 370

Aspergillus ATQMLESMITYNPRPTRAEVS DVANAVLDGADCIMLSGETARGNYPCAVTMMSETCAREAE 370

Trichoderma ATQMLESMIKNPRPTRAEIS DVANAVLDGADCIMLSGETARGNYPAESIHMEASAREAE 379

T. brucei ATQMLESMITSNPRPTRAEVS DVANAVLDGADCIMLSGETARGKYPNEVVQVMARICAREAE 355

T. borelli ATQMLDSMTHGPRPTRAEVS DVANAVLDGADCIMLSGETARGKYPVETVVVMARICAREAE 353

PotatoCytosolic ATQMLESMIKSPPPTRAEAT DVANAVLDGADCIMLSGETAAGAYPELAVKIMARICAREAE 356

TobaccoCytosolic ATQMLESMIKSPPPTRAEAT DVANAVLDGADCIMLSGETAAGAYPLAVGTMARICAREAE 354

B. subtilis ATQMLDSMQRNPRPTRAEAS DVANAVLDGADCIMLSGETAAGSYPVEAVQTMHNIAREAE 336

B. licheniforms ATQMLDSMQRNPRPTRAEAS DVANAVLDGADCIMLSGETAAGNYPVEAVQTMHNIAREAE 336

B. stearotherm. ATQMLDSMQRNPRPTRAEAS DVANAVLDGADCIMLSGETAAGQYPVEAVKTMHNIAREAE 337

B. psychrophils ATQMLDSMQRNPRPTRAEAS DVANAVLDGADCIMLSGETAAGIYPVEAVQTMHNIAREAE 336

E. coli TypeI ATQMLDSMIKNPRPTRAEAG DVANAVLDGADCIMLSGETARGKYPLEAVSMMARICAREAE 336

Synechocystis ATQMLDSMIQNSRPTRAEAS DVANAVLDGADCIMLSGETAAGQYPVKSVMARICAREAE 349

Lactococcus ATNMLESMTYNPRPTRAEIS DVANAVLDGADCIMLSGETAANGKYPRESVRTMARICAREAE 366

spirochete ATQMLHSMIENPRPTRAEVS DVANAVLDGADCIMLSGETAAGKYPIEAVKMMARICAREAE 330

Tobaccoplastid ATNMLESMLDHPPTRAEVS DVANAVLDGADCIMLSGETAAGKYPLKAVKMMARICAREAE 422

TobaccoCloroplast ASQLLESMEIYPIPTRAEVADSEAVRQRGDALMLSGESAMGQFPEKALTVMARICAREAE 457

Haemophilus ATQMMESMISNMPPTRAEVM DVANAVLDGADCIMLSGETAAGQYPSETVAMMARICAREAE 342

E. coli TypeII ATQMMESMITNMPPTRAEVM DVANAVLDGADCIMLSGETAAGQYPSETVAMMARICAREAE 342

Mycobacterium ATQMLDSMIENSPTRAEAS DVANAVLDGADCIMLSGETAAGKYPLAAVRTMARICAREAE 334

Corynebacterium ATQMLDSMIENSPTRAEAS DVANAVLDGADCIMLSGETAAGKYPNEVVQVMARICAREAE 334

Zymomonas ATAMLESMIKAPPTRAEVS DVANAVLDGADCIMLSGETAAGDWPHEAVNMARICAREAE 338

Leishmania ATQMLESMITYNPRPTRAEVS DVANAVLDGADCIMLSGETAAGKYPNEVVQVMARICAREAE 355

	H12->	<----H13----->	<-----H14----->	<S18->	<--H15-	
HumanR	AAVYHR---	QLFEELRRAAPLSRDPTEVTAIGAVEAAFKCC-	AAAIIVLTTTGRSAQLLS	485		
HumanL	AAVYHR---	QLFEELRRAAPLSRDPTEVTAIGAVEAAFKCC-	AAAIIVLTTTGRSAQLLS	454		
RatR	AAVYHR---	QLFEELRRAAPLSRDPTEVTAIGAVEASFKCC-	AAAIIVLTKTGRSAQLLS	485		
RatL	AAVYHR---	QLFEELRRAAPLSRDPTEVTAIGAVEASFKCC-	AAAIIVLTKTGRSAQLLS	454		
MouseM2	AAIYHL---	QLFEELRRLAPITSDPTEAAAVGAVEASFKCC-	SGAIIVLTKSGRSAHQVA	442		
RatM2	AAIYHL---	QLFEELRRLAPITSDPTEAAAVGAVEASFKCC-	SGAIIVLTKSGRSAHQVA	442		
HumanM2	AAIYHL---	QLFEELRRLAPITSDPTEATAVGAVEASFKCC-	SGAIIVLTKSGRSAHQVA	442		
HumanM1	AAVFHR---	KLFEELVRSSSHSTDLMEAMAMGSVEASYKCL-	AAALIVLTSGRSAHQVA	442		
CatM1	AAVFHR---	KLFEELVRSSSHSTDLMEAMAMGSVEASYKCL-	AAALIVLTSGRSAHQVA	441		
RabbitM1	AAVFHR---	KLFEELARSSSHSTDLMEAMAMGSVEASYKCL-	AAALIVLTSGRSAHQVA	441		
RatM1	AAVFHR---	LLFEELARASSQSDPLEAMAMGSVEASYKCL-	AAALIVLTSGRSAHQVA	442		
FrogMuscle	AAVFHR---	QLFEELRRVSPLTRDPTEATAVGAVEASFKCS-	SGAIIVLTKSGRSARLLS	438		
ChickenMuscle	AAVFHR---	QQFEELRHSVHHRPADAMAAAGAVEASFKCL-	AAALIVLTSGRSAHLVS	441		
S. cerevisiae1	QAIAYL---	PNYDDMRNCTPKPTSTTETVAASAVAAVFEQK-	AKAIIVLSTSGTTPRLVS	412		
S. cerevisiae2	SAIAHL---	ALYDDLDRDTPKPTSTTETVAASAAIALEQD-	CKAIIVLSTSGNTARLLS	414		
Yarrowia	KALAYA---	PLFNEMRRLTVRPTETVETIAISAVSASFEQQ-	FRAIIVLSTSGTSARLCS	408		
Emericella	VAIPHF---	NVFDLRLNLRPPTDTVESIAMAAVSASLELN-	AGAIIVLTTSGNTARMIS	426		
Aspergillus	VAIPHF---	NVFDLRLNLRPPTDTVESIAMAAVSASLELN-	AGAIIVLTTSGNTARYLS	426		
Trichoderma	NIIPYV---	SHFEEMCTLVKRPVSTVESCAMAAVRSALDLG-	AGGIIVLSTSGDSARLLS	435		
T. brucei	SATHDT---	VMFNSIKNLQKIPMCPPEEAVCS SAVASAFEVQ-	AKAMVLVSNTRGSRARLLS	411		
T. borelli	VMWMM---	AAFEAIKNLQSFPLIPEEAICSSAVNSIFELH-	AKAIIVLTTNTRGSRAMVVS	409		
PotatoCytosolic	SSLDNE---	AIFKEMIRCTPLPMSPLESLAS SAVRTANKAR-	AKLIIVLTRGGSTAKLVA	412		
TobaccoCytosolic	SHIDYP---	DVFKRIMSNAVPVMSPLESLAS SAVRTANSAR-	AKLILVLTTRGGSTAKLVA	410		
B. subtilis	EALNYK---	EILSKRRDQV--GMTITDAIGQSVHTAINLN-	AAIVTPTESGHTARMIA	390		
B. licheniformis	EALNKK---	KILSARSKQV--SMSITDAIGQSVHTAINLN-	VNAIVTPTESGHTARMIS	390		
B. stearotherm.	QALEHR---	DILSQRTKES--QTTITDAIGQSVHTALNLD-	VAAIVTPTVSGKTPQMVV	391		
B. psychrophils	AAIDYR---	SUVSTRREK--HGNMTEAIGQAAAYTAINLK-	VKAVLAPTESGHTAKMIA	390		
E. coli TypeI	RYMNSR---	LEFNNDNRK---LRITEAVCRGAVETAEKLD-	KPLIVVATQGGK SARAVR	388		
Synechocystis	VG-----	LHLVNNPPIENTETHALSEALVIDGILD-	IKYIVFTTSGFTSLLAS	398		
Lactococcus	TMLK-----	EYGRLHPERYDKSTVTEVVAASVKNAAEAMD-	VKLIIVLTSNTARLLS	419		
spirochete	KHR-----	KMTLYKDELFDKSI TRNYIIKCAIDATKLM-	AKAIIVDSLKGTARIMA	383		
Tobaccoplastid	SSLQKS---	TSSPSQSAAYKSHMGEMFAFHSSSMANTLS-	ETPIIVFTRTSGMAILLS	475		
TobaccoCloropt	RMWREQKRHEVIELPSIASSFSDSISEEICNSAAKMANLE-	VDALFVYTKNGHMASLLS	516			
Haemophilus	KMPS-----	INVSRRHMDKEFETIEESVAMSAVYAANHMKG-	VAAIVLTSSTGRTPLLLS	396		
E. coli TypeII	KMPS-----	INVSKRHLVDVQFDNVEEAIAMSAVYAANHLKG-	VTAIITMTESGRTALMVS	396		
Mycobacterium	EN-----	STAAPPLTHIPRTKRGVISYARIDIGERLD-	AKALVAFQTSGDTVRRLA	384		
Corynebacterium	TD-----	G-RVPDLTHIPRTKRGVISYARDIAERLN-	AKALVAFQTSGDTAKRVA	383		
Zymomonas	NAPGYI---	ERVRFPT--TPAEPPTVDALAEASAKTAETVG-	AKAIIVFTETGKTAQRVS	392		
Leishmania	SALNEY---	VFFNSIKKLQHIPMSADEAVCS SAVNSVYETK-	AKAMVVLVSNTRGSRARLVA	411		

	H15>	<S19>	<--H16-->	<S20-->	<H17-		
HumanR	R	R	---	SAQAARQVHLCR	GVFPFLLYR	REPPEA---IWADD 528	
HumanL	R	R	---	SAQAARQVHLCR	GVFPFLLYR	REPPEA---IWADD 497	
RatR	Q	Q	---	SAQAARQVHLSR	GVFPFLLYR	REPPEA---IWADD 528	
RatL	Q	Q	---	SAQAARQVHLSR	GVFPFLLYR	REPPEA---IWADD 497	
MouseM2	R	R	---	NPQTAQQAHLVYR	GIFPVLCR	DAVLN---AWAED 485	
RatM2	R	R	---	NPQTAQQAHLVYR	GIFPVLCR	DAVLD---AWAED 485	
HumanM2	R	R	---	NPQTAQQAHLVYR	GIFPVLCR	KDPVQE---AWAED 485	
HumanM1	R	R	---	NPQTAQQAHLVYR	GIFPVLCR	KDPVQE---AWAED 485	
CatM1	R	R	---	NHQTAQQAHLVYR	GIFPVVCR	KDPVQE---AWAED 488	
RabbitM1	R	R	---	NHQTAQQAHLVYR	GIFPVVCR	KDPVQE---AWAED 484	
RatM1	R	R	---	NPQTAQQAHLVYR	GIFPVLCR	DAVLD---AWAED 485	
FrogMuscle	R	R	---	NGQTAQQAHLVYR	GIFPVLYR	REAVHE---AWAED 481	
ChickenMuscle	R	R	---	NDQTAQQAHLVYR	GVFPVLCR	KQPAHD---AWAED 484	
S. cerevisiae1	K	K	---	CFRAARFVSHLYR	GVFPVFR	EKEPVS---DWTDD 455	
S. cerevisiae2	K	K	---	HARTARLAHLYR	GVFPFLYR	EPKRLD---DWGED 457	
Yarrowia	K	K	---	NAQAARFVSHLYR	GVYFFIYR	EKARASN-PAEWQHD 454	
Emericella	K	K	---	NPAATRYVSHLYR	GVWPFYR	EKKPDFNVKIWQED 473	
Aspergillus	K	K	---	NPAASRYVSHLYR	GVWPFYR	EKKPDFNVKVVQED 473	
Trichoderma	K	K	---	NPTTSRFVSHLYR	GVYFFLYR	EKKPDFNTVNWQED 482	
T. brucei	K	K	---	RLQTCRQLNVTR	SVVSVFYR	DAKSG---EDKD 453	
T. borelli	K	K	---	ELDVCRLLSITR	GTIPVYD	TEKLG---PDYD 451	
PotatoCytosolic	K	K	---	YRPAVPIILSVVY	PVLTDSFDWSIS	DETPARHSLVYRGLIPLLGE	GSAKAT---DSES 468
TobaccoCytosolic	K	K	---	YRPGMPILSVVY	PEIKTDSFDWTC	SDESPARHSLVYRGLVPVLH	AGSARAS---HEES 466
B. subtilis	K	K	---	YRPGAPIVAVTV	---	NDSISRKLALVSGVFAESG	ON---ASS 427
B. licheniformis	K	K	---	YRPGAPIVAVTV	---	NDAVSRKLSLVSGVFATSG	ON---HSS 427
B. stearotherm.	K	K	---	YRPGAPIVAVTS	---	NEAVSRRLALVSGVYTKEA	PH---VNT 428
B. psychrophils	K	K	---	YRPGCPVIAVTS	---	SEMCSRKLSLVSGVYPIV	GK---ASS 427
E. coli TypeI	K	K	---	YRPGDAPILALTR	---	NEKTAHQVLVSRGVVPQLV	KE---ITS 425
Synechocystis	N	N	---	QRPSVVPVIAFTS	---	SEKVTSLNLVSGIIPFLIN	EE---FDT 436
Lactococcus	K	K	---	KHRPDADILAITF	---	DEKVERGLMINVGVIPMTE	KP---AS 456
spirochete	T	T	---	YRASVPLFITTN	---	SERLARELALVSGVYSNLV	DNN---FKR 421
Tobaccoplastid	H	H	---	NRPSSTVIAFTN	---	NERVKORLALVSGVVPIM	DFS---SD 512
TobaccoChloroplast	R	R	---	CRPDCPIIAFTN	---	TTSVRRRLNLQVGLMPFRL	SFS---DD 553
Haemophilus	R	R	---	RISSCLPIFALSR	---	NQETLNLCALVSGVTPPIY	HGE---ESR 433
E. coli TypeII	R	R	---	RISSCLPIFAMSR	---	HERTLNLALVSGVTPVHF	DS---AND 433
Mycobacterium	R	R	---	RLHTEPLLLAFTA	---	WPEVRSQLAMVGTETFI	VPK---MQS 421
Corynebacterium	R	R	---	RLHTEPLLLAFTA	---	NEAVRSQALALVGTATFL	CEP---VSD 420
Zymomonas	R	R	---	RARPVAPILSLTP	---	DAEVARRLGLVWGAQPV	QVS---TVKT 429
Leishmania	K	K	---	RLQTCRQLNITR	---	GVESVFFDADKL---GHDEG 453	

```

--H17----->      <--S21-->      <S22-->
HumanR      VDRVQVQFGIESGKLRGFLRVGDLVIVVT-GW--RPGSGYTNIMRVLSISPIRKIHUPL-- 583
HumanL      VDRVQVQFGIESGKLRGFLRVGDLVIVVT-GW--RPGSGYTNIMRVLSISPIRKIRTPR-- 552
RatR        VDRVQVQFGIESGKLRGFLRVGDLVIVVT-GW--RPGSGYTNIMRVLSVSPIRKIRTPL-- 583
RatL        VDRVQVQFGIESGKLRGFLRVGDLVIVVT-GW--RPGSGYTNIMRVLSVSPIRS----- 547
MouseM2     VDLRVNVLAMDVGKARGFFKKGDVIVVLT-GW--RPGSGFTNIMRVVFPPIRB----- 535
RatM2       VDLRVNVLAMNVGKARGFFKKGDVIVVLT-GW--RPGSGFTNIMRVVFPPIRC----- 535
HumanM2     VDLRVNLFAMNVGKARGFFKKGDVIVVLT-GW--RPGSGFTNIMRVVFPPIRS----- 535
HumanM1     VDLRVNLFAMNVGKARGFFKKGDVIVVLT-GW--RPGSGFTNIMRVVFPPIRA----- 535
CatM1       VDLRVNVLAMNVGKARGFFKKGDVIVVLT-GW--RPGSGFTNIMRVVFPPIRKICHFM-- 539
RabbitM1    VDLRVNVLAMNVGKARGFFKKGDVIVVLT-GW--RPGSGFTNIMRVVFPPIRC----- 534
RatM1       VDLRVNVLAMNVGKARGFFKKGDVIVVLT-GW--RPGSGFTNIMRVVFPPIRN----- 535
FrogMuscle  VDSRVNFMAMDIGKARGFFKSGDVIVVLT-GW--RPGSGFTNIMRVVFPPIRS----- 531
ChickenMuscle VDLRVNLMNVGKARGFFKKGDLVIVVLT-GW--RPGSGYTNIMRVVFPPIRKIBYP-- 538
S. cerevisiae1 VEARINFGIEKAKKEFGILKKGDTVSVIQ-GF--KAGAGHSNPLQVSTVPPIRD----- 504
S. cerevisiae2 VHRRLKFGVEMARSFGMVDNGDTVSVIQ-GF--KGGVGHSNPLRISTVQGFPIRC---- 510
Yarrowia    VEEVRLKWMGDEAVLALGILNKGDVVVALQ-GW--TGGLATPPLSEFSSVSKLFENTNLLDYK 511
Emericella  VDRRLKKGWGINHGLKLGINKGDMIVCVQ-GW--RGGMGHTNIMRVVFPAAEEN----- 521
Aspergillus VDRRLKKGWGINHALKLGINKGDMIVCVQ-GW--RGGMGHTNIMRVVFPAAEEN----- 521
Trichoderma VDRRLKWAIVTRAIELKTLTAGDTVVVVQ-GW--KGGMGNTNMLRIVRADPDH----- 531
T. brucei    KERIVVKLGLDFAKKERYASTGDTVVVVH-AD--HVKGYPNQTRLIYLPPIRS----- 503
T. borelli   RENRVGLAIDVGKQMGVFEKGDVVAVH-AD--HHTKGFANQIRAIYKPIRA----- 501
PotatoCytosolic TEVRLLEAALKSAVTRGLCKPGDAVVALH----R-RIGSASVVIKICVVKPIRG----- 514
TobaccoCytosolic TEEVRLDFALQHAKTKGLCKQGDSVVALH----R-RVGTASVVIKIVTVKPIRC----- 512
B. subtilis  TDEVRLLEDAVQKSLNSGIVKHGDLIVVITA-GT--VGESGTTNMLMKVHTVGDIIAKGQGIGR 484
B. licheniforms TDEVRLLEKAVQKSLDTGIVRHGDLIVVITA-GA--VGEAGTTNMLMKVYVVDVAVKQGIGR 484
B. stearothersm. TDEVRLDVAVDAAVRSGLVKHGDLIVVITA-GVP--VGETGSTNMLMKVHVISDLLAKGQGIGR 486
B. psychrophils IDEVRLQESVEESVKHQYVGHGDLIVVITA-GVP--VGEAGTTNMLMKIHVIGDLLARGQGIGK 485
E. coli TypeI TDEVRYRLGKELALQSGLAHKGDVVVMVS-GAL--VP-SGTTNFTASVHVLPIRS----- 474
Synechocystis FEDVRIQQAELVLLRDRKMVEKGDQVILIMA-GIP--TKIPRGTNPLKIHRIPIRC----- 487
Lactococcus  TDDVRFVVAEKVALASGLVEAGDMIIIVA-GVP--VG-TGRTNIMRIRTVKPIRC----- 506
spirochete  TTEVRVVTSLKMLKEQGVVNDKDTVVIIS-GNPNRNIEKGTNFMINTVEDAIKGRNIPIR 480
Tobaccoplastid AEEVRFVRAIKLLLKSLVKDQGVVTLVQSGAQPIVRRHSTNHIQVRKVQSPIRG----- 566
TobaccoCloroplast MESVRLNKTFSLLKARGMIKSGDLIIAVS-----R-DMLQSIQVMNVPPIRS----- 597
Haemophilus TEACAKAAPQSLKEKGYLSTGDLVIVTQ-GGQ--CATQTNVQRTLIVEPIRC----- 482
E. coli TypeII GVAVRLASEAVNLLRDKGYLMSGDLVIVTQ-GDV--MSTVGSNTNTRILTVE----- 480
Mycobacterium TDGVRIRQVDKSLLELARYKRGDLVIVVA-GAP--PGTVGSTNLIHVHRIGEDD----VPIR 475
Corynebacterium TDDVRLMREVDRALLAMPEYNKGDVVVVA-GSP--PGVTGNTNMIHVHLLGDDTRIAKLPPIR 478
Zymomonas    LDEVRKLAETAKEYGFAKAGDRVVVVA-GEP--EGKAGTTNIVDVIEA----- 475
Leishmania   KERIVVAAGVEFAKSKGYVQTGDYCVVVIH-AD--HKVKGYNQTRILLVE----- 499

```

HumanR	-----	
HumanL	-----	
RatR	-----	
RatL	-----	
MouseM2	-----	
RatM2	-----	
HumanM2	-----	
HumanM1	-----	
CatM1	-----	
RabbitM1	-----	
RatM1	-----	
FrogMuscle	-----	
ChickenMuscle	-----	
S. cerevisiae1	-----	
S. cerevisiae2	-----	
Yarrowia	TYSMVIKSVNGGVLYKPIRB-----	531
Emericella	-----LGLSEPIRS-----	530
Aspergillus	-----LGLAEPIRA-----	530
Trichoderma	---L---GIGQMEPIRS-----	542
T. brucei	-----	
T. borelli	-----	
PotatoCytosolic	-----	
TobaccoCytosolic	-----	
B. subtilis	KSAYGPFVVVAQNAKEAEQKMTDGAVLVTRKSTDRDMIASLEKASALITEEGGLTSHAAVVG	544
B. licheniforms	KSAFGEVVIAQNAQEAAKKMKDGAVLVTRKSTDRDMMASLEKAAALITEEGGLTSHAAVVG	544
B. stearotherm.	KSAFGKAVVAKTAEERQKMVDGGILVTVSTADMMPAIEKAAALITEEGGLTSHAAVVG	546
B. psychrophils	DVAYGRTVVAKNAEALAYDTEGAILVTNASDRDMMPAIEKAGLITEEGGLTSHGAIVG	545
E. coli TypeI	-----	
Synechocystis	-----	
Lactococcus	-----	
spirochete	S-----	481
Tobaccoplastid	-----	
TobaccoChloroplast	-----	
Haemophilus	-----	
E. coli TypeII	-----	
Mycobacterium	I-----	476
Corynebacterium	S-----	479
Zymomonas	-----	
Leishmania	-----	

HumanR	-----	
HumanL	-----	
RatR	-----	
RatL	-----	
MouseM2	-----	
RatM2	-----	
HumanM2	-----	
HumanM1	-----	
CatM1	-----	
RabbitM1	-----	
RatM1	-----	
FrogMuscle	-----	
ChickenMuscle	-----	
S. cerevisiae1	-----	
S. cerevisiae2	-----	
Yarrowia	-----	
Emericella	-----	
Aspergillus	-----	
Trichoderma	-----	
T. brucei	-----	
T. borelli	-----	
PotatoCytosolic	-----	
TobaccoCytosolic	-----	
B. subtilis	LSLGIPVIVGLENATSILTDGQDITVDASRGAVYQGRASVLP	PIRS 589
B. licheniformis	LSLGIPVIVGMENATSILKEGEDITVDSARGAVYKGRASVLP	PIRS 589
B. stearotherm.	LSLGIPVIVGVENATTLFKDGGQEITVDGGFGAVYRGHASVLP	PIRS 591
B. psychrophils	LSLGIPVIVGVENATELIQHGKEITMDAESGVIYNGHASVLP	PIRS 590
E. coli TypeI	-----	
Synechocystis	-----	
Lactococcus	-----	
spirochete	-----	
Tobaccoplastid	-----	
TobaccoChloroplast	-----	
Haemophilus	-----	
E. coli TypeII	-----	
Mycobacterium	-----	
Corynebacterium	-----	
Zymomonas	-----	
Leishmania	-----	

Table A1. A Current List of Site Directed Mutations in PK Isozymes.

Point Mutation	Yeast Position	PK isozyme	Location	Ref.
R to Q	19	T. brucei	A-C DOM CONT	(71)
R to G	22	T. brucei	A-C DOM CONT	(71)
L to R	77	T. brucei	A-C DOM CONT	(71)
R to Q	77	Yeast	A-C DOM CONT	Current Study
E to K	89	Rabbit M1	Active Site	(142)
E to A	89	Rabbit M1	Active Site	(142)
E to D	89	Rabbit M1	Active Site	(142)
E to K/K to Q	89/86	Rabbit M1	Active Site	(142)
R to C	91	Rabbit M1		(80)
K to Q	236	Yeast	A-C DOM CONT	Current Study
K to M	240	Yeast	ACTIVE SITE	(143)
E to Q	242	Yeast	ACTIVE SITE	(52)
R to K	264	Yeast	ACTIVE SITE	(52)
M to R	289	B. stearothersophilus	A-C DOM CONT	(59)
K to Q	292	Yeast	A-C DOM CONT	Current Study
Q to N	299	Yeast	A-A SUB CONT	Current Study
Q to N	299	B. stearothersophilus	A-A SUB CONT	(59)
T to M	311	Rabbit M1	A-A SUB CONT	(80)
T to M	311	Yeast	A-A SUB CONT	Current Study
T to M	311	Yeast	A-A SUB CONT	(109)
T to M	311	Rabbit M2	A-A SUB CONT	(79)
D to E	327	B. stearothersophilus	A-C DOM CONT	(34)
Q to K	348	Rabbit M1	A-A SUB CONT	(80)
Y to F	360	Rat M2	C-C SUB CONT	(76)
F to Y	360	Rat M1	C-C SUB CONT	(77)
A to R	369	Rat M1	C-C SUB CONT	(77)
R to A	369	Yeast	C-C SUB CONT	Current Study
R to A	369	Rat M2	C-C SUB CONT	(76)
A to S/P to S	372/373	Rat M2	C-C SUB CONT	(76)
S to A/S to P	372/373	Rat M1	C-C SUB CONT	(77)
S to P	373	Rabbit M1	C-C SUB CONT	(144)
T to L	379	Rat M2	C-C SUB CONT	(76)
L to T	379	Rat M1	C-C SUB CONT	(77)
S to P	384	Yeast	C-C SUB CONT	(78)
E to A	392	Yeast	C-C SUB CONT	Current Study
C to L	394	Rat M2	C-C SUB CONT	(76)
L to C	394	Rat M1	C-C SUB CONT	(77)
I to L	399	Rat M2	C-C SUB CONT	(76)
L to I	399	Rat M1	C-C SUB CONT	(77)
T to E	403	Yeast	FBP binding site	Current Study
T to K	403	Yeast	FBP binding site	Current Study
T to R	406	Yeast	FBP binding site	Current Study
R to Q	409	Yeast	A-C DOM CONT	Current Study
K to E	413	Yeast	A-C DOM CONT	Current Study
K to Q	413	Yeast	A-C DOM CONT	Current Study
Y to F	414	Rabbit M1	C-C SUB CONT	(144)
Y to F	436	Yeast	A-C DOM CONT	Current Study
Y to S	436	Yeast	A-C DOM CONT	Current Study
W to Y	437	B. stearothersophilus	A-C DOM CONT	(34)
A to K	458	Yeast	FBP binding site	Current Study
R to Q	459	Yeast	FBP binding site	Current Study
F to V	466	T. brucei	A-C DOM CONT	(71)

VITA

Aron W. Fenton

Candidate for the Degree of

Doctor of Philosophy

Thesis: MOLECULAR DISSECTION OF THE ALLOSTERIC REGULATION OF
YEAST PYRUVATE KINASE BY FRUCTOSE-1,6-BISPHOSPHATE

Major Field: Biochemistry and Molecular Biology

Biographical:

Education: Graduated from Sharon-Mutual High School, Mutual, Oklahoma in May 1991; received Bachelor of Science degree in Biochemistry and Molecular Biology from Oklahoma State University, Stillwater, Oklahoma in December 1993. Completed the requirements for the Doctor of Philosophy degree with a major in Biochemistry and Molecular Biology at Oklahoma State University in December 1999.

Research Experience: 1992-93: Special Research Student, Department of Biochemistry and Molecular Biology, Oklahoma State University, Stillwater, OK
1993: Undergraduate Research Technician, Department of Animal Science, Oklahoma State University, Stillwater, OK
1994: Research Technician, Department of Biochemistry and Molecular Biology, Oklahoma State University, Stillwater, OK
1994-present: Ph.D. Candidate, Department of Biochemistry and Molecular Biology, Oklahoma State University, Stillwater, OK

Honors: American Institute of Chemists Award, Distinguished Freshman Scholarship, High School Class Valedictorian

Professional Memberships: Sigma Xi; Phi Lambda Upsilon, National Honorary Chemical Society; Gamma Sigma Delta, Honor Society of Agriculture; Biophysics Journal Club; Biochemistry and Molecular Biology Journal Club